

The Pennsylvania State University

The Graduate School

John and Willie Leone Family Department of Energy and Mineral Engineering

DEVELOPMENT OF AN ARTIFICIAL NEURAL NETWORK BASED EXPERT SYSTEM
FOR RATE TRANSIENT ANALYSIS TOOL IN MULTILAYERED RESERVOIRS
WITH OR WITHOUT CROSS FLOW

A Thesis in

Energy and Mineral Engineering

by

Jafar M-Amin

© 2015 Jafar M-Amin

Submitted in Partial Fulfillment
of the Requirements
for the Degree of

Master of Science

May 2015

The thesis of Jafar M-Amin was reviewed and approved* by the following:

Turgay Ertekin

Professor of Petroleum and Natural Gas Engineering

Head, John and Willie Leone Family Department of Energy and Mineral Engineering

Thesis Advisor

Eugene Morgan

Assistant Professor of Petroleum and Natural Gas Engineering

Shimin Liu

Assistant Professor of Energy and Mineral Engineering

Luis F. Ayala H.

Associate Professor of Petroleum and Natural Gas Engineering;

Associate Department Head for Graduate Education

*Signatures are on file in the Graduate School

Abstract

The Artificial Neural Network has been used in a variety of complex conditions where the non-linear relationships between existing variables can be difficult to understand. Forecasting the reservoir production along with resembling the reservoir behavior are the main goals of using simulators. To reduce the number of runs by a simulator, the Artificial Neural Network is used to predict the relationship between variables using a history matching technique. The Artificial Neural Network (ANN) mainly consists of two solution parts. The first part is called forward solution and is used to obtain production properties from parameters generated using the simulator. Using an inverse solution enables users to obtain reservoir or well design data based on production data such as production rate and cumulative production.

The artificial neurons are mathematical functions that handle multiplying, summing and activating the neurons to be transformed to a desired goal, an output. Different scenarios have been implemented following the Artificial Neural Network application to the petroleum industry. As the number of layers in a multilayer reservoir increases, neural network requires more time and computations. By using optimization methods and applying them to the ANN, the tool decides on the best design in which the least error is achieved. The developed tool has been assessed based on the comparison of simulator parameters and ANN learned variables.

To enhance the utilization of the tool, a graphic user interface (GUI) has been created to help users access the data and results efficiently. The GUI is itself considered to be an auxiliary tool and based on the data provided as inputs, results would be available.

Table of Contents

List of Figures	vii
List of Tables	xiv
Aknowledgemnet	xvi
Nomenclature units	xvii
Chapter 1 Introduction	1
Chapter 2 Literature Review	3
2.1 Multilayered reservoir.....	3
2.2 Rate Transient Analysis	7
2.3 Artificial Neural Network.....	8
2.3.1 History and Application.....	8
2.3.2 ANN Structure	12
2.3.3 Transfer Functions	14
2.3.4 Learning and Training algorithm	16
Chapter 3 Problem Statement	18
Chapter 4 Generation of training sets	21
4.1 Grid Blocks Sensitivity Analysis	22
4.2 Range of reservoir parameters	24
4.3 Well design parameters.....	25
Chapter 5 Artificial Neural Network development.....	27
5.1 Artificial Neural network design	27

5.2 Multilayered neural network development	29
5.2.1 Two-layered reservoir network.....	29
5.2.1.1 Forward artificial Neural network	29
5.2.1.2 Inverse well design artificial neural network.....	31
5.2.1.3 Inverse reservoir parameters Artificial Neural Network	32
5.2.2 Three-layered reservoir network.....	33
5.2.2.1 Forward artificial Neural network	33
5.2.2.2 Inverse well design Artificial Neural Network.....	34
5.2.2.3 Artificial Neural Network inverse reservoir parameters.....	35
5.2.3 Four-layered reservoir network.....	36
5.2.3.1 Forward Artificial Neural Network	36
5.2.3.2 Inverse well design Artificial Neural Network.....	37
5.2.3.3 Inverse reservoir parameters Artificial Neural Network	38
5.3 Graphical User Interface (GUI)	39
5.3.1 Forward ANN forecasting production profile.....	40
5.3.2. Inverse forecasting well design parameters	41
5.3.3. Inverse forecasting reservoir parameters	42
Chapter 6 Results and Discussions	43
6.2 Result of Three-layered reservoir network Artificial Neural.....	54
6.3 Results for Four-layered reservoir artificial neural network.....	66
6.5 Supplemental Approach.....	83
Chapter 7 Summary, conclusion and recommendation	86
7.1 Results Summary	86
7.2 Conclusion	88

7.3 Future recommendations.....	88
References.....	89
Appendix A.....	92
Data sample of the three-layered reservoir generated by the simulator.....	92
Appendix B.....	104
Forward network and simulator comparison plots in two-layered reservoir	104
Appendix C.....	118
Forward network and simulator comparison plots in three-layered reservoir	118
Appendix D.....	132
Forward network and simulator comparison plots in three-layered reservoir	132

List of Figures

Figure 1 wellbore in a multilayered reservoir (Ehlig-Economides, 1987).....	4
Figure 2 A simple biological neuron structure An ANN structure with reference to brain neurons	9
Figure 3 Schematic diagram of the simplest multilayer feedforward backproppagation.....	11
Figure 4 Criteria or termination of training and selection of optimum network architecture	13
Figure 5 Table of all transfer functions used for artificial neural network	15
Figure 6 Cumulative production curves plotted with different grid blocks	23
Figure 7 GUI screenshot of three-layered reservoir.....	39
Figure 8 GUI results for forward solution of three-layered reservoir	40
Figure 9 GUI results of well design inverse tool for three-layered reservoir	41
Figure 10 GUI results of reservoir properties inverse tool for three-layered reservoir.....	42
Figure 31 data set 433 of gas rate and cumulative production data of ANN and CMG	46
Figure 32 data set 443 of gas rate and cumulative production data of ANN and CMG	46
Figure 41 Figure 41 Inverse well design for drainage area.....	48
Figure 42 Figure 41 Inverse well design for Bottom hole pressure	48
Figure 43 Inverse porosity results for CMG and ANN.....	50
Figure 44 Inverse porosity results for CMG and ANN.....	51
Figure 45 Inverse initial reservoir pressure results for CMG and ANN.....	51
Figure 46 Inverse vertical permeability results for CMG and ANN.....	52
Figure 47 Inverse vertical permeability results for CMG and ANN.....	52
Figure 48 permeability results for CMG and ANN	53
Figure 49 permeability results for CMG and ANN	53
Figure 52 Data set 22 of forward network for three-layered system	56
Figure 53 Data set 18 of forward network for three-layered system	56

Figure 80 Bottom Hole Pressure results for CMG and ANN	58
Figure 81 Drainage Area results for CMG and ANN	58
Figure 82 Permeability layer 1 results for CMG and ANN	60
Figure 83 Permeability layer 2 results for CMG and ANN	61
Figure 84 Permeability layer 3 results for CMG and ANN	61
Figure 85 vertical permeability of layer 1 results for CMG and ANN	62
Figure 86 vertical permeability of layer 2 results for CMG and ANN	62
Figure 87 vertical permeability layer 3 and initial reservoir pressure results for CMG and ANN	63
Figure 88 initial reservoir pressure results for CMG and ANN	63
Figure 89 porosity layer 1 results for CMG and ANN	64
Figure 90 porosity layer2 results for CMG and ANN	64
Figure 91 porosity layer 3 results for CMG and ANN	65
Figure 108 Data set 260 forward solution for four-layered reservoir	68
Figure 109 Data set 252 forward solution for four-layered reservoir	68
Figure 122 Bottom Hole pressure results from four-layered reservoir results	70
Figure 123 Drainage area results for four-layered reservoir	70
Figure 124 Permeability layer 1 plots for CMG Vs ANN	72
Figure 125 Permeability layer 2 plots for CMG Vs ANN	73
Figure 126 Permeability layer 3 plots for CMG Vs ANN	73
Figure 127 Permeability layer 4 plots for CMG Vs ANN	74
Figure 128 Vertical Permeability layer 1 plots for CMG Vs ANN	74
Figure 129 Vertical Permeability layer 2 plots for CMG Vs ANN	75
Figure 130 Vertical Permeability layer 3 plots for CMG Vs ANN	75
Figure 131 Vertical Permeability layer 4 plots for CMG Vs ANN	76

Figure 132 Initial Reservoir pressure plots for CMG Vs ANN	76
Figure 133 porosity layer 1 and porosity layer 1 plots for CMG Vs ANN.....	77
Figure 134 porosity layer 2 plots for CMG Vs ANN.....	77
Figure 135 porosity layer 3 plots for CMG Vs ANN.....	78
Figure 136 porosity layer 4 plots for CMG Vs ANN.....	78
Figure 137 Two plots represent two data sets of production rate for blind data set	79
Figure 138 Two plots represent two data set of cumulative production	80
Figure 139 ANN results in red compare to CMG results in blue for gas rate for 70 data sets	81
Figure 140 ANN results in red compare to CMG results in blue for cumulative gas for 70 data sets.....	81
Figure 141 Error distribution map for 70 blind data sets as for 30 values Cumulative production	82
Figure 142 Error distribution map for 70 blind data sets for 30 values of Cumulative production	82
Figure 143 Two-layered and three-layered similarity approach in gas rate.....	84
Figure 144 Two-layered and three-layered similarity approach in cumulative production	85
Figure 11 data set 12 of gas rate and cumulative production data of ANN and CMG	104
Figure 12 data set 15 of gas rate and cumulative production data of ANN and CMG	104
Figure 13 data set 26 of gas rate and cumulative production data of ANN and CMG	105
Figure 14 data set 30 of gas rate and cumulative production data of ANN and CMG	105
Figure 15 data set 36 of gas rate and cumulative production data of ANN and CMG	106
Figure 16 data set 52 of gas rate and cumulative production data of ANN and CMG	106
Figure 17 data set 86 of gas rate and cumulative production data of ANN and CMG	107
Figure 18 data set 109 of gas rate and cumulative production data of ANN and CMG	107
Figure 19 data set 131 of gas rate and cumulative production data of ANN and CMG	108
Figure 20 data set 144 of gas rate and cumulative production data of ANN and CMG	108
Figure 21 data set 152 of gas rate and cumulative production data of ANN and CMG	109

Figure 22 data set 159 of gas rate and cumulative production data of ANN and CMG	109
Figure 23 data set 171 of gas rate and cumulative production data of ANN and CMG	110
Figure 24 data set 188 of gas rate and cumulative production data of ANN and CMG	110
Figure 25 data set 221 of gas rate and cumulative production data of ANN and CMG	111
Figure 26 data set 253 of gas rate and cumulative production data of ANN and CMG	111
Figure 27 data set 310 of gas rate and cumulative production data of ANN and CMG	112
Figure 28 data set 322 of gas rate and cumulative production data of ANN and CMG	112
Figure 29 data set 373 of gas rate and cumulative production data of ANN and CMG	113
Figure 30 data set 393 of gas rate and cumulative production data of ANN and CMG	113
Figure 33 data set 451 of gas rate and cumulative production data of ANN and CMG	114
Figure 34 data set 456 of gas rate and cumulative production data of ANN and CMG	114
Figure 35 data set 458 of gas rate and cumulative production data of ANN and CMG	115
Figure 36 data set 473 of gas rate and cumulative production data of ANN and CMG	115
Figure 37 data set 502 of gas rate and cumulative production data of ANN and CMG	116
Figure 38 data set 503 of gas rate and cumulative production data of ANN and CMG	116
Figure 39 data set 554 of gas rate and cumulative production data of ANN and CMG	117
Figure 40 data set 560 of gas rate and cumulative production data of ANN and CMG	117
Figure 50 Data set 8of forward network for three-layered system	118
Figure 51 Data set 15 of forward network for three-layered system	118
Figure 54 Data set 61 of forward network for three-layered system	119
Figure 55 Data set 29 of forward network for three-layered system	119
Figure 56 Data set 557 of forward network for three-layered system	120
Figure 57 Data set 518of forward network for three-layered system	120
Figure 58 Data set 467 of forward network for three-layered system	121

Figure 59	Data set 460 of forward network for three-layered system	121
Figure 60	Data set 453 of forward network for three-layered system	122
Figure 61	Data set 402 of forward network for three-layered system	122
Figure 62	Data set 371 of forward network for three-layered system	123
Figure 63	Data set 366 of forward network for three-layered system	123
Figure 64	Data set 339 of forward network for three-layered system	124
Figure 65	Data set 298 of forward network for three-layered system	124
Figure 66	Data set 291 of forward network for three-layered system	125
Figure 67	Data set 245 of forward network for three-layered system	125
Figure 68	Data set 224 of forward network for three-layered system	126
Figure 69	Data set 206 of forward network for three-layered system	126
Figure 70	Data set 200 of forward network for three-layered system	127
Figure 71	Data set 177 of forward network for three-layered system	127
Figure 72	Data set 156 of forward network for three-layered system	128
Figure 73	Data set 151 of forward network for three-layered system	128
Figure 74	Data set 140 of forward network for three-layered system	129
Figure 75	Data set 122 of forward network for three-layered system	129
Figure 76	Data set 105 of forward network for three-layered system	130
Figure 77	Data set 91 of forward network for three-layered system	130
Figure 78	Data set 86 of forward network for three-layered system	131
Figure 79	Data set 62 of forward network for three-layered system	131
Figure 92	data set 532 forward solution for four-layered reservoir	132
Figure 93	data set 600 forward solution for four-layered reservoir	132
Figure 94	data set 530 forward solution for four-layered reservoir	133

Figure 95 data set 515 forward solution for four-layered reservoir	133
Figure 96 data set 497 forward solution for four-layered reservoir	134
Figure 97 data set 440 forward solution for four-layered reservoir	134
Figure 98 data set 423 forward solution for four-layered reservoir	135
Figure 99 data set 405 forward solution for four-layered reservoir	135
Figure 100 data set 381 forward solution for four-layered reservoir	136
Figure 101 data set 333 forward solution for four-layered reservoir	136
Figure 102 data set 328 forward solution for four-layered reservoir	137
Figure 103 data set 309 forward solution for four-layered reservoir	137
Figure 104 Data set 305 forward solution for four-layered reservoir	138
Figure 105 Data set 281 forward solution for four-layered reservoir	138
Figure 106 Data set 276 forward solution for four-layered reservoir	139
Figure 107 Data set 264 forward solution for four-layered reservoir	139
Figure 108 Data set 260 forward solution for four-layered reservoir	140
Figure 109 Data set 252 forward solution for four-layered reservoir	140
Figure 110 Data 234 set 305 forward solution for four-layered reservoir	141
Figure 111 Data set 232 forward solution for four-layered reservoir	141
Figure 112 Data set 192 forward solution for four-layered reservoir	142
Figure 113 Data set 174 forward solution for four-layered reservoir	142
Figure 114 Data set 163 forward solution for four-layered reservoir	143
Figure 115 Data set 142 forward solution for the four-layered reservoir	143
Figure 116 Data set 137 forward solution for the four-layered reservoir	144
Figure 117 Data set 134 forward solution for the four-layered reservoir	144
Figure 118 Data set 128 forward solution for the four-layered reservoir	145

Figure 119 Data set 83 forward solution for the four-layered reservoir	145
Figure 120 Data set 62 forward solution for the four-layered reservoir	146
Figure 121 Data set 8 forward solution for the four-layered reservoir	146

List of Tables

Table 1 Random grid block size for the reservoir.....	23
Table 2 Parameters range for the reservoir	24
Table 3 Parameters range for the well	26
Table 4 Forward network's inputs and outputs for two-layered system.....	29
Table 5 Forward network's functional links for two-layered system	30
Table 6 Inverse well design network's inputs and outputs for two-layered system	31
Table 7 Inverse reservoir parameters network's inputs and outputs for two-layered system	32
Table 8 Forward network's inputs and outputs for three-layered system.....	33
Table 9 Inverse well design network's inputs and outputs for three-layered system	34
Table 10 Inverse reservoir parameters network's inputs and outputs for three-layered system	35
Table 11 Forward network's inputs and outputs for four-layered system	36
Table 12 inverse well design network's inputs and outputs for four-layered system.....	37
Table 13 Inverse reservoir parameters network's inputs and outputs for a four-layered system.....	38
Table 14 Forward Two-layered network results	45
Table 15 Two-layered system production profile error for all 30 values.....	45
Table 16 Two-layered inverse well design ANN results	47
Table 17 Inverse well design for two later-reservoir results and error	49
Table 18 Inverse reservoir properties results	50
Table 19 Forward ANN for three-layered reservoir results	54
Table 20 Forward network for three-layered system results.....	55
Table 21 Inverse well design Solution for three-layered reservoir	57
Table 22 ANN and CMG results and comparison for the three-layered reservoir	59
Table 23 Inverse reservoir properties optimum network results for three-layered Reservoir.....	60

Table 24 Forward solution results for Cumulative production and production rate	66
Table 25 optimum network of Forward solution for four-layered reservoir	67
Table 26 Inverse well design optimum network	69
Table 27 Inverse well design results for four-layered reservoir	71
Table 28 Inverse reservoir properties optimum network for four-layered reservoir.....	72
Table 29 Network results for 70 blind data set	80

Acknowledgements

I would like to express my greatest gratitude to Dr. Ertekin for his valuable advice and guidance. I have had honor to be under his supervision during the thesis completion and having courses that contribute to the wealth of my knowledge and industry experience.

Moreover, I would like to thank my committee members for the defense, Dr. Liu for his attitude and effort and Dr. Morgan for his kindness and generosity regarding spending his valuable time throughout thesis and course.

I would like to thank my sponsor during Master's study, Fulbright and Amideast for the precious opportunity to study in such a prestigious academic institution, the Pennsylvania State University.

Lastly, Special thanks to my life's greatest support and my soul mate, Amelie and her great family for their love, support and kindness.

Nomenclature units

ANN	Artificial Neural Network
L	Block Length (ft)
BHP	Bottom Hole Pressure (psi)
C	Cumulative gas production (SCF)
A	Drainage Area (acre)
G	Gas rate (SCF/D)
k	Horizontal Permeability (md)
pi	Initial Reservoir Pressure (psi)
h	Layer Thickness (ft)
phi	Porosity (%)
T	Reservoir Temperature (F)
h	Thickness(ft)
k _v	Vertical Permeability (md)
SCF/d	Standard Cubic Feet per day

Chapter 1 Introduction

Many of the reservoir and well parameters can be estimated using well logs, lab experiments on core samples and seismic data. Moreover, reservoir simulators can provide these data with acceptable approximation. Using CMG¹ IMEX as a simulator to model heterogeneous, single porosity and single permeability reservoir will be effective and a well is vertically drilled throughout the multilayered reservoir. All the layers within the reservoir boundary have been perforated thoroughly enabling variety of formations to be included in the simulation.

The goal of the Artificial Neural Network model is to find reservoir properties and production forecast using the technique of mimicking the neuron function of the human brain. In addition to reducing the cost, this tool can save a tremendous amount of time compared to the time consuming simulator and the fact that a simulator requires obtaining some data in the field.

In this expert tool, effort has been extended to predict where the reservoir layers are interconnected within the layers as called crossflow. The magnitude of vertical permeability of adjacent layers is an indicator of the cross flow. Using both supervised and unsupervised techniques in the Artificial Neural Network enables the network to predict the variables with accuracy and helps the tool to select a proper structure as optimum results.

Chapter two depicts the simple structure of neurons in artificial neural network with the explanation of hidden layers and transfer functions along with the application and history of using ANN in various fields such as biology, medicine, computer analysis and nuclear power.

¹ Computer Modelling Group: A reservoir simulation

In chapter three, the problems that are supposed to be solved has been studied and proper solution for each problem suggested.

In chapter four, the data generation process is discussed and the comparison between the simulator and neural network data is achieved. Chapter five covers the structure and theory of the tool using MATLAB². In chapter six, the results will be discussed with the regression and error criteria. Chapter seven includes the conclusion, summary and future recommendations for this study.

² high-level language and interactive numerical computation

Chapter 2 Literature Review

2.1 Multilayered reservoir

A multilayered reservoir is a reservoir consists of horizontally homogeneous and isotropic layers and each layer may have different properties compare to others. These reservoirs mostly have shorter life and higher gas production compared to single layered reservoirs. The efficiency of having less perforation and completion job cost in addition to requiring less interpretation time for well test analysis are the benefits of multilayered reservoirs (Gas Well Testing Handbook, 2003). These layers mostly have different gas rates and even pressure transients, which is due to its unique formation. There have been efforts since the 1960's to identify the characteristics of a multilayered reservoir and its layers behavior within the whole system.

Generally, the pressure differences between layers can lead to reservoir fluid to flow, only if there are communications among the layers. The wellbore commingled system exists if the layers have no flow in between and the crossflow only occurs in wellbore. In the wellbore commingled system, vertical permeability among layers is very small or equal zero. The flow most likely comes from a less permeable layer to the more permeable one. This is due to the fact that formation pressure in less permeable layers is higher than that in the more permeable one. Permeability is of very high importance when it comes to crossflow since flow direction among layers can be determined from permeability (Park, 1989). To identify the layers' properties and behavior, a certain number of analytical methods as well as numerical simulators are adopted and an example of multilayered reservoir has been illustrated in Figure 1.

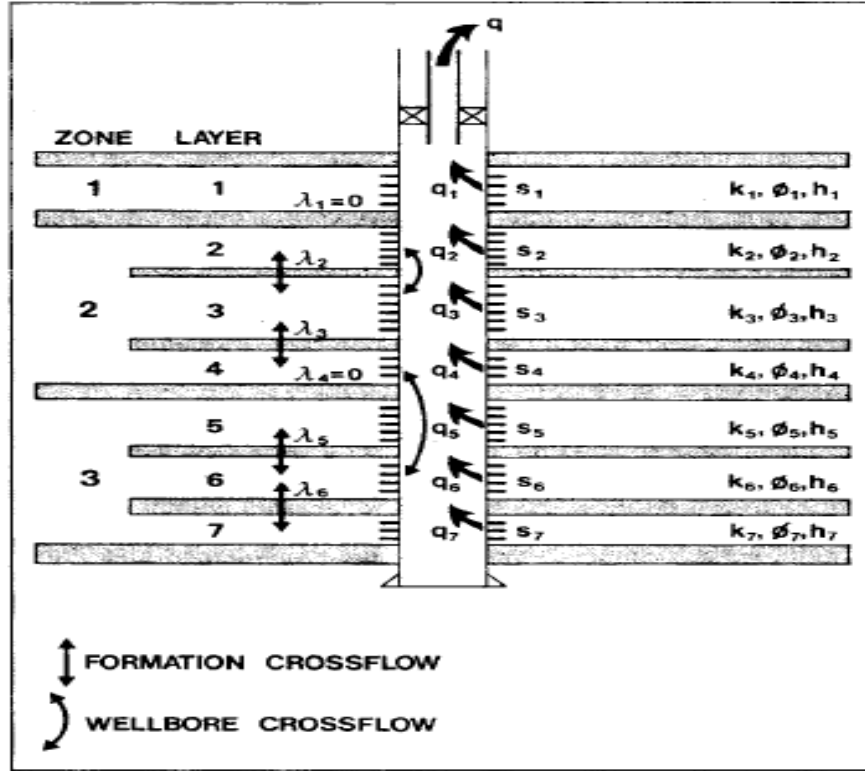


Figure 1 wellbore in a multilayered reservoir (Ehlig-Economides, 1987)

One of the early studies on commingled flow (no crossflow in wellbore) was performed and analyzed by Lefkovits. In an effort to obtain layer properties using analytical methods, thickness, permeability, porosity and vertical permeability have been identified thoroughly. For a commingled system, Tariq and Ramey developed a beneficial algorithm for numerical inversion of Laplace equations. This algorithm has been used in many experiments and publications. On the other hand, the crossflow between layers in multilayered reservoirs using differential equations in two-dimensional systems were developed by the Jacquard formula.

Bourdet developed a model of infinite two-layered reservoirs with mentioning skin factor. Later on, Ehlig-Economides and Joseph suggested a similar model to Bourdet's with an unlimited number of layers which is applicable to constant pressure boundary with cross flow.(Ehlig-Economides ,SPE 14167, 1987)

The crossflow of the layers depends on porosity of the layer. If the porosity of a less permeable layer is small in comparison to that of more permeable layers, it is more likely that the flow occurs for long periods of time. On the other hand, if the porosity of a less permeable reservoir is larger than that of a more permeable layer, the crossflow effect will be reduced since the pressure in the less permeable reservoir is higher than that of the more permeable one.

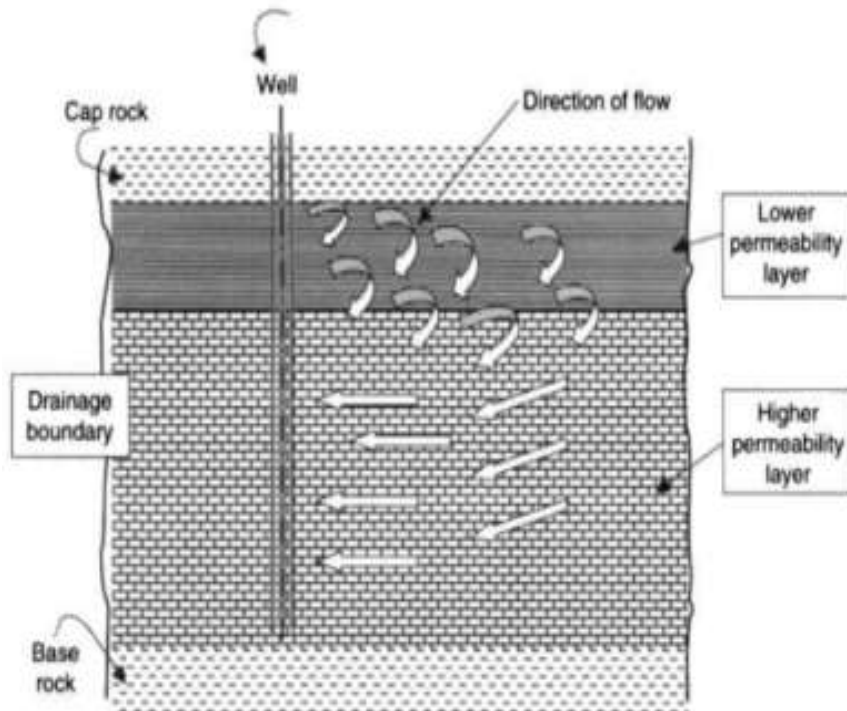


Figure 2 Schematic view of flow direction in multilayered reservoir (Gas Well Testing Handbook, 2003).

A multilayered gas reservoir with crossflow behaves similarly to a homogeneous single layer reservoir with cross flow with the same pore volume and dimensions only if the product of thickness-permeability (kh) of both are equal (Gas Well Testing Handbook, 2003).

In multilayered reservoir with I number n number of layers , the total $(kh)_t$ is equal to the sum of all layers (kh) as illustrated in equation below:

$$(kh)_t = \sum_k^n (kh)_i , k = 1$$

Using the production rate of layer (q), the permeability of each layer can be obtained. For a reservoir with n number of layers, permeability of a single layer is dependent of total rate (q_t), layer rate (q_i), permeability (k) , total reservoir thickness (h_t) and layer thickness (h_i). Therefore equation below is prepared:

$$k_i = \frac{q}{q_t} * \left[\frac{kh_t}{h_i} \right]$$

2.2 Rate Transient Analysis

In specific, rate transient analysis is advantageous to reservoir evaluation and it helps obtaining reservoir properties such as permeability, porosity and thickness. In rate transient analysis, the bottom hole pressure is kept constant during the test. The bottom hole pressure varies from 15 to 50 percent of reservoir initial pressure in order to cover as many reservoir parameters range as possible. On the other hand, pressure transient analysis evaluates the reservoir pressure, heterogeneity, reservoir boundary, skin and fracture parameters. In pressure transient analysis, production rate is fixed at a certain rate to analyze the pressure transient. There are many types of pressure transient analyses such as pressure buildup test, drawdown test, fall off test, drill stem test where the sequence of the well shut in and well type vary.

In this study, the production data has been evaluated using both the simulator and Artificial Neural Network (ANN) results. The data extracted from the simulator is based on reservoir properties and well parameters. Both production rate and cumulative production have been plotted for each set of parameters values on different reading time intervals. These points are selected and will be used in the neural network to resemble curves. Using these points and a few more parameters, the model can predict the well design or reservoir properties accordingly.

2.3 Artificial Neural Network

2.3.1 History and Application

As a computational model for processing data, Artificial Neural Network has been used in a variety of science branches, medical researches and marketing purposes. An Artificial Neural Network comprises of processing units that resemble neurons in the human brain. A common reason of using the Artificial Neural Network is when the parameters' relationships cannot be obtained analytically or it is difficult to obtain them considering time and human effort.

In the oil and gas industry where production of hydrocarbons is a key factor to investors, the Artificial Neural Network can forecast production with the help of mimicking the biological nervous system of the brain. Although simulators are widely common to be used to forecast the production and variables, there are some disadvantage with simulators. In order to use simulators, skilled individuals who have knowledge of mathematics, physics and basic reservoir engineering are required. Moreover, Simulators mostly rely on data that extracted from field operations such as well logging, core analysis and well testing which can be very expensive to run and process. Considering the amount of time that simulators take to analysis and simulate a reservoir given the broad range of data, it is quite efficient to utilize artificial neural network to avoid time consuming simulations.

McCulloch and Pitts proposed the first simplified neuron model in 1943. Since that time, Artificial Neural Network has been used in engineering analysis and predictions (Cleveland, Cutler J ,Encyclopedia of Energy,2007).

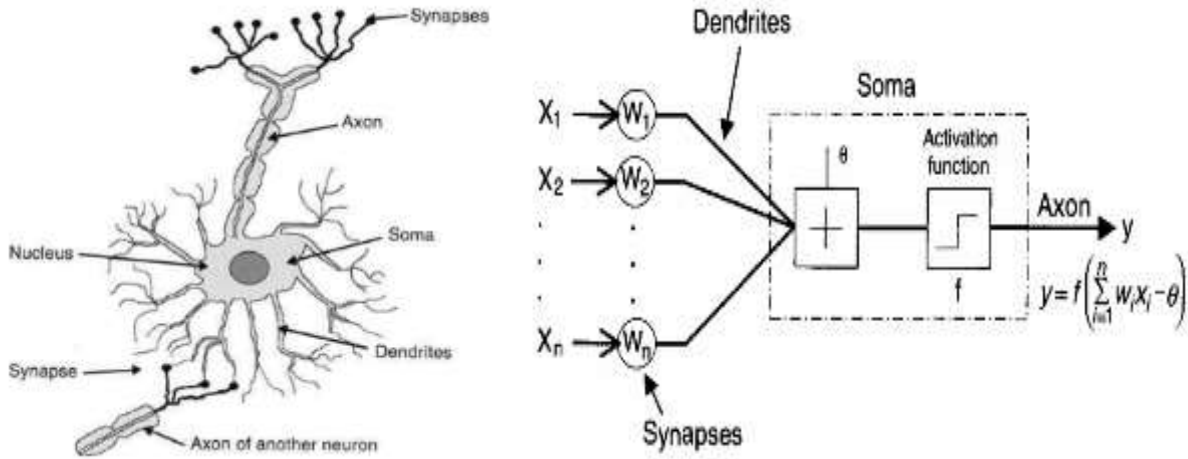


Figure 2 Above Left: a simple biological neuron structure showing the Axon and Dendrites which resemble input and output, respectively. Above Right: An ANN structure with reference to brain neurons (Cleveland, Cutler J ,Encyclopedia of Energy,2007).

Artificial Neural Network performance can be assessed by calculated error between the network output and target, training time and other properties. The ANN structure, mainly consists of neurons, hidden layers, transfer functions and algorithms are substantial to achieve the goal. The least error, which is the best prediction case or referred as our network solution, depends on trial and error the majority of the time (Haykin 1994).The simple biological neuron structure in two different diagrams are shown in Figure 2.

There are few features that have been built in the Artificial Neural Network which enable us to monitor and obtain favorable results in a more professional and comprehensive way. There are two ways to obtain reliable data through neural network: supervised and unsupervised. For supervised method supervising the input and output is done by assigning inputs and outputs individually. The unsupervised operate the network in a way to have all of the data as one input given to the system and ultimately, the network is able to classify the data, pictures or maps the users are interested in examining.

Features such as pattern classification, clustering and function approximation for casting and optimization would be used in both supervised and unsupervised neural networks. In contrast to supervised learning, the unsupervised learning classifies the examples based on their similarities and provides the classified groups of data.

Many ANN's have been utilized to solve problems. Some problems may be exclusively suitable to be fixed by specific types of neural networks. We should pay attention to the factors that are decisive in order to pick the appropriate type. ANN's consist of many types such as Hopfields networks, Adaptive Resonance Theory (ART) networks, Kohonen networks, Backproppagation networks, Recurrent networks, Counterpropagation networks and Radial basis function (RBF) networks. Amongst all of these network types, the Backproppagation type is widely used, especially in engineering applications.

A backproppagation network consists of input layers and variables assigned to the input layers and an output layer with target data. The most important part of this network is the hidden layer in which the nodes affiliated with the layer are in charge of detecting nonlinearities between input and output. The term backproppagation is rooted in the methods of correcting errors which is coming backward from output passing hidden layers nodes and all the way to inputs.

These types of networks are useful in many branches as they can be used for forecasting, classification of data, pattern recognition, modelling and data mining (Hassoun, 1995). In this study, we have used BPANNs as a mean to find solutions for problems and predict the necessary part of unknowns such as cumulative gas production and gas rate along with other reservoir and well design parameters.

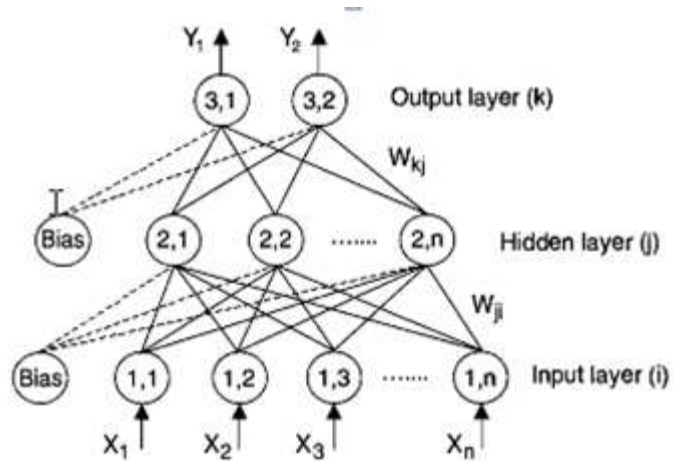


Figure 3 Schematic diagram of the simplest multilayer feedforward backpropagation with an input layer (i), a hidden layer (j) and an output layer (k) (Cleveland, Cutler J ,Encyclopedia of Energy).

In backpropagation ANNs alone, there are two different solution types we can use. Feedforward backpropagation is a common way of problem solving in which it obtains the error by means of gradient descent for data sets. There are two actions inside the BPANNs : first would be the forward solution into the hidden layer from inputs, second the backward would be the error computation by adjusting proper weights. All input nodes will be multiplied by their proper weights and be summed with hidden nodes. A simple BPANNs structure has been shown in Figure 3.

A transfer function will come to picture when one hidden node has been identified, then activating the nodes from a hidden layer. Lastly, we will convert it to a value between -1 and +1 which is done by transfer functions. The selection of the transfer function can be critical to obtaining close data to the target. Essentially, this function has to be selected for each hidden layer. Depending on the structure and final goal, hidden layers can be more than one based on the accuracy level required throughout the data computation, and history matching time may be compromised with large numbers of hidden layers.

The transfer function assigns the sign to all nodes of a layer to another layer and so on. The weights that have been added to the input layers are selected by networks but can be revised if the result of all activation process and multiplication ends up far from the known target. In this case, the second part of the data computation begins with modifying the results based on interconnected weights and assigned new values, which would bring the output and target as close as possible. This process will repeat itself until the specified tolerance, which can be assigned by the network developer based on the limitations of the study. The last activation will go from the last hidden layers (or the hidden layer if only one) to the output layer and the regressions can be analyzed (I.A Basheer, 2000).

2.3.2 ANN Structure

A typical structure of an ANN consists of an input layer, hidden layer(s), neurons and an output layer. Though it may appear simple, there can be millions of computational forward and backward sweeps inside which happens with the presence of neurons from all layers. Obviously, every network can have different structures or architecture based on the goal of the project. There is always an optimum structure in which the least error, best result is reached which can be established based on trial and error. As shown in Figure 4, once the testing and training lines approached closely to a point, optimum network is reached and after this point, lines will extend far from each other that implies over fitting has happened and the network has started memorizing instead of training.

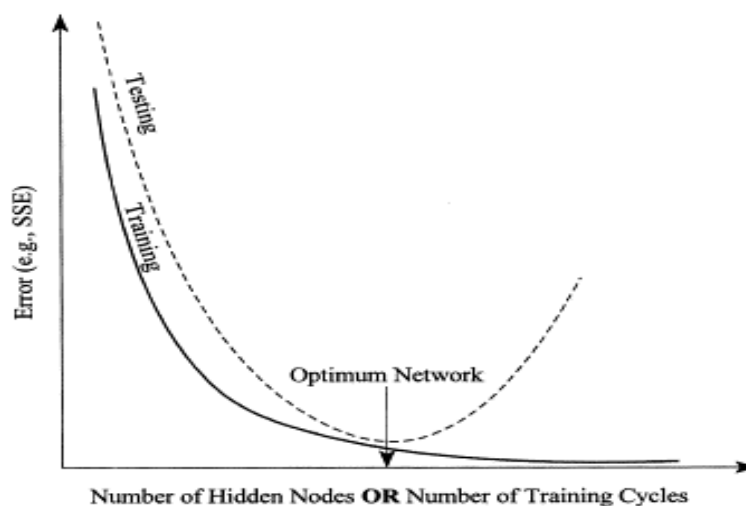


Figure 4 Criteria or termination of training and selection of optimum network architecture (I.A Basheer, 2000)

Since there is no general formula about the ideal number of hidden layers or neurons in which the network is optimum, the process requires trial and error. There are some assumptions based on experience to determine these unknowns. There are some rules of thumb that can be useful such as the one in which the number of neurons is roughly equal to the product of output and input numbers divided by two. Again, these rules of thumb will not always be reliable, but

sometimes a great deal of accuracy would be achieved considering the effect of these changes on other important parts of a network.

2.3.3 Transfer Functions

The activation generation in neural networks is performed by transfer functions in addition to simulating nodes from different layers. There are a variety of transfer function types, but the most widely used ones are Hard-Limit transfer function, which set the function neurons zero if the function argument is less than zero and it is to equal one if the function argument is greater or equal to one. The log-sigmoid transfer function, or Logsig, will take the neuron, which can be any number, and convert it in a zero to one range data. This transfer function is widely used in multilayer backproppagation network. The other common function is called Hyperbolic Tangent Sigmoid or briefly known as Tansig, which is a powerful function along with Purelin (a linear function mostly designated for output layer). The complete list of different types of transfer functions used in neural networks is shown in the Figure 5 on the next page with schematic structures and specific signs.

The selection of the transfer function can be a critical factor especially when the number of the hidden layers increases. In general, transfer function selection of a network is based on trial and error. It is not surprising that similar networks have embedded different types of transfer functions and have yielded close results to the favorite target.

Name	Input/Output Relation	Icon	MATLAB Function
Hard Limit	$a = 0 \quad n < 0$ $a = 1 \quad n \geq 0$		hardlim
Symmetrical Hard Limit	$a = -1 \quad n < 0$ $a = +1 \quad n \geq 0$		hardlims
Linear	$a = n$		purelin
Saturating Linear	$a = 0 \quad n < 0$ $a = n \quad 0 \leq n \leq 1$ $a = 1 \quad n > 1$		satlin
Symmetric Saturating Linear	$a = -1 \quad n < -1$ $a = n \quad -1 \leq n \leq 1$ $a = 1 \quad n > 1$		satlins
Log-Sigmoid	$a = \frac{1}{1 + e^{-n}}$		logsig
Hyperbolic Tangent Sigmoid	$a = \frac{e^n - e^{-n}}{e^n + e^{-n}}$		tansig
Positive Linear	$a = 0 \quad n < 0$ $a = n \quad 0 \leq n$		poslin
Competitive	$a = 1$ neuron with max n $a = 0$ all other neurons		compet

Figure 5 Table of all transfer functions used for artificial neural network

2.3.4 Learning and Training algorithm

The learning rule in which the weight and bias for the network are properly determined is known as training algorithm. Generally the data set would be divided into three parts: training set, validating set and testing sets. Training set would usually contains the majority parts of the data since the training process is the core part of the network. The training set is the one the network attempts to establish , check and compute the nodes in layers. On the other hand, it is important to have separate training, validation and testing sets without overlap or known as blind set, so the network can be tested against the testing set without the mutually observed nodes.

The decreasing error in training and testing sets is a good sign noting that the network is training itself. Once the learning is being conducted successfully, the training rate would be larger in order to gain more nodes and neurons trained. If the error fluctuates with high training rate, then the network is forgetting while training. The optimum training rate is the one where the network has a steady decrease in error. If the error in the test data is still considerably high despite the fact that the training sets' error is low, the training network has reached its best results and training the network beyond this point would be unnecessary. This undesirable condition happens if the data set chosen for training has some flaws or the range is out of limited criteria (I.A Basheer, 2000).

If the error in both training and testing data decreases but does not reach a desirable error, the training cannot be resumed and should be stopped accordingly. After a certain point, the training and testing curves would split and cause the network to memorize the data sets rather than to learn. The preferred solution to this problem is to introduce new hidden layers and increase the number of neurons.

Training algorithms or learning rules are important for the success of the network because of conducting task such as weight initialization; computation order management and algorithms entities. There are many types of algorithms in different ANN tools. For the MATLAB toolbox, few algorithms are introduced and among them, the most common ones are scaled such as conjugate gradient or `Trainscg`, conjugate gradient or `Traincgb`, resilient propagation or `Trainrp`, Bayesian regularization or `Trainbr` and Levenberg-Marquardt or `Trainlm`.

Chapter 3 Problem Statement

Production prediction is a critical issue for the implementation of oil and gas projects that require investments. Many companies would like to spend their capital on the projects that return cash that far surpasses the cost. The idea of Net Present Value (NPV) and cash flow in the oil and gas industry are dependent on factors such as total production, oil and Gas price, market challenges, etc. Some of these factors can be controlled while the others are difficult to handle. It is obvious that in a reasonably high gas price, production increase would bring fortune to investors in addition to the demand and supply situation.

It is important to estimate the profit for any investment. In the energy sector, particularly for oil and gas, the production forecasting is a key to boost the economy. To estimate or forecast the production, there have been many models suggested and for the majority of them, certain types of data are necessary to be taken from the field. Data collected from rock samples, seismic survey, well testing operation and well logging is conventional types of practices in in-situ experiments. For simulators, all the mentioned data should be used to acquire an efficient model for production and rate of delivery. The considerable amount of time consumed to develop a model using simulators, which can be costly, is not very efficient therefore numerical reservoir simulators cannot be very reliable. Moreover, models created by simulators often face difficulty giving reliable data since the uncertainty and other external factors affect the quality of the prediction.

ANN has been tested and approved as a strong tool to predict variables with satisfying results. Basically, artificial neural network as an intelligent expert system tries to mimic the relationship among different variables and predict or provide the behavior of system with low

prediction error. In this study and by using MATLAB, the ANN has been trying to mimic the data generated by CMG-CMOST simulator and its results will be compared to that of simulator. The reservoir has been simulated using the CMG-Builder and the gas rate and cumulative productions have been estimated using CMG-IMEX in both tables and graphs based on data generated for well design and reservoir parameters.

Reservoir parameters include horizontal and vertical permeability, porosity, layer thickness and initial reservoir pressure for a multilayered reservoir. The well design consists of drainage area and bottom hole pressure specifically. Generally, there are two wide common ways to perform well test analysis on a reservoir. One is pressure transient analysis which monitors the pressure by having gas rate as a constant value. Consequently, by fixing the pressure, we can monitor gas rate and that is our goal: to create a tool as a rate transient analysis. Once the reservoir and well design data ranges given to the simulator, all data including reservoir properties and production profile are generated and extracted. Until now, all of the production data and other properties have been generated using the simulator. Using MATLAB to design artificial neural network, the reservoir parameters and well parameters were put as input as well as the production profile.

By training the ANN, the tool will start mimicking data and find complex relationships among variables. The time needed to complete the training depends on structure type consisting of epochs, layers, neurons and error tolerance. In this step the production data generated by the simulator and the data from trained ANN will be compared. The calculated error or regression is a major factor to determine whether the ANN could be able to forecast properly and whether it is reliable. If it is not reliable, this may be indicative of the need for modification. This solution type is called the forward ANN while the second solution type is called the inverse ANN. In

inverse reservoir properties, the goal is to obtain reservoir parameters by using well design and a production profile from the simulator. The third solution part is called inverse II ANN or inverse well design which predicts well design, provided that reservoir parameters and production profile are known and have been fed to network.

Chapter 4 Generation of training sets

The reservoir model is built using CMG-IMEX in a Cartesian grid system, helps to generate the data for the reservoir and well design parameters and production profile. Production profile data have been stored in two separated text files: one for gas rate and the other for cumulative production for covering data for 15 years study. Afterwards, parameters have been tested in both forward and inverse modes.

The assumptions considered for this model are as follows:

- ❖ Homogeneous and isotropic reservoir
- ❖ One vertical well only in the center of the drainage area
- ❖ Dry gas reservoir
- ❖ Single porosity
- ❖ Gravity effect is negligible
- ❖ The well perforated fully in the reservoir layers
- ❖ Rate transient analysis under specific bottom hole pressure
- ❖ Total production period of 15 years
- ❖ Constant reservoir temperature

4.1 Grid Blocks Sensitivity Analysis

Grid blocks can be a factor in enhancing numerical simulator and help improve the model efficiency. It is obvious that the larger the block sizes, the less accurate the model can be created compared to the model of a smaller block size. The smaller grid size models are not necessarily preferable. It is about the balance and when the size shrinks, the simulator consumes more time to compute all the properties assigned into each block of the reservoir especially if the drainage area is large.

As mentioned earlier, the purpose behind using ANN is to save both time and money. Therefore, a sensitivity analysis is performed to select the optimum grid size in which the balance between time and accuracy can be reached. The concept here is to compare the generated production profiles proportioned to their grid size. To understand the relationship between grid size and production profile, Figure 6 has been prepared for this purpose. The production curves (cumulative production) have been generated based on the number of blocks. In this practice, the number of blocks increases until the cumulative production differences proportionate to two consequent numbers of blocks are negligible. According to the figure, for the reservoir of 50*50 blocks, the optimum block size was chosen to be 93 ft.

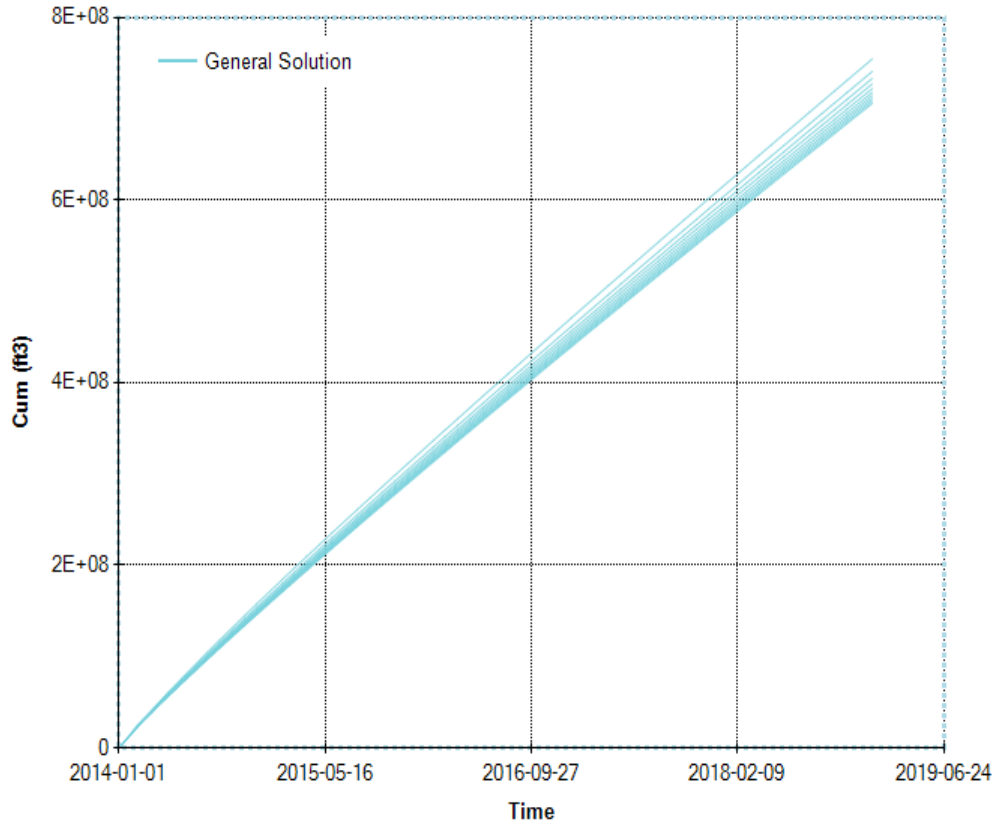


Figure 6 Cumulative production curves plotted with different grid blocks

Table 1 Random grid block size for the reservoir

No of blocks	Grid block size
100	46.66905
90	51.8545
80	58.33631
70	66.67007
60	77.78175
50	93.3381
40	116.6726
30	155.5635
20	233.3453
10	466.6905

4.2 Range of reservoir parameters

As mentioned earlier, in order to generate the data that will be used for production profile, a range of data is assigned to each variable using CMG_CMOST. These data have been extracted from different reservoir perspectives to be used to create a homogeneous and isotropic model. The study period in which the study has been performed is 15 years and during this period the production rate and cumulative production will be recorded and compared with the ANN data to estimate the prediction success.

Feed forward solution is the tool which provides the production profile based on reservoir parameters and well design data. To obtain reservoir parameters, well design parameters along with production rate and cumulative production are needed, but first of all we need to generate synthetic data that can be used as reservoir parameters. We do this by assigning each reservoir parameter a range to generate a set of data. In this study we utilized 600 sets of data. To address the rate transient analysis, the bottom hole pressure was put to a constant value for each run with 600 different values among all runs. The table below illustrates the ranges for generating the entries of data sets.

Table 2 Parameters range for the reservoir

Parameters	Symbol	Minimum	Maximum	Unit
Horizontal Permeability	k	0.1	5	md
Vertical permeability	k_v	.001	0.1*k	md
Porosity	ϕ	7	20	%
Initial Reservoir Pressure	p_i	2000	8000	psi
Thickness	h	20	100	ft.
Reservoir Temperature	T	200		F
Depth	D	9000		ft.

4.3 Well design parameters

The model in this study is a gas reservoir consists of horizontal multilayers and the first scenario starts with two-layered reservoir then three and four-layered systems will be modeled. The well drainage area is changing while the well is kept in the center. The well designed in this model is a producing well with constant bottom hole pressure since we study the rate transient analysis to observe the production rate over limited time. To predict the well design, the inverse solution has been used in which the production profile and reservoir parameters are recorded to obtain the unknowns (bottom hole pressure and drainage area).

The bottom hole pressure in this study for all 600 data sets ranges from 15 percent to 50 percent of the initial reservoir pressure. In order to obtain production rate, sandface pressure has been kept constant. To develop an expert tool which enables us to forecast how many wells are needed to meet future production from a region, the drainage area has been added to the tool to acquire the estimation of the drainage area for each well and likewise number of wells required for the whole allocated area. In an attempt to predict the total numbers of well for a project, the well design parameters is a useful tool to assess the drainage area which will be used for identifying number of wells. Simply by having production data and some reservoir properties, the well design ANN will predict drainage area where a vertical well will be placed .By dividing the total allocated area over the drainage area, the optimum number of wells needed to meet the production is predicted.

$$\text{Number of wells} = \frac{\text{Total allocated area in acre}}{\text{Drainage area in acre}}$$

The second parameter that is predicted in this network, bottom hole pressure, is specified in which if the well produce in this pressure condition, the production profile provided as input will be achieved. In Table 3 the parameters range for well design ANN have been illustrated.

Table 3 Parameters range for the well

Parameters	Symbol	Minimum	Maximum	Unit
Bottom Hole Pressure	BHP	$0.15* p_i$	$0.5* p_i$	psi
Reservoir drainage area	A	80	500	acre

Chapter 5 Artificial Neural Network development

Once all the training data have been generated using CMG simulator, it is time to develop the ANN to assess the prediction. The ultimate goal of this model is to forecast the cumulative production and production rate in addition to the well design and the reservoir parameters. MATLAB has been used to develop the neural network modified by each scenario's inputs and outputs. The inputs needed to train the network are extracted from CMG_CMOST.

5.1 Artificial Neural network design

The tool to predict production profile of a well is called the forward neural network in which the inputs are two files of cumulative production and production rates along with the third file consists of reservoir parameters and well design. The network data set inside ANN has been divided into three sets of training, validating and testing sets. Of the 600 data sets, 90 percent or 540 data sets have been assigned to be used as training sets and 5 percent of that, equal to 30 data sets, devoted to validation test in addition to the 5 percent or 30 data sets for testing sets.

In general, the benefit of having larger sets assigned to training would trigger the training enhancement where the majority part of the whole data sets will be trained and then tested only with the other 30 data sets that have not been introduced to the training. It is very important to test the network after completion of the training and validation. It is imperative to test the network with blind data set or the data out of training set to show that the network has strong ability of obtaining relationships between parameters of any kind. There have been studies on the selection of number of data sets for each three partitions but for higher accuracy the training sets have been increased.

The structure of the network has many important parts such as hidden layers, number of neurons, transfer function, and training algorithm. All of the mentioned parts are decisive and will effectively enhance the network efficiency which lead to optimum utilization of system. Functional links have been used repeatedly in this network group because of its high efficiency and influence on the training. Functional link is a mathematical relationship between various data to relate these data while the network has been put into training. There is no absolute rule for selecting functional links and it is implemented by trial and error. The number of functional links and their mathematical format are mostly based on specified acceptable error.

There are some networks that will only require few functional links while the others may need at least 20 or more. Generally, the method of utilizing functional links is to combine all the parameters with less error (easily predictable by network) with other variable to enhance the network productivity. The nodes in the layers will most probably link the variables better with other strong related parameters when they are linked together. Scaling is another factor powering the network. This practice will use mathematical functions to interpret the data to a new set of data which will be ranged in a different scale to help the network provide a better correlation. For instance, logarithmic values of initial reservoir pressure or permeability have been taken. Similarly, a multiplier of 1/100 is applied to thickness. Thickness can be obtained from well logs, well testing and seismic data and in order to provide a strong model with powerful prediction, thickness has been removed from output for inverse solution and only presented in the input of the forward solution.

5.2 Multilayered neural network development

5.2.1 Two-layered reservoir network

In the two-layered reservoir, the simplest network in this study, reservoir properties distributed to two-layereds and the vertical well has been perforated along these two-layereds completely. In this network there are five reservoir parameters in addition to two well design parameters. Gas rate and cumulative production value have been read on days 1, 10, 15, 20, 30, 45, 60, 80 and then on every three months interval until the end of production period which in total adds up to 30 values .

5.2.1.1 Forward artificial Neural network

In forward ANN , the five reservoir parameters along with two well design parameters are inputs while the 30 data sets of each consisting 30 values of cumulative production and production rates are unknowns. Thickness of layers have been used as input only in the forward ANN. Table 4 refers to the properties used for the forward solution.

Table 4 Forward network's inputs and outputs for two-layered system

	Two-layered reservoir	Unit
Input	Horizontal permeability (K_1, K_2)	md
	Vertical permeability (K_{v1}, K_{v2})	md
Reservoir parameters	Porosity (ϕ_1, ϕ_2)	%
	Thickness (h_1, h_2)	ft.
	Reservoir Initial pressure, p_i	Psi
Input Well design	Bottom Hole Pressure, BHP	Psi
	Reservoir Drainage Area	acre
Output	Gas rate Reading of days 1, 10,15,20,30,45,60,80 and 22 more readings from day 80 for each 3 month interval	SCF/day
	Cumulative gas production Reading of days 1, 10,15,20,30,45,60,80 and 22 more readings from day 80 for each 3 month interval	SCF

Functional links, as mentioned earlier have been used in all networks based on the complexity and integrity of the scenario and will contribute to a better results for the network. Table 5 consists of links that have been used in a two-layered reservoir network. In fact, bottom hole pressure and initial reservoir pressure have the most influence on the production of the reservoir, therefore the network will have less difficulty forecasting these parameters. The best way to select functional links is to link the least difficult predicted parameters to the most strong and effective data and as shown in Table 5, most of the links include one of the bottom hole pressure (BHP) or initial reservoir pressure(p_i).

Table 5 Forward network's functional links for two-layered system

Functional links	$K_1 \cdot h_1, \text{Log}(\text{BHP}^{.35}), \text{Log}(K_1^{.65}), \text{Log}(L^{.1.5}),$ $\text{Log}(h_2^{.2.7}), (\text{Log}(k_2^{.55})), (k_{v1}) \cdot (\text{Log}(h_2)) / \phi_1,$ $(k_{v2} \cdot \phi_2), (K_{v1})^{.2}, (K_{v1}) \cdot \log(\text{BHP}),$ $(\phi_1) \cdot (\log(p_i)) / \text{Log}(k_{v1}), (k_{v4} \cdot \phi_1) / (\log(L))$ $\text{Log}(p_i / K_{v1}), \text{Log}(\text{BHP} \cdot K_{v2})$
------------------	---

5.2.1.2 Inverse well design artificial neural network

In an inverse well design in which the reservoir parameters are known as inputs along with production rate and cumulative to predict the well design, bottom hole pressure and drainage area are unknowns and will be compared with simulator results to assess the accuracy of the network results. Seven parameters from reservoir and 30 data sets from each production rate and cumulative production have been set into the network.

This model can predict whether there is formation crossflow by having vertical permeability less than or equal to 0.01 md.

Table 6 Inverse well design network's inputs and outputs for two-layered system

	Two-layered reservoir	Unit
Input Reservoir parameters	Horizontal permeability (K_1, K_2)	md
	Vertical permeability (Kv_1, Kv_2)	md
	Porosity (ϕ_1, ϕ_2)	%
	Reservoir Initial pressure, pi	Psi
Input Production profile	Gas rate Reading of days 1, 10,15,20,30,45,60,80 and 22 more readings from day 80 for each 3 month interval	SCF/day
	Cumulative gas production Reading of days 1, 10,15,20,30,45,60,80 and 22 more readings from day 80 for each 3 month interval	SCF
Output Well design	Bottom Hole Pressure, BHP	Psi
	Reservoir Drainage Area	acre
Input Functional links	$(BHP.^{.5})$	
	$(Kv1.^{.2})$	
	$Kv2.*\log(\phi_1)$	
output Functional links	$\log(BHP)./(Kv1)$	
	$\log(Pi.*Kv2)$	
	$\log(Pi).*(K2)$	

The functional links in this network have been presented in both inputs and outputs to enhance the network recovery and relate the weak inputs and outputs to strong ones such as initial reservoir pressure and bottom hole pressure.

5.2.1.3 Inverse reservoir parameters Artificial Neural Network

In inverse ANN with well design and production rate and cumulative production as input, the reservoir parameters are unknown and we are trying to obtain them from the inverse solution. In this network which is more complex comparing to previous networks, the number of functional links has increased to obtain satisfying error. The number of unknowns (reservoir parameters) is seven and will be compare to the simulator results after the network has been trained to assess the accuracy.

Table 7 Inverse reservoir parameters network's inputs and outputs for two-layered system

	Two-layered reservoir	Unit
Input Production profile	Gas rate Reading of days 1, 10,15,20,30,45,60,80 and 22 more readings from day 80 for each 3 month interval	SCF/day
	Cumulative gas production Reading of days 1, 10,15,20,30,45,60,80 and 22 more readings from day 80 for each 3 month interval	SCF
Input Well design	Bottom Hole Pressure, BHP	Psi
	Reservoir Drainage Area	acre
Output Reservoir parameters	Horizontal permeability (K_1, K_2)	md
	Vertical permeability (K_{v1}, K_{v2})	md
	Porosity(ϕ_1, ϕ_2)	%
	Reservoir Initial pressure, Pi	Psi
Input Functional links	$(K_{v1}^{.5}), (K_{v2}^{.2}); (K_{v1}^{.2}); (K_2^{.2}); (k_1) \cdot \log(\text{BHP}),$ $(K_2 \cdot (\log(\text{Pi})) / K_{v1}); (\phi_2 \cdot k_2) / (L),$ $(k_{v2} \cdot K_2) / (\log(\text{BHP})), \log(\text{BHP}^{.35}); \log(\text{Pi}^{.65}); \log(L^{.1.5}),$ $(K_{v1} \cdot \phi_1); (k_{v1}) \cdot \log(\phi_2) / \log(\text{Pi}),$ $(\text{Pi}) \cdot \log(K_2); (K_{v1}) \cdot \log(\text{BHP}); (K_{v2}) \cdot \phi_2,$ $(K_1) \cdot \log(\text{BHP}); ((K_1 \cdot \text{Pi})) / (K_{v2})$	
output Functional links	$\log(K_1) / \text{BHP}, \log(\text{BHP}) / (K_{v1}), \log(\text{Pi}) / (K_{v2}),$ $\text{Log}(K_1 \cdot \phi_1); (\phi_2) \cdot (K_2), (K_2) \cdot (\log(L)), \log(\text{BHP}) \cdot (K_2); \dots$ $\text{Log}(K_{v1} \cdot (\text{BHP})); \log(K_{v2}) \cdot (\text{Pi}); (K_{v2}) \cdot (\phi_1) / (K_1); \dots$ $\log(K_{v1}) \cdot (K_2); (K_{v2}^{.5}); (K_{v1}^{.5})$	

5.2.2 Three-layered reservoir network

In a three-layered reservoir, three layers constitute the reservoir and the vertical well has been perforated along these three layers completely. In this system there are 13 reservoir parameters in addition to two well design parameters. The 30 values of each production rate and cumulative production have been presented as well.

5.2.2.1 Forward artificial Neural network

In forward ANN, the 13 reservoir parameters along with two well design are inputs while the 30 values of cumulative production and production rates are unknowns. Thickness of layers have been the input but will not be present in the inverse section.

Table 8 Forward network's inputs and outputs for three-layered system

	Three-layered reservoir	Unit
Input Reservoir parameters	Horizontal permeability (K_1, K_2, K_3)	md
	Vertical permeability (K_{v1}, K_{v2}, K_{v3})	md
	Porosity (ϕ_1, ϕ_2, ϕ_3)	%
	Thickness (h_1, h_2, h_3)	ft.
	Reservoir Initial pressure, P_i	Psi
Input Well design	Bottom Hole Pressure, BHP	Psi
	Reservoir Drainage Area	acre
Output	Gas rate Reading of days 1, 10,15,20,30,45,60,80 and 22 more readings from day 80 for each 3 month interval	SCF/day
	Cumulative gas production Reading of days 1, 10,15,20,30,45,60,80 and 22 more readings from day 80 for each 3 month interval	SCF

5.2.2.2 Inverse well design Artificial Neural Network

In an inverse well design in which the reservoir parameters were defined as input along with production rate and cumulative to predict the well design, bottom hole pressure and acreage are unknowns and will be compared with the simulator to assess the accuracy of the network results. In Inverse tool, k_v or vertical permeability has been computed to state the communication between the layers within single reservoir. Vertical permeability less or equal 0.01 is assumed to be zero therefore the commingled system is suggested.

Table 9 Inverse well design network's inputs and outputs for three-layered system

	Three-layered reservoir	Unit
Input Reservoir parameters	Horizontal permeability (K_1, K_2, K_3)	md
	Vertical permeability (K_{v1}, K_{v2}, K_{v3})	md
	Porosity (ϕ_1, ϕ_2, ϕ_3)	%
	Reservoir Initial pressure, P_i	Psi
Input Production profile	Gas rate Reading of days 1, 10,15,20,30,45,60,80 and 22 more readings from day 80 for each 3 month interval	SCF/day
	Cumulative gas production Reading of days 1, 10,15,20,30,45,60,80 and 22 more readings from day 80 for each 3 month interval	SCF
Output Well design	Bottom Hole Pressure, BHP	Psi
	Reservoir Drainage Area	acre
Input Functional links	$(BHP.^{.5})$	
	$(K_{v1}.^{.2})$	
	$K_{v2}.*\log(\phi_1)$	
	$(K_{v3}.*\log(L))./(\log(BHP))$	
	$(\log(L).*\log(P_i))./(K_2)/100$	
	$\log(K_1).*((BHP))./(K_{v1})$	
Output Functional links	$\log(P_i)./(K_{v2})$	
	$\log(P_i)./(K_{v3})$	

As the number of layers increases, the network complexity will increase. The best strategy to minimize the error and improve the network efficiency is to increase the functional links and number of hidden layers.

5.2.2.3 Artificial Neural Network inverse reservoir parameters

In this case, the numbers of unknowns are 10 and the inputs are well design parameters (BHP and Drainage Area) in addition to 30 data of production rate and 30 data of cumulative production. Table 10 shows the parameters as inputs and outputs.

Table 10 Inverse reservoir parameters network's inputs and outputs for three-layered system

	Three-layered reservoir	Unit
Input Production profile	Gas rate Reading of days 1, 10,15,20,30,45,60,80 and 22 more readings from day 80 for each 3 month interval	SCF/day
	Cumulative gas production Reading of days 1, 10,15,20,30,45,60,80 and 22 more readings from day 80 for each 3 month interval	SCF
Input Well design	Bottom Hole Pressure, BHP	Psi
	Reservoir Drainage Area	acre
output Reservoir parameters	Horizontal permeability (K_1, K_2, K_3)	md
	Vertical permeability (K_{v1}, K_{v2}, K_{v3})	md
	Porosity(ϕ_1, ϕ_2, ϕ_3)	%
	Reservoir Initial pressure, P_i	Psi
Input Functional links	$(K_{v1}^{.5}), (K_{v2}^{.2}); (K_{v1}^{.2}); (K_2^{.2}); (\phi_1) \cdot \log(\text{BHP}),$ $(K_{v3} \cdot (\log(L)) / K_{v1}); (\phi_2 \cdot k_2) / (L),$ $(k_{v2} \cdot K_2) / (\log(\text{BHP})), \log(\text{BHP}^{.35}); \log(P_i^{.65}); \log(L^{.15}),$ $(K_{v1}) \cdot \phi_1; (k_{v1}) \cdot \log(\phi_2) / \log(P_i),$ $(P_i) \cdot \log(K_2); (K_{v1}) \cdot \log(\text{BHP}); (K_{v2}) \cdot \phi_2,$ $(K_{v2}) \cdot \log(\text{BHP}); ((K_2 \cdot K_{v1})) / (\text{BHP})$	
output Functional links	$\log(K_1) / K_{v1}, \log(K_{v2}) / (\text{BHP}), \log(P_i) / (K_{v3}),$ $\text{Log}(K_3 \cdot \phi_1), (\phi_2) \cdot (K_2)$	

5.2.3 Four-layered reservoir network

In the four-layered reservoir, all the four layers have been perforated completely. In this system there are 17 reservoir parameters in addition to two well design parameters. The 30 values of each production rate and cumulative production have been generated as well.

5.2.3.1 Forward Artificial Neural Network

In this network, the highest complexity and accordingly highest error compared to other networks concluded due to the increase in reservoir layer. The increase in number of layers have led the network inputs content to increase up to 17 properties, 5 more than the previous three-layered network. Using proper functional links and structure optimization is the key to satisfy the target.

Table 11 Forward network's inputs and outputs for four-layered system

	Four-layered reservoir	Unit
Input Reservoir parameters	Horizontal permeability (K_1, K_2, K_3, K_4)	md
	Vertical permeability (Kv_1, Kv_2, Kv_3, Kv_4)	md
	Porosity ($\phi_1, \phi_2, \phi_3, \phi_4$)	%
	Reservoir Initial pressure, P_i	Psi
	Thickness (h_1, h_2, h_3, h_4)	ft.
Input Well design	Bottom Hole Pressure, BHP	Psi
	Reservoir Drainage Area	acre
Output	Gas rate Reading of days 1, 10,15,20,30,45,60,80 and 22 more readings from day 80 for each 3 month interval	SCF/day
	Cumulative gas production Reading of days 1, 10,15,20,30,45,60,80 and 22 more readings from day 80 for each 3 month interval	SCF

5.2.3.2 Inverse well design Artificial Neural Network

The thickness has been removed from the network. For the inverse well design in which the reservoir parameters were defined as the input along with production rate and cumulative gas values to predict the well design, bottom hole pressure and acreage are unknowns and will be compared with the simulator's results to assess the accuracy of the network results.

Table 12 inverse well design network's inputs and outputs for four-layered system

	Four-layered reservoir	Unit
Input Reservoir parameters	Horizontal permeability (K_1, K_2, K_3, K_4)	md
	Vertical permeability ($K_{v1}, K_{v2}, K_{v3}, K_{v4}$)	md
	Porosity ($\phi_1, \phi_2, \phi_3, \phi_4$)	%
	Reservoir Initial pressure, P_i	Psi
Input Production profile	Gas rate Reading of days 1, 10,15,20,30,45,60,80 and 22 more readings from day 80 for each 3 month interval	SCF/day
	Cumulative gas production Reading of days 1, 10,15,20,30,45,60,80 and 22 more readings from day 80 for each 3 month interval	SCF
Output Well design	Bottom Hole Pressure, BHP	Psi
	Reservoir Drainage Area	acre
Input Functional links	$(K_{v4} \cdot \phi_1)^{0.5}$	
	$(K_{v1} \cdot \phi_1)^2$	
	$K_{v2} \cdot \log(\phi_1)$	
Output Functional links	$\log(\text{BHP}) / (K_{v1})$	
	$\log(\text{BHP} / K_{v1})$	
	$\log(P_i) / (K_4)$	

5.2.3.3 Inverse reservoir parameters Artificial Neural Network

In this network, the number of unknowns are 13 and the inputs are well design parameters (BHP and drainage area) in addition to 30 data points of production rate and 30 data points of cumulative production. In this section, 13 parameters are unknown and 60 data from the production profile with two well design parameters such as bottom hole pressure and drainage area considered as the inputs. Obviously due to the complexity of the network, the large number of functional links have been utilized.

Table 13 Inverse reservoir parameters network's inputs and outputs for a four-layered system

	Four-layered reservoir	Unit
Input Production profile	Gas rate Reading of days 1, 10,15,20,30,45,60,80 and 22 more readings from day 80 for each 3 month interval	SCF/day
	Cumulative gas production Reading of days 1, 10,15,20,30,45,60,80 and 22 more readings from day 80 for each 3 month interval	SCF
Input Well design	Bottom Hole Pressure, BHP	Psi
	Reservoir Drainage Area	Acre
Input Reservoir parameters	Horizontal permeability (K_1, K_2, K_3, K_4)	md
	Vertical permeability (Kv_1, Kv_2, Kv_3, Kv_4)	md
	Porosity ($\phi_1, \phi_2, \phi_3, \phi_4$)	%
	Reservoir Initial pressure, P_i	Psi
Input Functional links	$(\phi_4.^{.2.7}), (\phi_1.^{.1.7}) (Kv1.^{.5}), (Kv2.^{.2}), (Kv1.^{.2}), (K2.^{.2}),$ $(k1).^{\log(Pi)}$ $(K4.^{\log(BHP)})/Kv1), (\phi_2.^{k2})/L)$ $(kv2.^{K2})/(\log(BHP)), \log(BHP.^{.35}), \log(Pi.^{.65}), \log(L.^{1.5})$ $(Kv1).^{\phi_1}, (kv1).^{\log(\phi_2)}/\log(Pi)$ $(Pi).^{\log(K2)}, (Kv1).^{\log(BHP)}, (Kv2).^{\phi_2}$ $(K1).^{\log(BHP)}, ((K1.^{Pi}))/BHP)$	
Output Functional links	$\log(K1)/Kv1), \log(BHP)/(Kv2)), \log(Pi)/(Kv3),$ $\text{Log}(K3).^{\phi_1}), (\phi_2).^{K2}), (K2).^{\log(L)}, \log(BHP).^{\phi_3}$	

5.3 Graphical User Interface (GUI)

In order to facilitate the user accessibility to this model, Graphical User Interface has been introduced within MATLAB to illustrate the data contributed to inputs and outputs. There are basically three types of GUI forms based on three different solution types which will be schematically shown in this section. The three types of solutions that resulted in different types of data are as follows:

1. Forward ANN forecasting production profile
2. Inverse forecasting well design parameters
3. Inverse forecasting reservoir parameters

This panel is very easy to use and by inserting sample data for each inputs spots, the network results will be presented. Figure 7 shows the GUI graphic model.

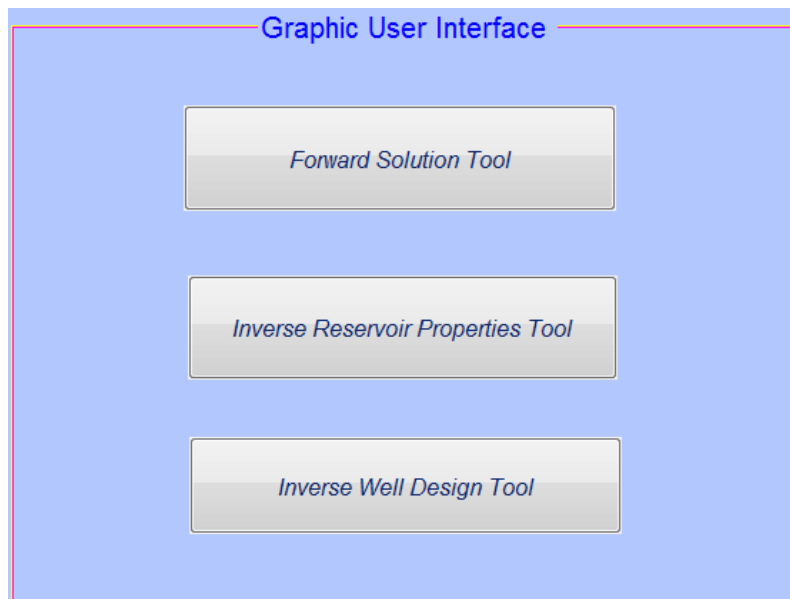


Figure 7 GUI screenshot of three-layered reservoir

5.3.1 Forward ANN forecasting production profile

In this panel, reservoir parameters and well design data will be imported as the inputs. There is a radio button in which by pressing , will bring the results based on inputs as two production curves. Production rate and cumulative production will be graphed over entire production time. Figure 8 presents the forward solution GUI with all data included

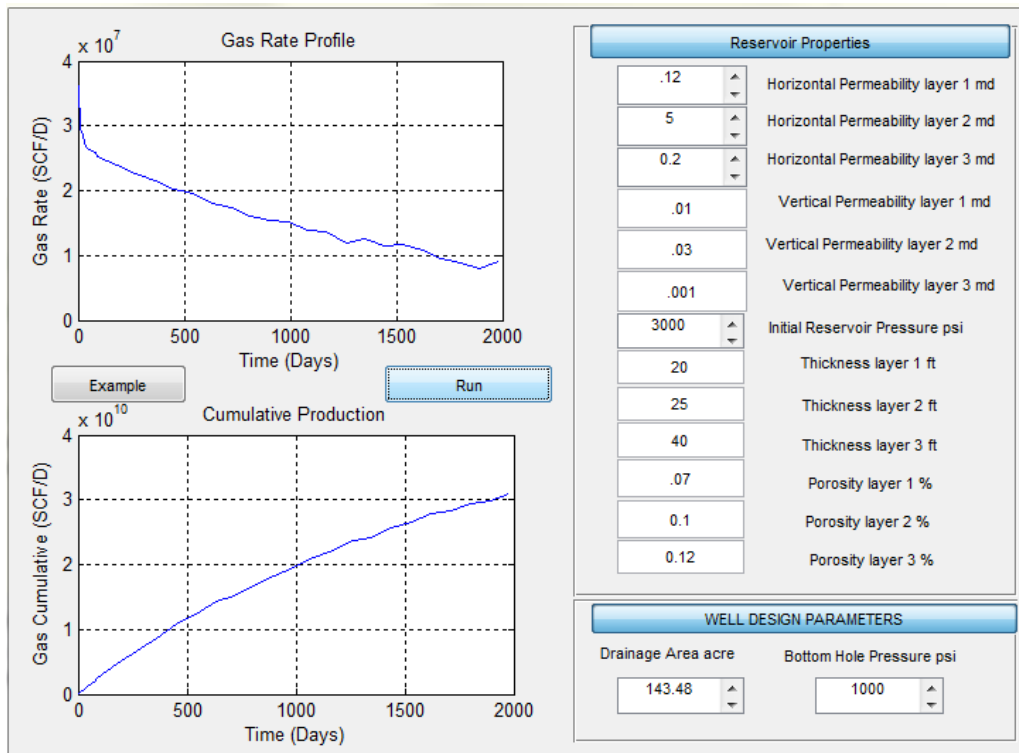


Figure 8 GUI results for forward solution of three-layered reservoir

5.3.2. Inverse forecasting well design parameters

In this section, while the reservoir parameters are known, with the help of production data the well design parameters including bottom hole pressure and drainage area will be predicted and placed in designated box under well parameters panel as shown in Figure 9.

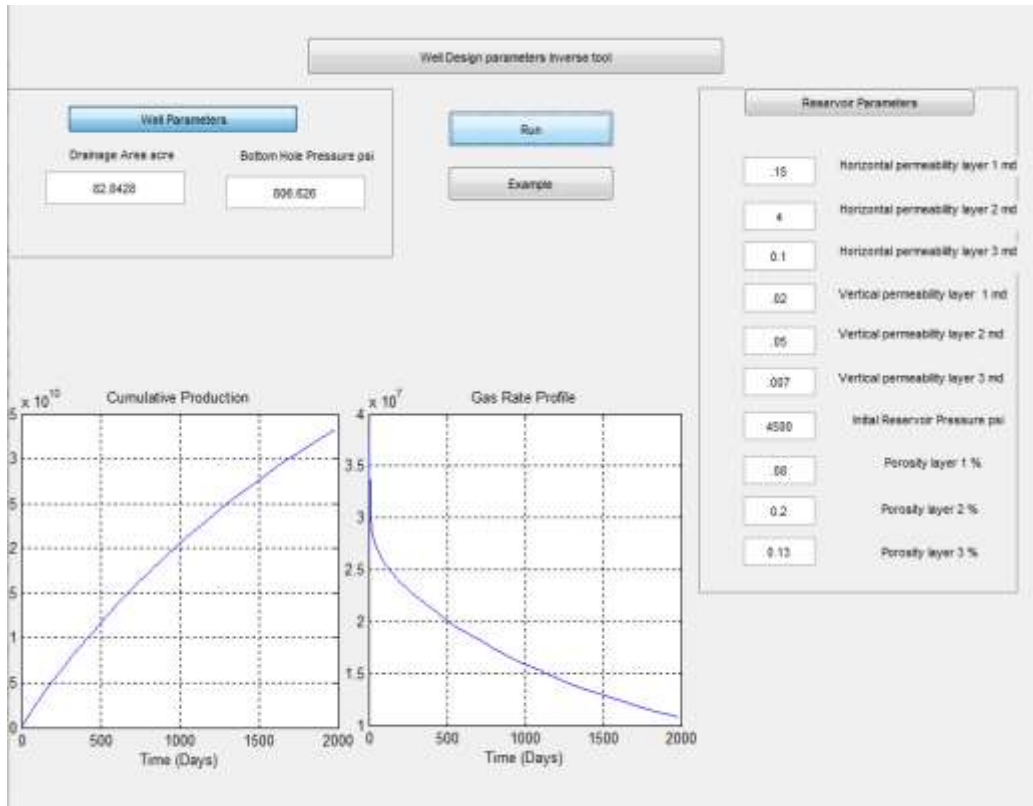


Figure 9 GUI results of well design inverse tool for three-layered reservoir

5.3.3. Inverse forecasting reservoir parameters

In this panel, well design data are known along with production rate and cumulative production (as curves) to predict the reservoir parameters such as horizontal permeability, vertical permeability, porosity,..etc. The reservoir properties appear in designated area in the left side of the Figure 10.

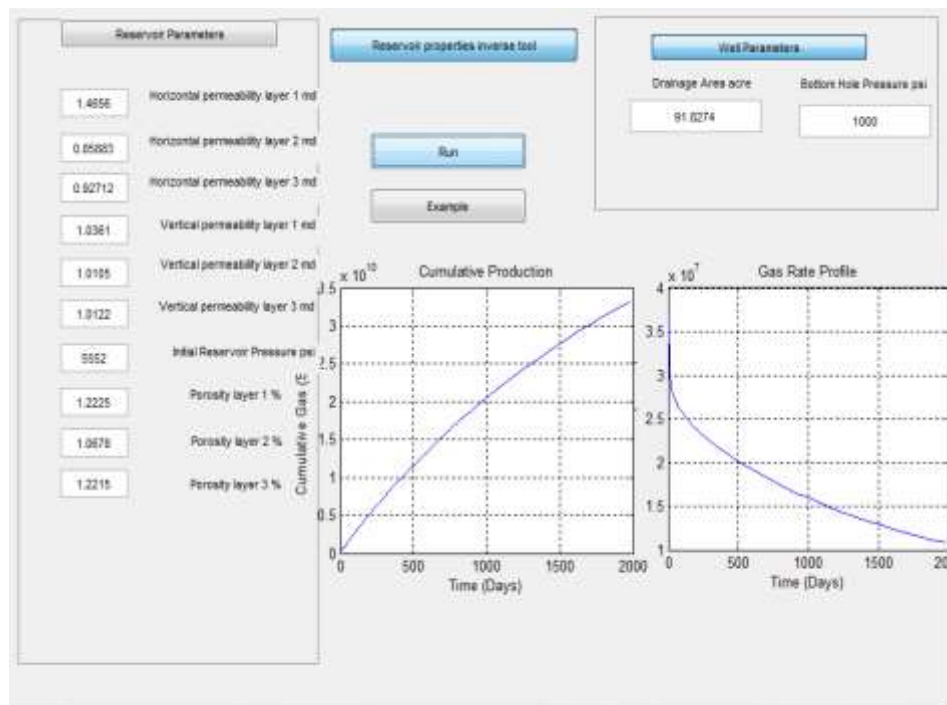


Figure 10 GUI results of reservoir properties inverse tool for three-layered reservoir

Chapter 6 Results and Discussions

In this section, the network results will be reviewed and discussed for three different scenarios such as two-layered system, three-layered system and four-layered system. For each scenario, there are three solution networks starting with Forward ANN which provides production profile and two inverse solutions where the reservoir parameters and well design data will be disclosed respectively.

The measurement for assessing whether the result will be acceptable is mostly performed by the difference between actual data and trained data or will be referred as CMG generated data and ANN generated data. The error between these two sets of data for all scenarios are based on the error and regression. The simple way of calculating error is percentage error and is shown below:

$$\text{Error} = \left| \frac{\text{CMG} - \text{ANN}}{\text{CMG}} \times 100 \right|$$

The important assessment tool for the network is most likely to be the average error. First of all, the error for all parameters have been calculated using simple equation mentioned above. After, all the errors within the data set will be summed then the result will be divided by the number of data points that exist in that data set and the final average error is ready to be presented. In this study, both average error and single data point error have been plotted and presented with maximum and minimum error in each data set.

6.1 Result of two-layered reservoir network Artificial Neural Network

Forward ANN results

As mentioned earlier, 30 values are read for production rate and cumulative production on days 1, 10, 15, 20, 30, 45, 60, 80 and every three months interval for the rest of production time. Five percent of the total 600 data sets have been assigned to testing while 90 percent are used to train the network and the rest are used in validation. Therefore, 30 data sets have been used to estimate and assess the network accuracy. The 30 data sets for each parameters of well design (two parameters for bottom hole pressure and drainage area) and parameters of reservoir (nine parameters including horizontal permeability, vertical permeability, porosity, initial reservoir pressure and thickness) along with 60 data of both production rate and cumulative production have been selected.

Since the network has been optimized as such to provide the best results (least error), the optimum network is identified with specific information including the number of hidden layers and number of neurons of each layer. It is highly recommended to follow the optimum network restrains to achieve the favorable result. The transfer function for all networks is Tansig (for hidden layers) and Purelin (for output layer as linear function) based on the efficiency and satisfying results. The Table 14 and Table 15 show the optimum network results .

Table 14 Forward Two-layered network results

ERROR	AVERAGE CUMULATIVE ERROR				AVERAGE GAS RATE ERROR	
RECOMMENDED NETWORK	1%				3.6%	
Hidden Layer	1	2	3	4	5	6
Neurons	84	86	87	90	89	86

Table 15 Two-layered system production profile error for all 30 values

Average error		1.60%	3.60%	Average error		1.60%	3.60%
No	Run	Error C	Error G	No	Run	Error C	Error G
1	12	2.1	4.6	16	253	1.8	2.5
2	15	1.2	3.7	17	310	1.3	5.5
3	26	0.9	1.6	18	322	3.3	4.6
4	30	0.9	2	19	373	0.8	1.6
5	36	3.2	6.1	20	393	2.1	1.9
6	52	0.8	2	21	433	2.9	7.5
7	86	0.9	4.2	22	443	1.6	3.4
8	109	3.7	3	23	451	1.8	7.6
9	131	2.4	5.9	24	456	2.3	3.3
10	144	2	5	25	458	0.8	2.3
11	152	0.6	3.3	26	473	0.9	1.4
12	159	1.1	2.4	27	502	0.9	4.2
13	171	1	1.9	28	503	0.8	2.1
14	188	1.2	3	29	554	2.3	2.7
15	221	1.3	5	30	560	3.3	4.2

All the figures starting from figure 11 to Figure 40 indicating the result of ANN and simulator are shown in appendix II .These figures represent all 30 data set for cumulative production on top and gas rate below for 30 values assigned to each. Results of CMG are presented in red circles for gas rate curve and ANN results are in green circles and vice versa according to figures legends. Figure 31 and 32 as example have been shown in the next page.

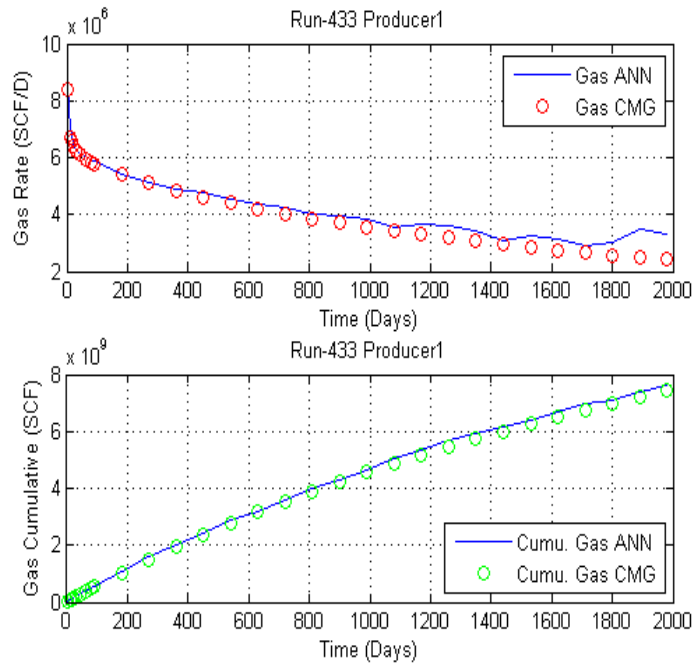


Figure 11 data set 433 of gas rate and cumulative production data of ANN and CMG

Though both CMG and ANN points follow the same trend, the error is increase in the end of intervals for gas rate values.

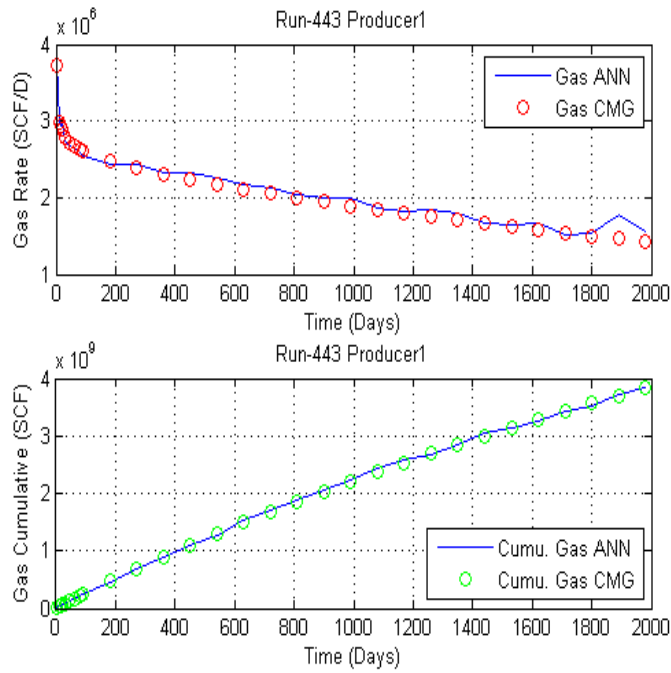


Figure 12 data set 443 of gas rate and cumulative production data of ANN and CMG

Inverse well parameters ANN for two-layered reservoir

In this network, the bottom hole pressure and drainage area were predicted with optimum network design with an average error of 4 and 1 percent respectively. The optimum network consists of two hidden layers with 41 neurons and 42 neurons respectively.

Table 16 Two-layered inverse well design ANN results

PARAMETERS	BOTTOM HOLE PRESSURE AVERAGE ERROR	DRAINAGE AREA AVERAGE ERROR
RECOMMENDED	4%	1%
Hidden Layer	1	2
Neurons	41	42

In Figure 41 and Figure 42 , a pretty good match between CMG and ANN results proves the high accuracy and forecasting potential of this network. Table 17 show the results for both bottom hole pressure and drainage area .

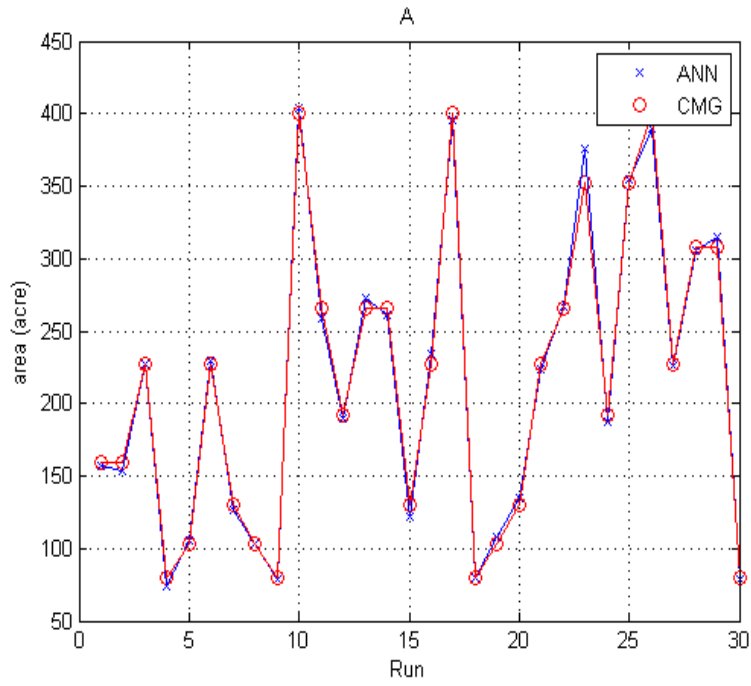


Figure 13 Figure 41 Inverse well design for drainage area

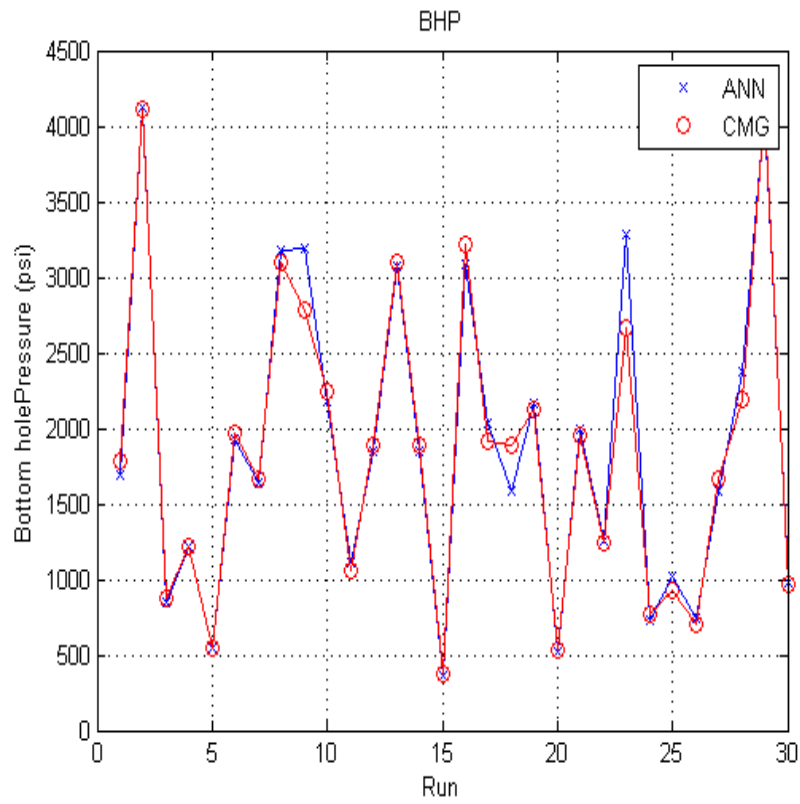


Figure 14 Figure 41 Inverse well design for Bottom hole pressure

Table 17 Inverse well design for two later-reservoir results and error

		ANN		CMG		Error	
No	Run	BHP	Drainage Area(acre)	BHP	Drainage Area(acre)	BHP Error	Drainage Area error
1	28	1693.4	156.8	1788.9	159.5	5.3	0.8
2	32	4122.6	153.9	4111.1	159.5	-0.3	1.8
3	64	855	226.9	881.5	227.6	3	0.1
4	74	1220.7	74.1	1219.8	80.0	-0.1	3.7
5	80	543.3	105.0	545.7	103.5	0.4	-0.7
6	108	1921.2	229.0	1969.2	227.6	2.4	-0.3
7	157	1632.8	126.9	1670.4	130.0	2.3	1.2
8	167	3183.3	102.9	3096.3	103.5	-2.8	0.3
9	190	3191	78.3	2784	80.0	-14.6	1
10	198	2175.8	404.1	2240.8	400.0	2.9	-0.5
11	258	1111	258.9	1063	266.1	-4.5	1.4
12	266	1849.9	189.3	1888.9	192.0	2.1	0.7
13	280	3074.1	273.0	3096.3	266.1	0.7	-1.3
14	362	1851.7	260.6	1888.9	266.1	2	1
15	367	364.2	121.7	377.8	130.0	3.6	3.2
16	370	3089.1	233.9	3222.2	227.6	4.1	-1.4
17	401	2038.2	395.7	1913.6	400.0	-6.5	0.5
18	416	1586.9	80.0	1888.9	80.0	16	0
19	426	2157.9	108.2	2129.6	103.5	-1.3	-2.3
20	468	517.6	134.3	533.3	130.0	3	-1.6
21	469	1999.8	224.0	1955.6	227.6	-2.3	0.8
22	487	1263	266.9	1244.5	266.1	-1.5	-0.1
23	494	3276.8	375.8	2666.7	352.3	-22.9	-3.3
24	509	732.9	187.7	770.4	192.0	4.9	1.1
25	532	1021.7	355.0	922.2	352.3	-10.8	-0.4
26	539	737.6	389.2	700	400.0	-5.4	1.4
27	543	1588.4	226.2	1670.4	227.6	4.9	0.3
28	555	2372.8	305.8	2192.6	307.7	-8.2	0.3
29	569	4080	315.3	4111.1	307.7	0.8	-1.2
30	578	981.6	79.1	966.7	80.0	-1.5	0.5

Inverse reservoir parameters ANN for two-layered reservoir

In this network, seven parameters were predicted with optimum network design with an average error of 1, 5, 4, 10, 1, 1 and 1 percent by below table respectively. The optimum network has five hidden layers and the number of neurons shown in Table 18.

Table 18 Inverse reservoir properties results

PARAMETERS	K1	K2	KV1	KV2	PI	PHI1	PHI2
RECOMMENDED	1%	5%	4%	10%	1%	1%	1%
HIDDEN LAYER	1	2	3	4	5		
NEURONS	95	100	105	96	98		

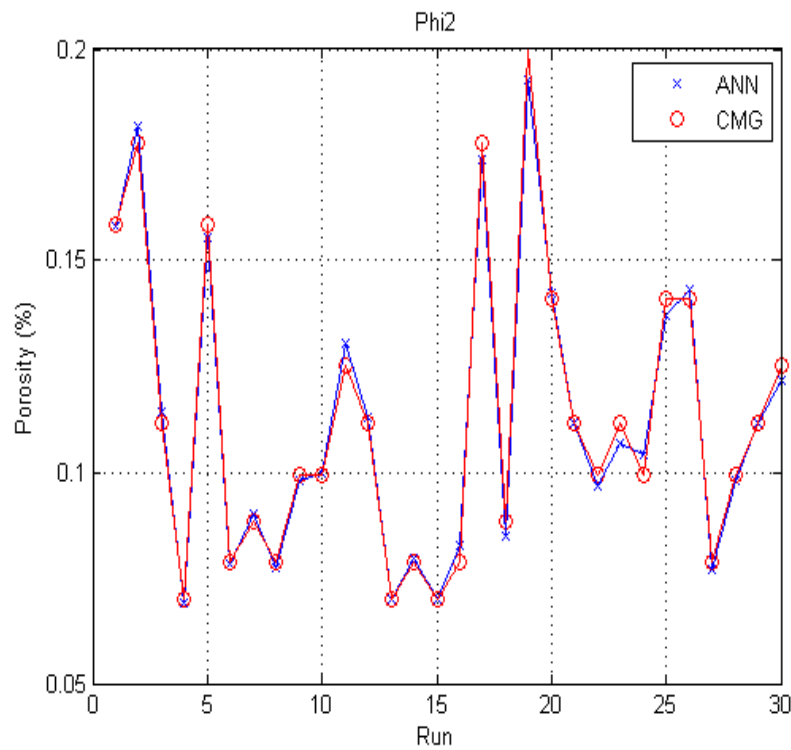


Figure 15 Inverse porosity results for CMG and ANN

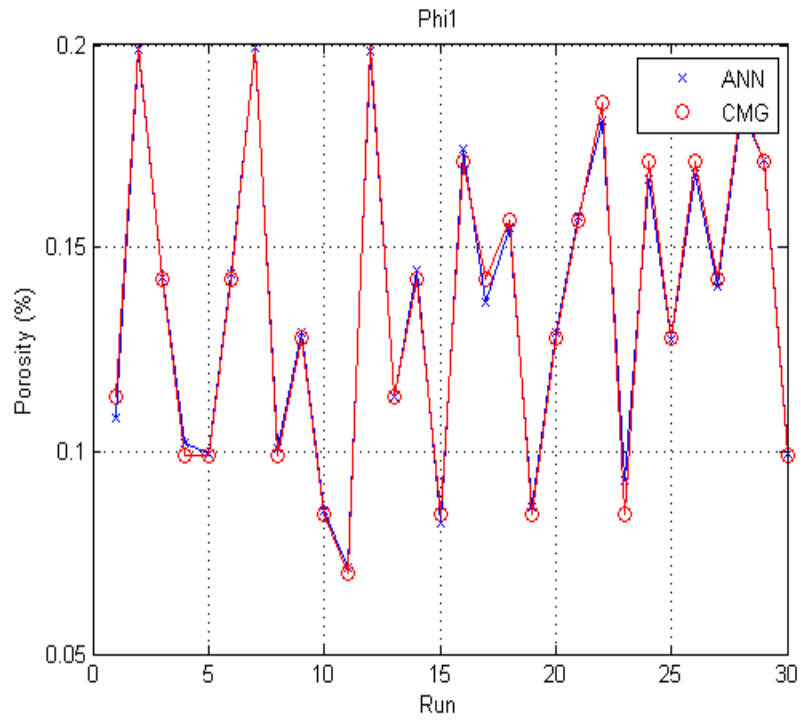


Figure 16 Inverse porosity results for CMG and ANN

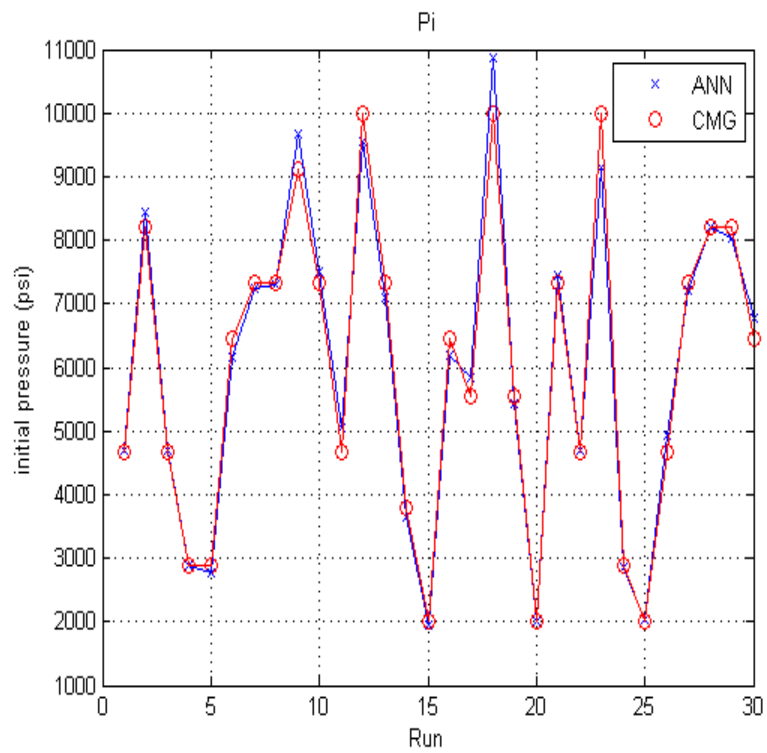


Figure 17 Inverse initial reservoir pressure results for CMG and ANN

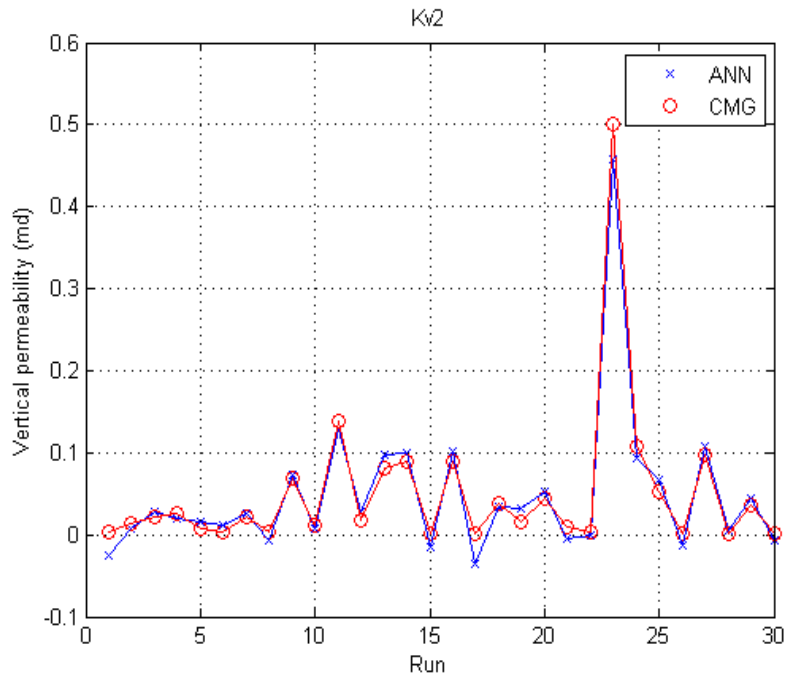


Figure 18 Inverse vertical permeability results for CMG and ANN

Due to small value of vertical permeability, the error is expected to be relatively higher compare to other properties.

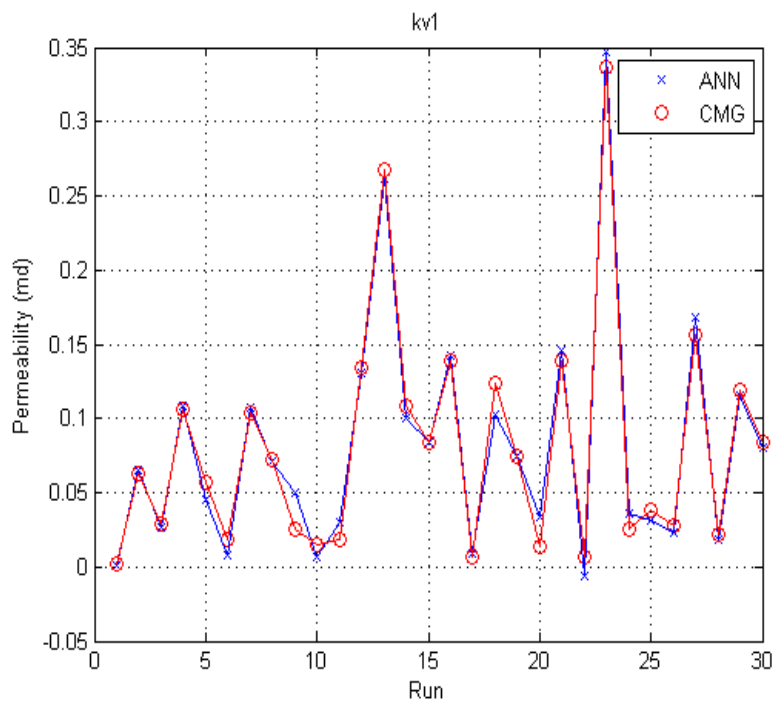


Figure 19 Inverse vertical permeability results for CMG and ANN

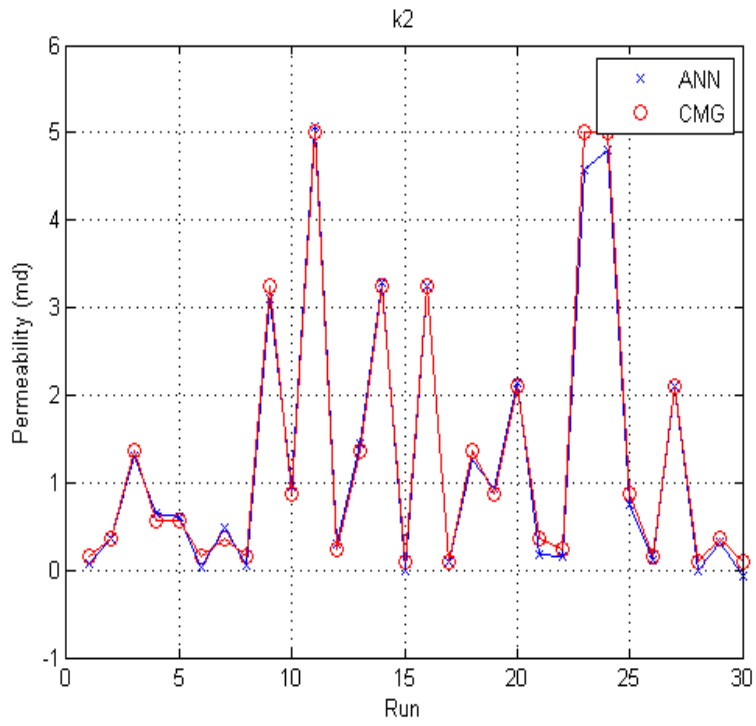


Figure 20 permeability results for CMG and ANN

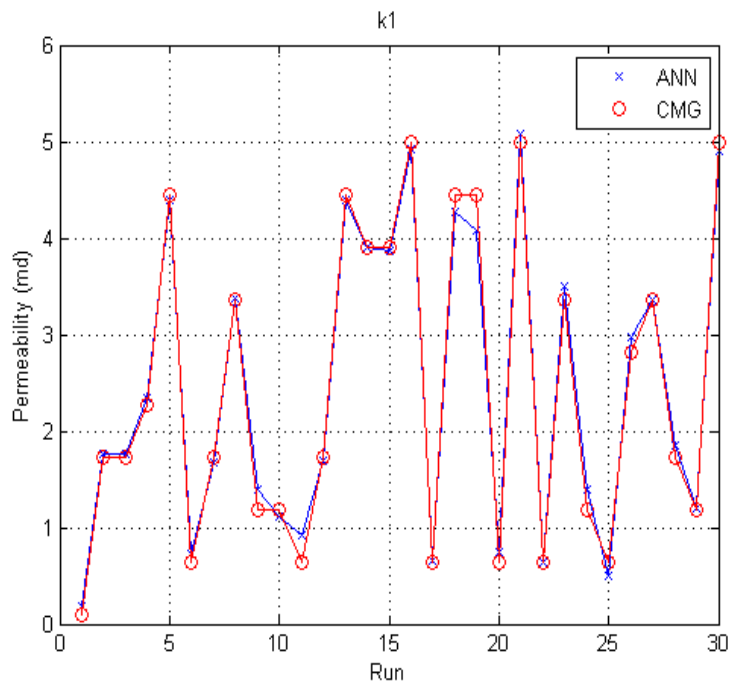


Figure 21 permeability results for CMG and ANN

6.2 Result of Three-layered reservoir network Artificial Neural

Forward ANN production forecasting

In this network, the complexity increases when one more layer has been added to the the system. Putting into account extra layer, that leads to have four more input parameters, the network still has a very good match with actual data from the simulator. The average error for production rate of 30 data sets is 4 % and for Cumulative production is 2 % with recommended network shown in Table 19.

Table 19 Forward ANN for three-layered reservoir results

ERROR	AVERAGE CUMULATIVE ERROR				AVERAGE GAS RATE ERROR	
RECOMMENDED NETWORK	2%				4%	
Hidden Layer	1	2	3	4	5	6
Neurons	72	78	77	80	75	75

In Table 20, the average error for 30 values of all 30 data sets have been presented.

Table 20 Forward network for three-layered system results

Average error		2.00%	4.00%	Average error		2.00%	4.00%
No	Run	Error C	Error G	No	Run	Error C	Error G
1	8	2.5	3.78	16	200	2.56	3.16
2	15	4.91	5.84	17	206	2.62	5.92
3	18	1.69	3.87	18	224	2.39	10.69
4	22	2.98	5.75	19	245	2	2.98
5	29	2.42	5.68	20	291	2.53	5.57
6	61	1.93	3.69	21	298	2.81	3.17
7	62	1.3	1.84	22	339	1.16	2.25
8	86	2.92	3.83	23	366	2.93	4.29
9	91	3.24	2.67	24	371	2.69	4.19
10	105	1.58	5.77	25	402	2.98	4.88
11	122	1.13	2.84	26	453	0.8	1.95
12	140	1.86	6.34	27	460	4.15	14.18
13	151	0.85	1.15	28	467	2.67	6.11
14	156	1.37	3.8	29	518	10.28	11.33
15	177	2.08	5.6	30	557	0.95	2.23

All the figures starting from figure 50 to Figure 79 indicating the result of ANN and simulator are shown in appendix III .These figures represent all 30 data set for cumulative production on top and gas rate below for 30 values assigned to each. Results of CMG are presented in red circles for gas rate curve and ANN results are in green circles and vice versa according to figures legends. Figure 52 and 53 as example have been shown in the next page.

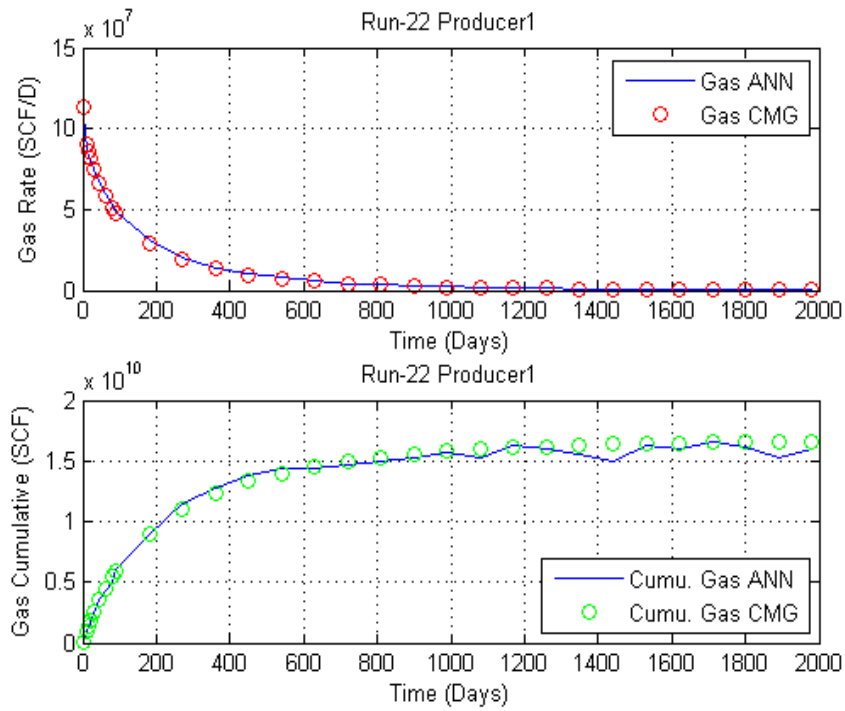


Figure 22 Data set 22 of forward network for three-layered system

In Figure 52 with high fluctuation of data, still the model can follow the trend with low error.

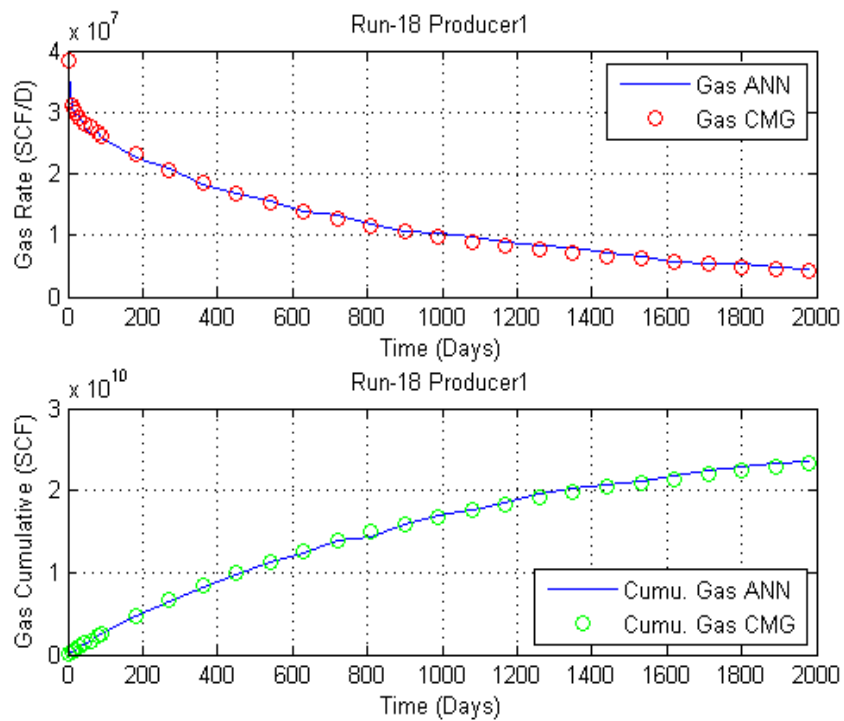


Figure 23 Data set 18 of forward network for three-layered system

Inverse Well Design parameters ANN for the three-layered reservoir

In this network, two parameters (BHP and drainage area) were predicted by optimum network design with an average error of 6 and 2 percent respectively. The optimum network consists of two hidden layers and the number of neurons are 78 and 84 respectively.

Table 21 Inverse well design Solution for three-layered reservoir

PARAMETERS	BOTTOM HOLE PRESSURE AVERAGE ERROR	DRAINAGE AREA AVERAGE ERROR
OPTIMUM NETWORK	6%	2%
HIDDEN LAYER	1	2
NEURONS	78	84

Figures 80 and 81 shows the network results that is compared to results of the simulator data.

Table 22 show the results for both bottom hole pressure and drainage area for whole 30 data sets.

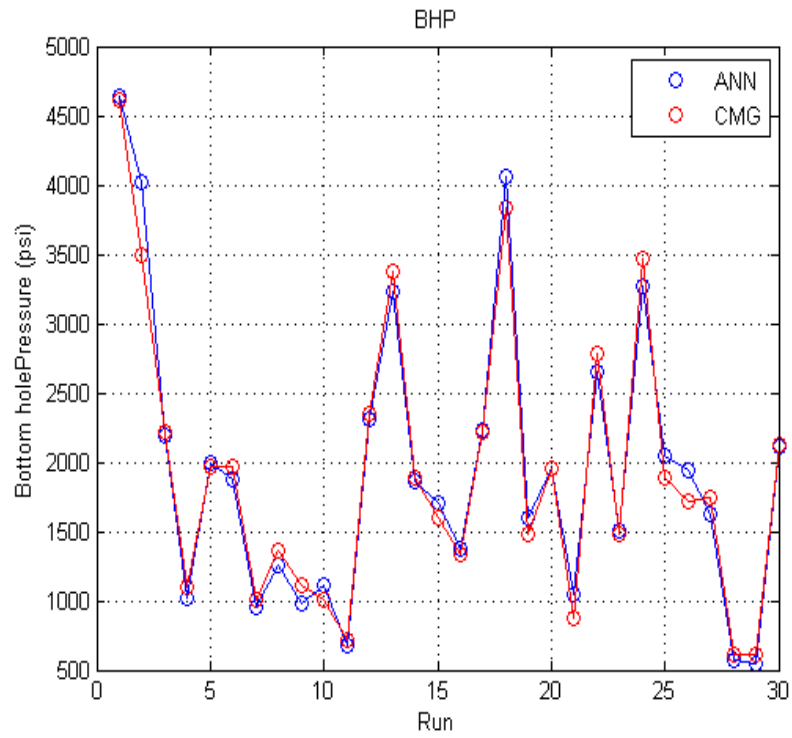


Figure 24 Bottom Hole Pressure results for CMG and ANN

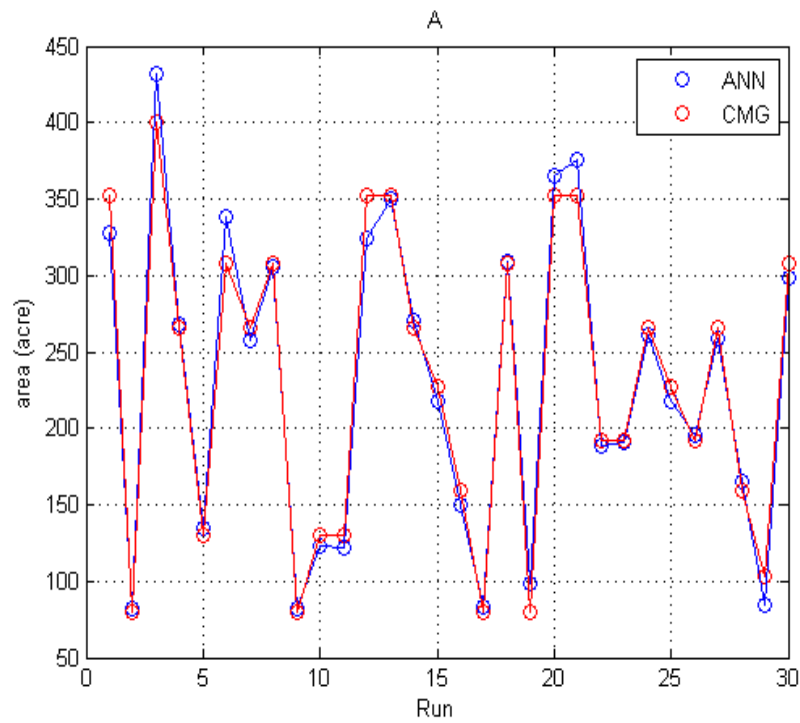


Figure 25 Drainage Area results for CMG and ANN

Table 22 ANN and CMG results and comparison for the three-layered reservoir

No	Run	ANN		CMG		Error	
		BHP	Drainage Area (acre)	BHP	Drainage Area (acre)	Block Length	Drainage Area error
1	10	4641.5	327.2828	4611.1	352.3322	-0.7	3.6
2	17	4014.9	82.26256	3492.6	79.97755	-15.0	-1.4
3	34	2187.8	431.7617	2219.7	399.9604	1.4	-3.9
4	52	1014.1	268.5292	1100.0	266.1387	7.8	-0.4
5	89	1997.4	134.4126	1969.2	129.9603	-1.4	-1.7
6	98	1869.2	338.814	1970.4	307.7223	5.1	-4.9
7	117	954.0	257.2522	1000	266.1387	4.6	1.7
8	119	1260.2	306.0161	1366.7	307.7223	7.8	0.3
9	173	981.6	82.34721	1107.4	79.97755	11.4	-1.5
10	184	1118.1	123.1129	1000	129.9603	-11.8	2.7
11	209	676.8	122.4537	713.6	129.9603	5.2	2.9
12	219	2311.6	324.2731	2345.7	352.3322	1.5	4.1
13	227	3232.0	350.1811	3381.5	352.3322	4.4	0.3
14	236	1858.7	270.1751	1888.9	266.1387	1.6	-0.8
15	242	1704.8	218.0795	1595.1	227.5651	-6.9	2.1
16	261	1377.6	149.4895	1332.1	159.4732	-3.4	3.2
17	291	2226.1	82.96498	2219.7	79.97755	-0.3	-1.9
18	294	4061.3	308.953	3833.3	307.7223	-5.9	-0.2
19	326	1592.2	99.05049	1481.5	79.97755	-7.5	-11.3
20	338	1956.1	365.4689	1955.6	352.3322	0.0	-1.8
21	366	1042.7	376.0032	881.493	352.3322	-18.3	-3.3
22	369	2644.9	188.5557	2784.0	192.0099	5.0	0.9
23	399	1512.9	190.6434	1481.5	192.0099	-2.1	0.4
24	419	3269.5	261.5943	3471.6	266.1387	5.8	0.9
25	489	2049.7	217.6591	1888.9	227.5651	-8.5	2.2
26	503	1935.1	196.1439	1718.5	192.0099	-12.6	-1.1
27	515	1628.7	258.6215	1742.0	266.1387	6.5	1.4
28	532	568.5	165.2608	611.12	159.4732	7.0	-1.8
29	577	539.9	84.63292	611.12	103.4597	11.6	9.6
30	579	2112.8	298.0413	2129.6	307.7223	0.8	1.6

Inverse ANN reservoir parameters results for three-layered system

In this network, ten parameters were predicted by optimum network design with the average error of 4.1, 2.6, 7.7, 7.4, 12, 16, 0.7, 1, 0.6 and 3 percent respectively shown in table below. The optimum network has three hidden layers and number of neurons has been shown in Table 23.

Table 23 Inverse reservoir properties optimum network results for three-layered Reservoir

Parameters	K1	K2	K3	kv1	kv2	Kv3	Pi	phi1	phi2	phi3
Recommended	4.1%	2.6 %	7.7%	7.4%	12%	16%	0.7%	1%	0.6%	3%
Hidden layer	1	2	3							
Neurons	94	97	96							

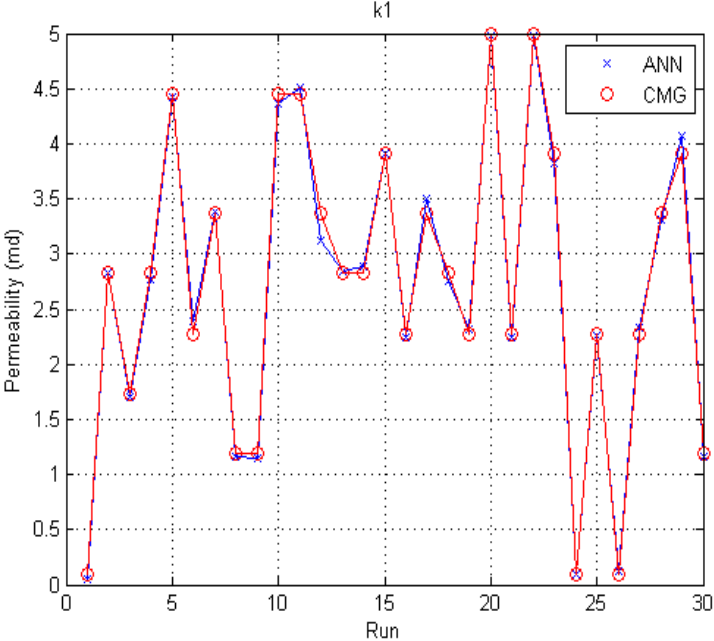


Figure 26 Permeability layer 1 results for CMG and ANN

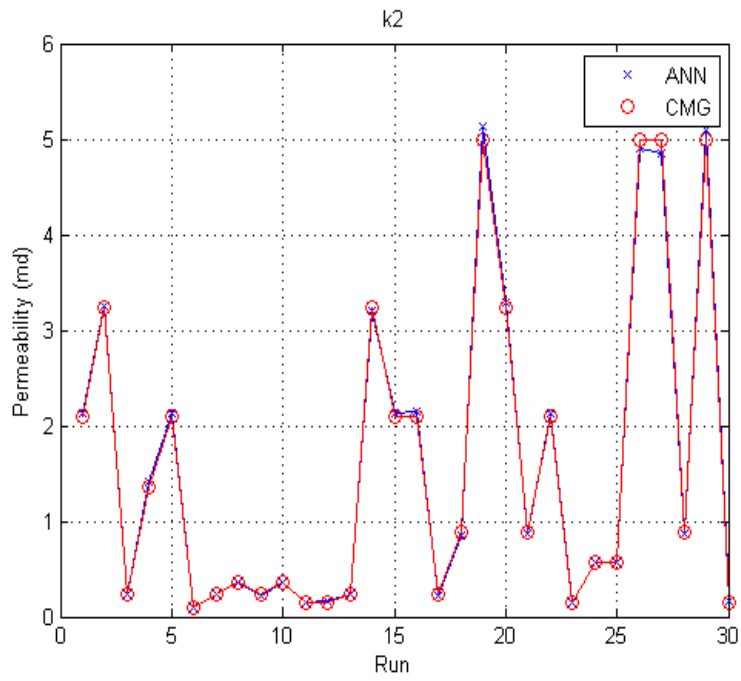


Figure 27 Permeability layer 2 results for CMG and ANN

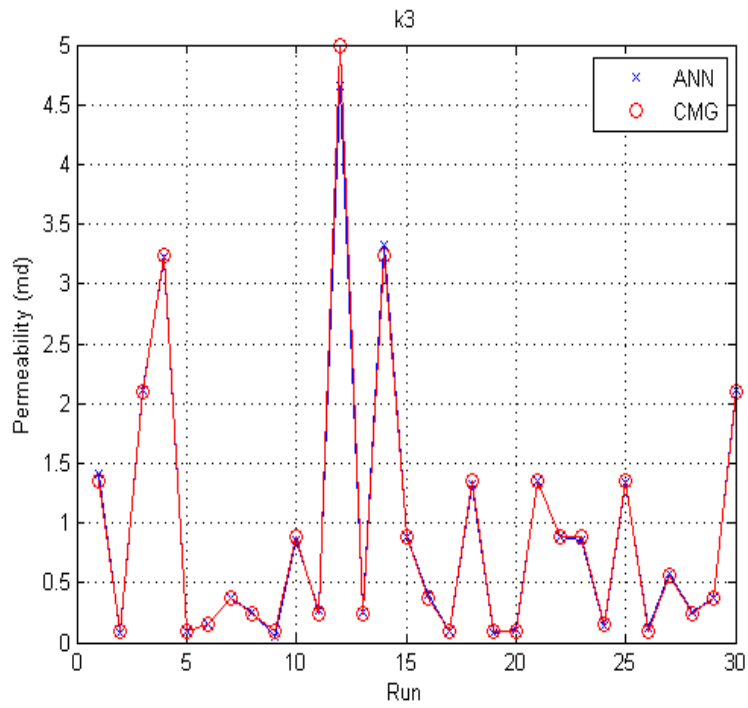


Figure 28 Permeability layer 3 results for CMG and ANN

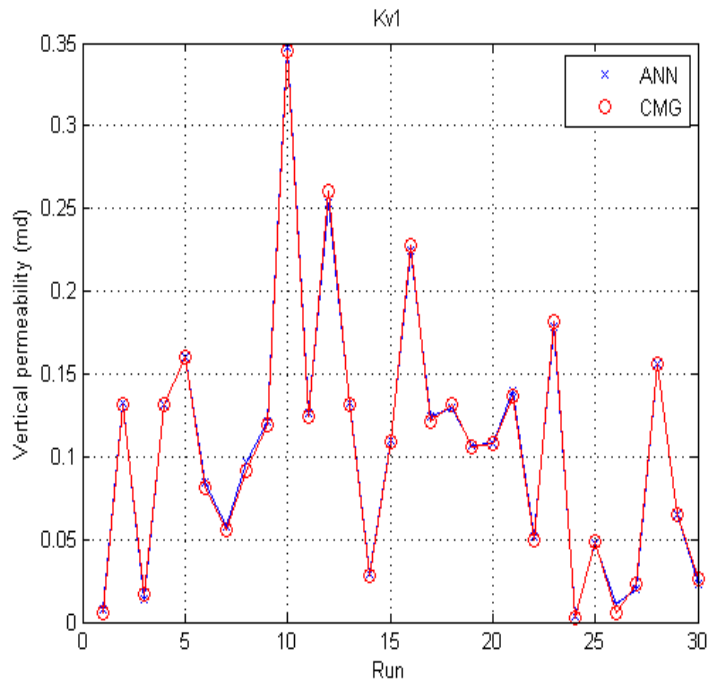


Figure 29 vertical permeability of layer 1 results for CMG and ANN

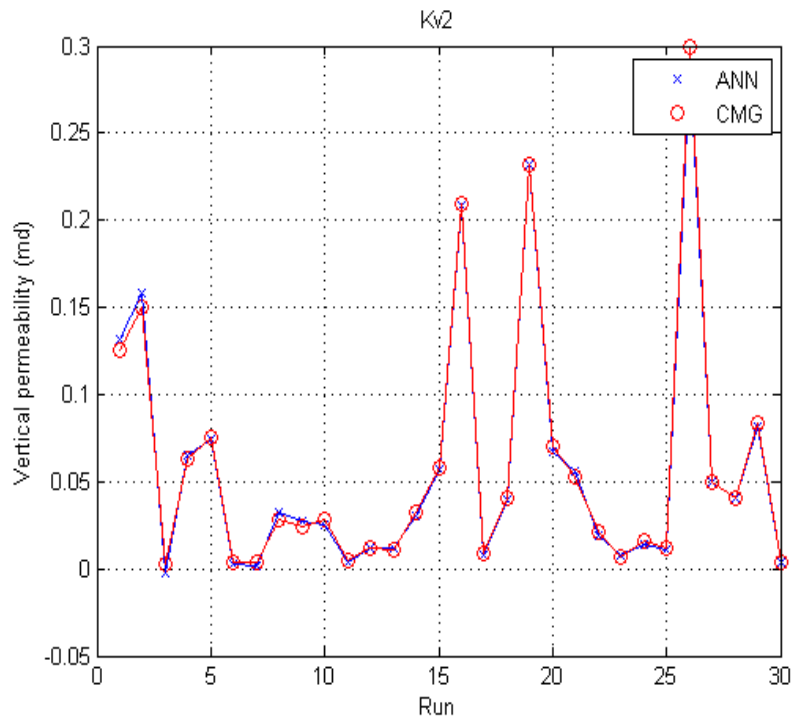


Figure 30 vertical permeability of layer 2 results for CMG and ANN

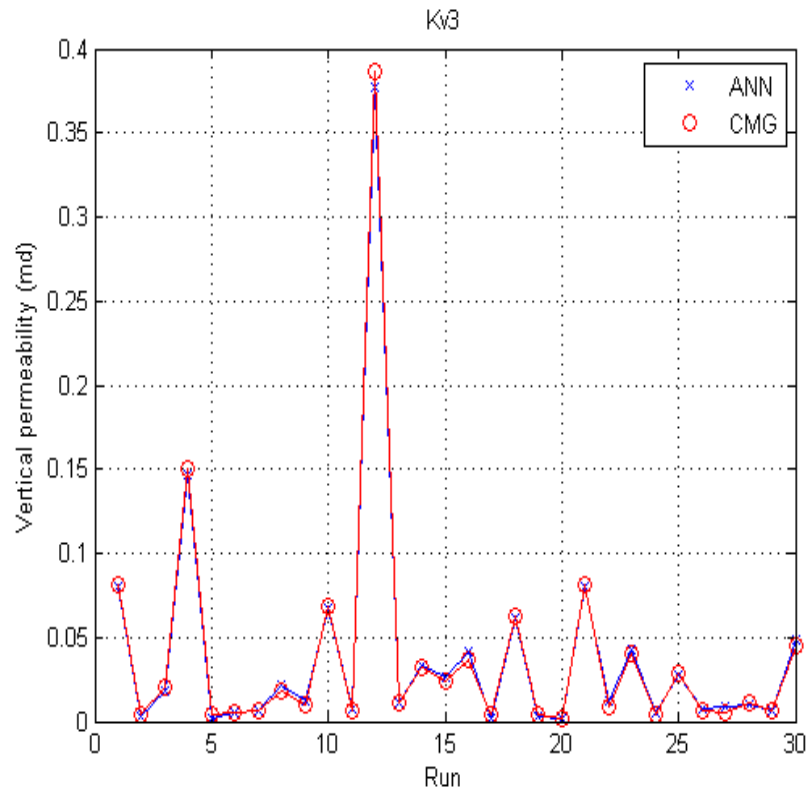


Figure 31 vertical permeability layer 3 and initial reservoir pressure results for CMG and ANN

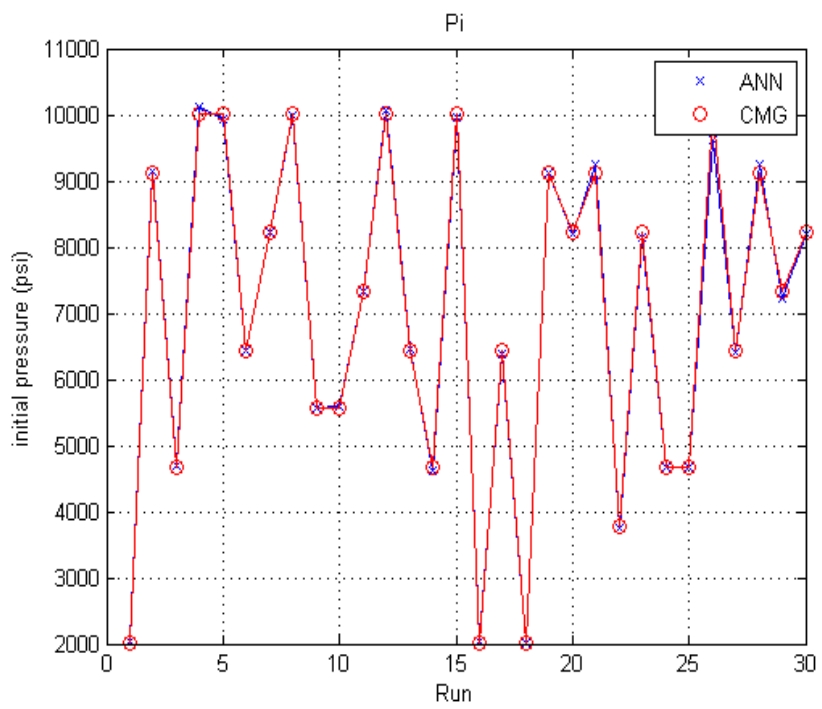


Figure 32 initial reservoir pressure results for CMG and ANN

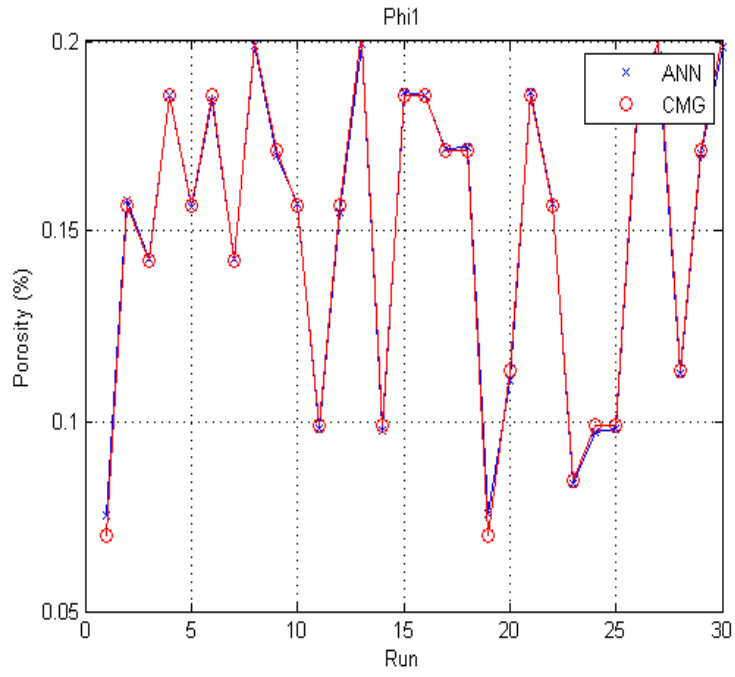


Figure 33 porosity layer 1 results for CMG and ANN

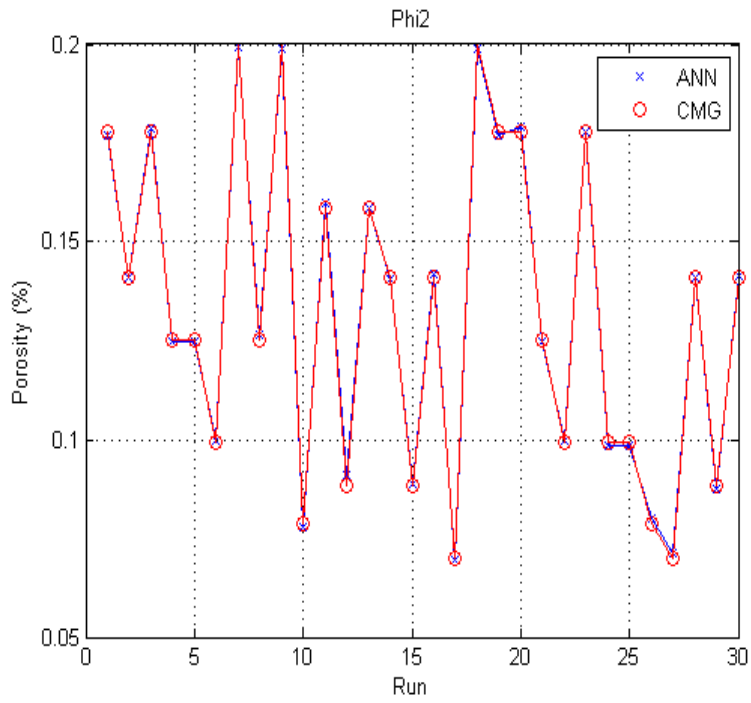


Figure 34 porosity layer2 results for CMG and ANN

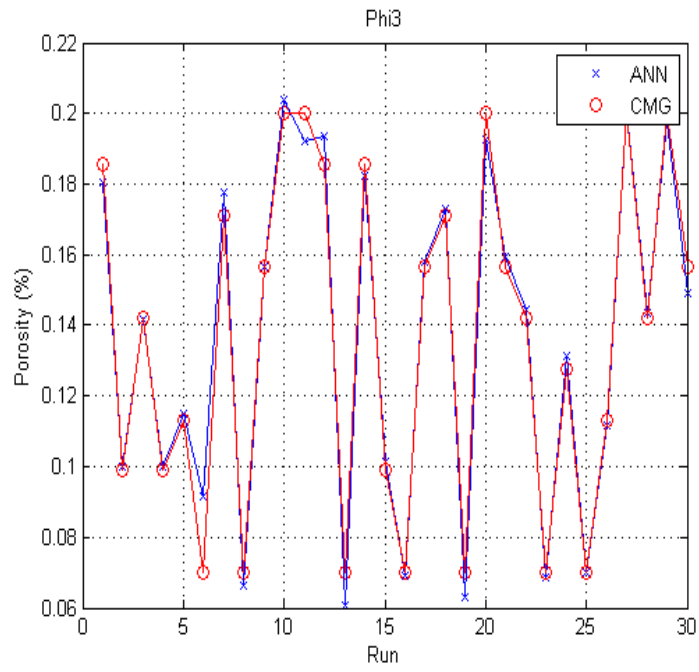


Figure 35 porosity layer 3 results for CMG and ANN

6.3 Results for four-layered reservoir artificial neural network

Forward ANN for production forecasting

In this network, the complexity increases when one more layer has been added to the system. Putting into account, increase in layer leads to having eight more input parameters compared to the two-layered system, the network still has a very good match with actual data from the simulator. The average error for production rate of 30 data set is 1.5 percent and for cumulative production is 5 percent with the recommended network design shown in table 25.

Table 24 Forward solution results for Cumulative production and production rate

Average error		1.50%	5.00%	Average error		1.50%	5.00%
No	Run	Error C	Error G	No	Run	Error C	Error G
1	8	1.30%	7.60%	16	276	0.60%	2.90%
2	62	2.30%	22.60%	17	281	0.80%	2.60%
3	83	0.80%	5.40%	18	305	1.80%	6.10%
4	128	0.90%	10.70%	19	309	0.70%	1.60%
5	134	2.10%	3.30%	20	328	1.50%	3.40%
6	137	1.40%	7.30%	21	333	1.70%	6.80%
7	142	1.50%	4.50%	22	381	1.50%	3.80%
8	163	1.40%	6.00%	23	405	1.10%	2.60%
9	174	2.80%	4.10%	24	423	1.90%	8.20%
10	192	1.40%	6.40%	25	440	0.80%	3.60%
11	232	1.50%	3.00%	26	497	1.80%	3.80%
12	234	1.60%	2.90%	27	515	1.40%	4.30%
13	252	1.20%	2.50%	28	530	0.80%	2.30%
14	260	1.50%	5.00%	29	532	0.80%	3.60%
15	264	0.90%	2.30%	30	600	1.40%	2.50%

Table 25 optimum network of Forward solution for four-layered reservoir

ERROR	AVERAGE CUMULATIVE ERROR				AVERAGE GAS RATE ERROR	
RECOMMENDED NETWORK	1.5%				5%	
Hidden Layer	1	2	3	4	5	6
Neurons	89	99	93	99	91	93

All the figures starting from figure 92 to Figure 121 indicating the result of ANN and simulator are shown in appendix IV .These figures represent all 30 data set for cumulative production on top and gas rate below for 30 values assigned to each. Results of CMG are presented in red circles for gas rate curve and ANN results are in green circles and vice versa according to figures legends. Figure 108 and 109 as example have been shown in the next page.

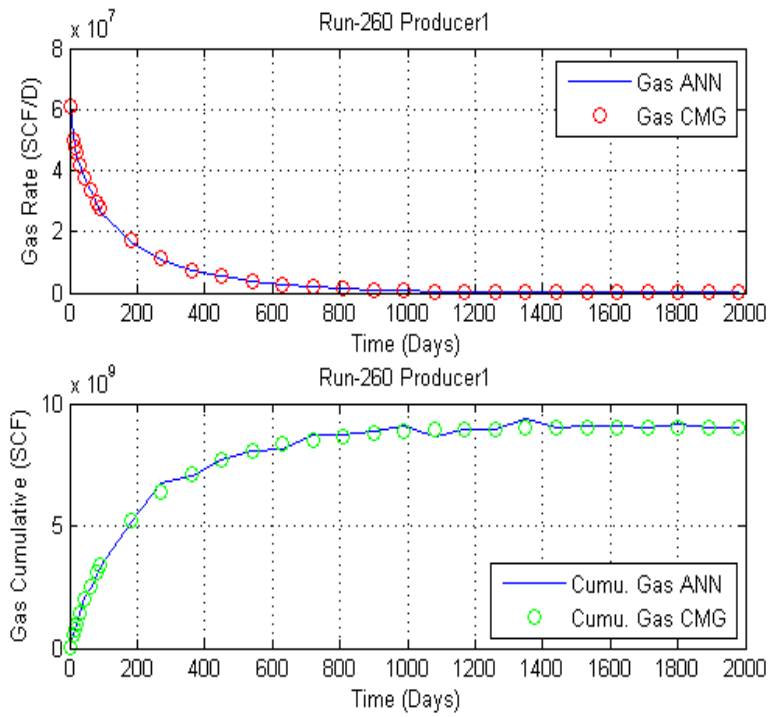


Figure 36 Data set 260 forward solution for four-layered reservoir

Sharp edges in ANN curve of Figure 108 show that both results are following the same trend.

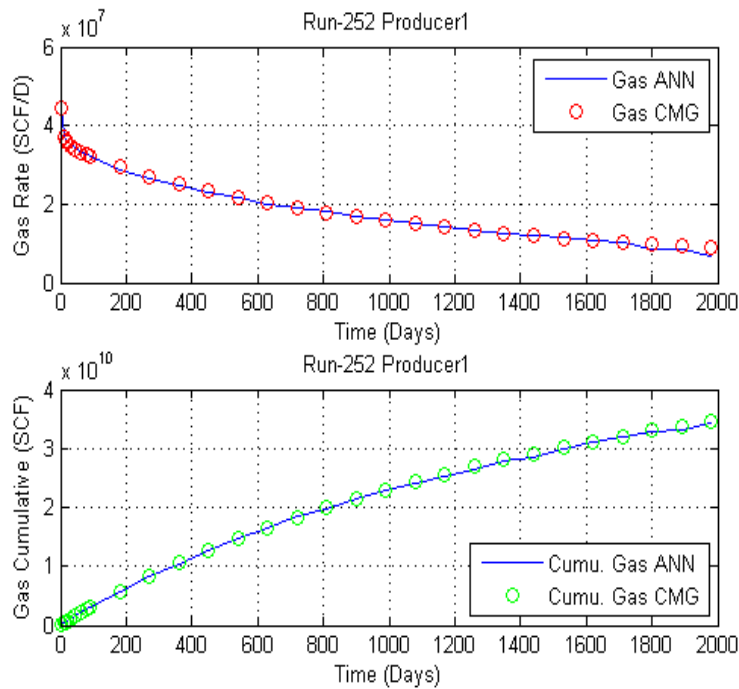


Figure 37 Data set 252 forward solution for four-layered reservoir

Inverse well parameters ANN for four-layered reservoir

In this network, the bottom hole pressure and drainage area are predicted with optimum network design with the average errors of 6 and 2 percent, respectively. The optimum network has two hidden layers with 34 neurons and 35 neurons, respectively in Table 26.

Table 26 Inverse well design optimum network

PARAMETERS	BOTTOM HOLE PRESSURE AVERAGE ERROR	DRAINAGE AREA AVERAGE ERROR
RECOMMENDED	6%	2%
Hidden Layer	1	2
Neurons	34	35

Figure 122 and Figure 123 illustrate the following trends and for drainage area in Figure 123, some points on ANN curve show high error while the others completely match the CMG data. Table 27 show the results for both simulator and ANN network for 30 data sets of bottom hole pressure and drainage area.

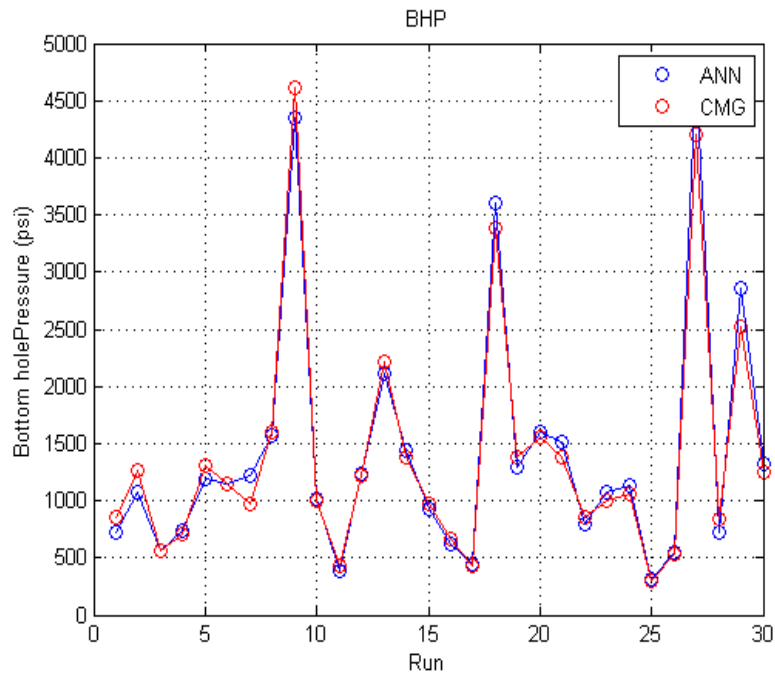


Figure 38 Bottom Hole pressure results from four-layered reservoir results

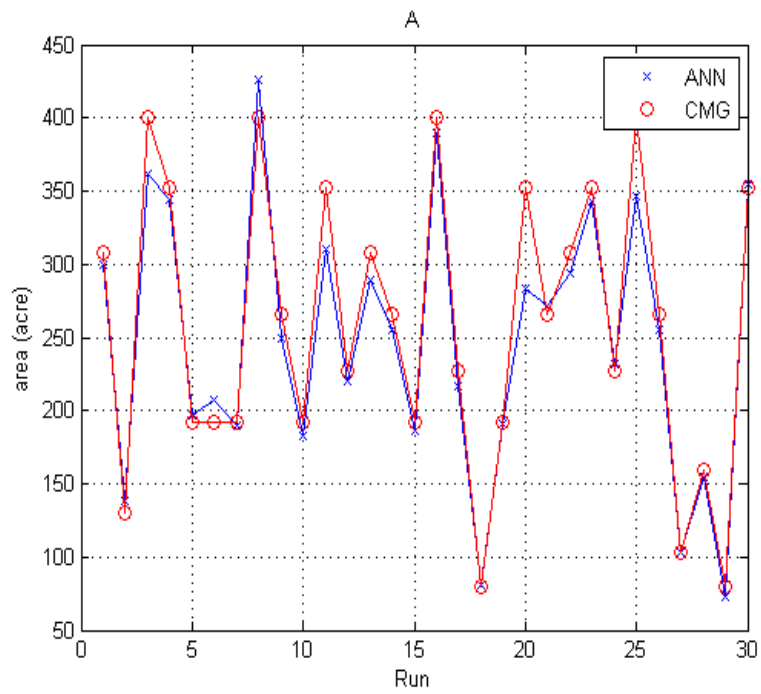


Figure 39 Drainage area results for four-layered reservoir

Table 27 Inverse well design results for four-layered reservoir

No	Run	ANN		CMG		Error	
		BHP	Drainage Area(acre)	BHP	Drainage Area(acre)	BHP Error	Drainage Area error
1	55	725.8	299.5733	860.5	299.5733	15.6	1.3
2	83	1069.3	138.7018	1265.5	138.7018	15.5	-3.3
3	100	567.7	361.383	566.7	361.383	-0.2	4.9
4	113	741.1	343.7302	713.6	343.7302	-3.9	1.2
5	121	1186.5	197.2025	1301.2	197.2025	8.8	-1.3
6	147	1140.9	207.8713	1154.3	207.8713	1.2	-4.0
7	162	1223.3	190.0437	966.7	190.0437	-26.6	0.5
8	177	1573.0	425.6913	1595.1	425.6913	1.4	-3.2
9	205	4355.9	248.9575	4611.1	248.9575	5.5	3.3
10	233	1013.0	182.8317	1007.4	182.8317	-0.6	2.4
11	254	388.4	310.1139	433.3	310.1139	10.4	6.2
12	256	1242.1	220.1889	1219.8	220.1889	-1.8	1.6
13	332	2107.9	289.2494	2219.7	289.2494	5.0	3.0
14	345	1435.3	254.9108	1385.2	254.9108	-3.6	2.1
15	350	922.1	186.1866	966.7	186.1866	4.6	1.5
16	352	619.8	390.3203	658.0	390.3203	5.8	1.2
17	357	440.5	216.9412	433.3	216.9412	-1.7	2.4
18	367	3604.5	80.76206	3381.5	80.76206	-6.6	-0.5
19	382	1295.2	190.4778	1385.2	190.4778	6.5	0.4
20	405	1604.6	283.5631	1553.1	283.5631	-3.3	10.3
21	418	1511.9	271.4383	1385.2	271.4383	-9.1	-1.0
22	477	796.1	294.312	860.5	294.312	7.5	2.2
23	501	1075.6	342.7617	1000.0	342.7617	-7.6	1.4
24	503	1128.6	232.0761	1063.0	232.0761	-6.2	-1.0
25	505	307.8	347.0055	300.0	347.0055	-2.6	6.9
26	530	542.6	255.3334	533.3	255.3334	-1.7	2.1
27	541	4748.5	102.9816	4201.2	102.9816	-13.0	0.2
28	544	725.2	154.2835	833.3	154.2835	13.0	1.6
29	559	2854.7	72.87405	2525.9	72.87405	-13.0	4.5
30	565	1320.0	354.5655	1244.5	354.5655	-6.1	-0.3

Inverse reservoir parameters ANN for four-layered reservoir

In this network, 13 parameters were predicted with optimum network design with average errors of 3, 11, 13, 10, 18, 44, 43, 48, 1, 1, 5, 1 and 5 percent, respectively. The optimum network has two hidden layers with 31, 32 and 38 neurons respectively. Due to a very small value for vertical permeability, the average error exceeded 40 percent but upon closer examination, the difference between the actual data of 0.02 and the predicted value of 0.21 are very small and negligible in the reservoir scale regardless of the error.

Table 28 Inverse reservoir properties optimum network for four-layered reservoir

Parameters	K1	K2	K3	K4	kv1	kv2	Kv3	Kv4	Pi	phi1	phi2	phi3	Phi4
Recommended	3%	11%	13%	10%	18%	44%	43%	48%	1 %	1%	5%	1%	1%
Hidden layer	1	2	3										
Neurons	31	32	38										

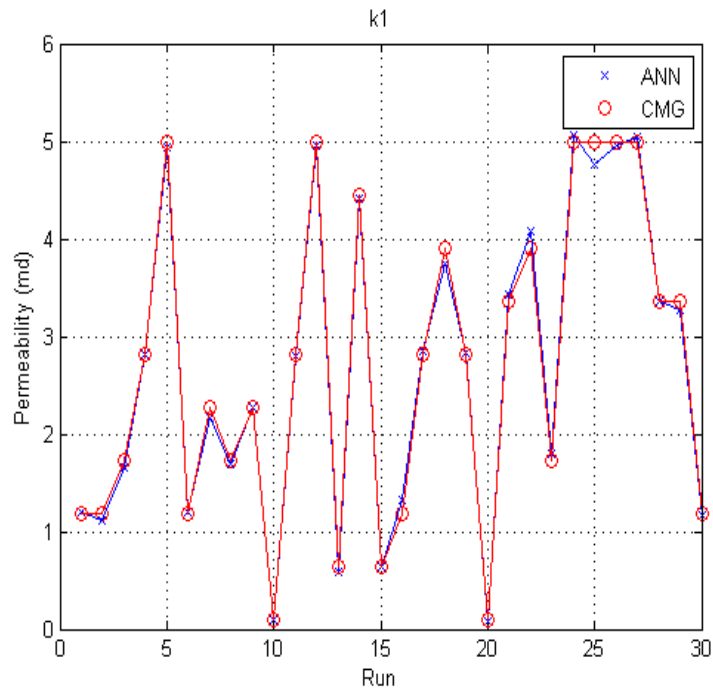


Figure 40 Permeability layer 1 plots for CMG Vs ANN

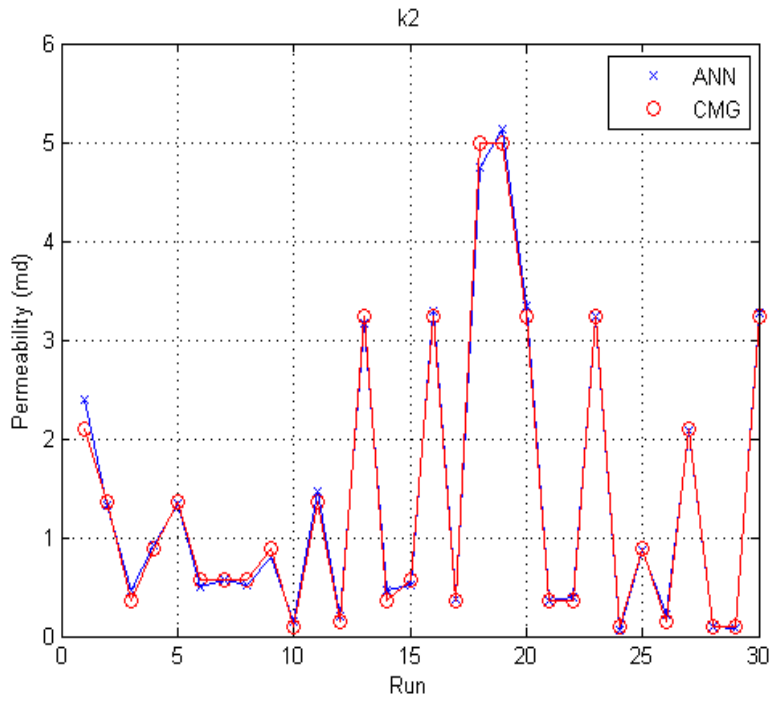


Figure 41 Permeability layer 2 plots for CMG Vs ANN

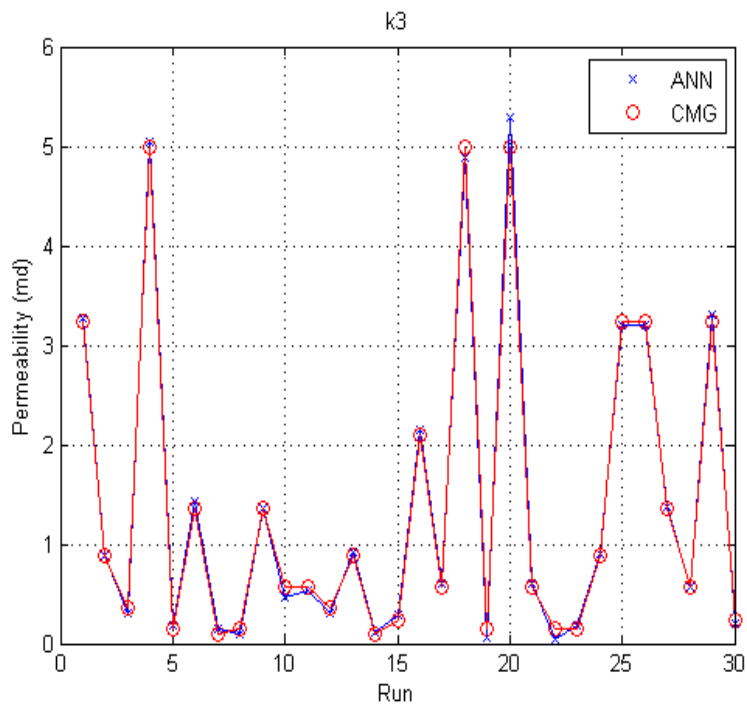


Figure 42 Permeability layer 3 plots for CMG Vs ANN

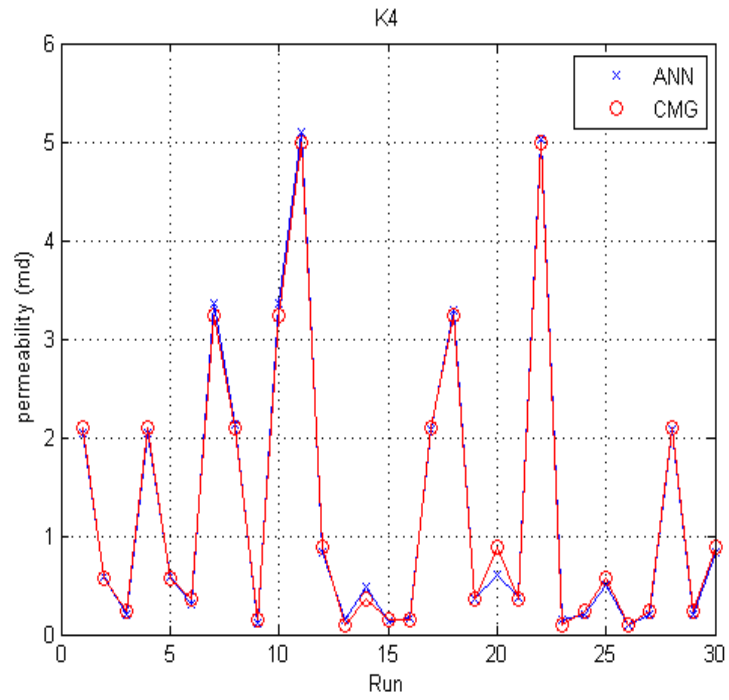


Figure 43 Permeability layer 4 plots for CMG Vs ANN

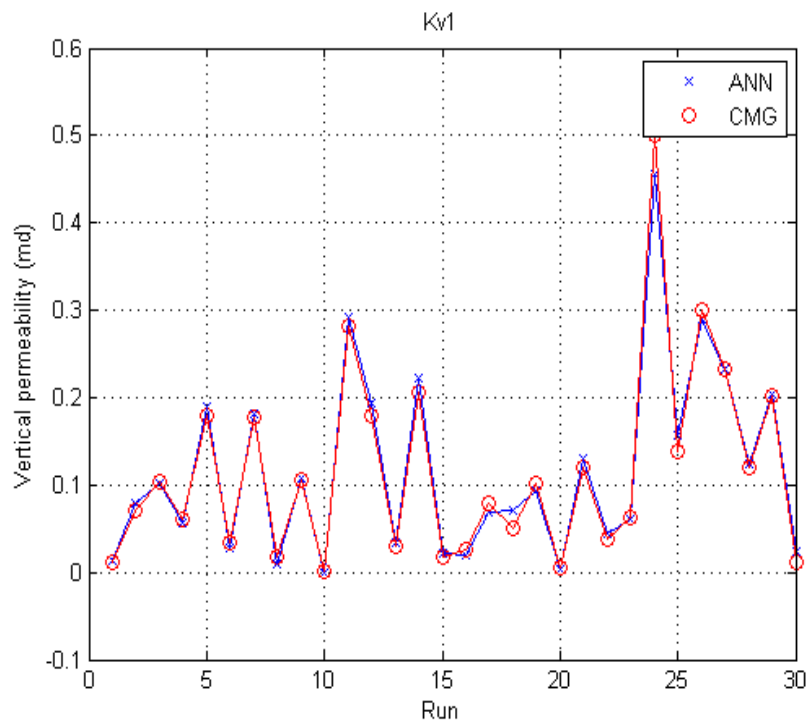


Figure 44 Vertical Permeability layer 1 plots for CMG Vs ANN

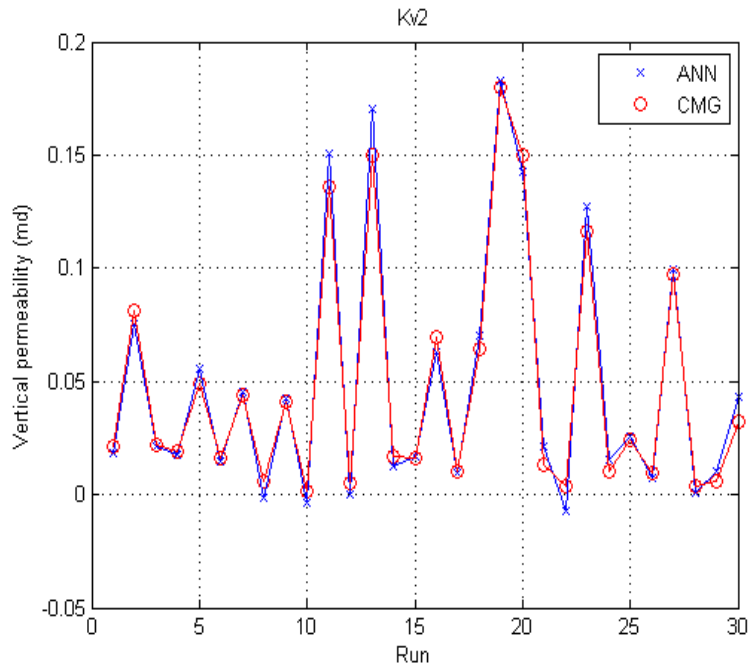


Figure 45 Vertical Permeability layer 2 plots for CMG Vs ANN

Highest error for vertical permeability which is still applicable for data measured in field is shown in Figure 129.

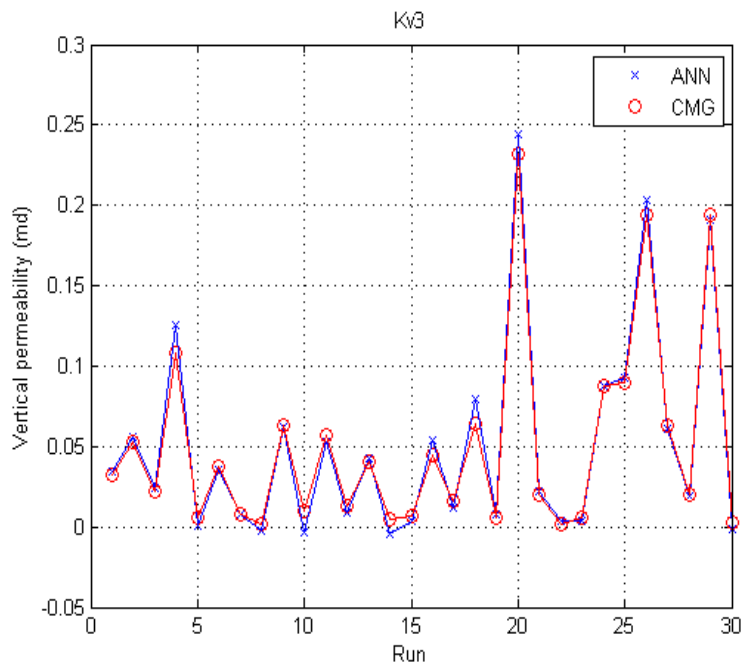


Figure 46 Vertical Permeability layer 3 plots for CMG Vs ANN

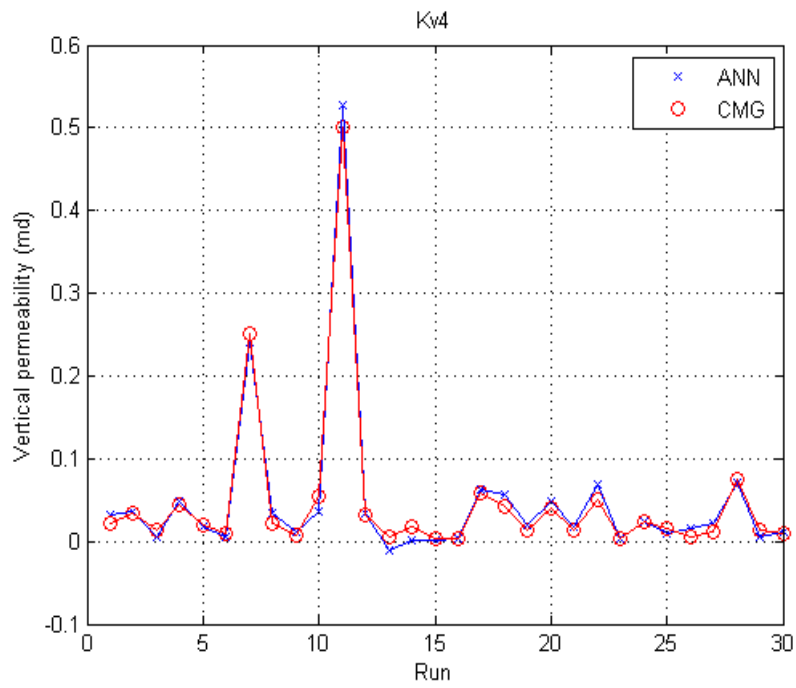


Figure 47 Vertical Permeability layer 4 plots for CMG Vs ANN

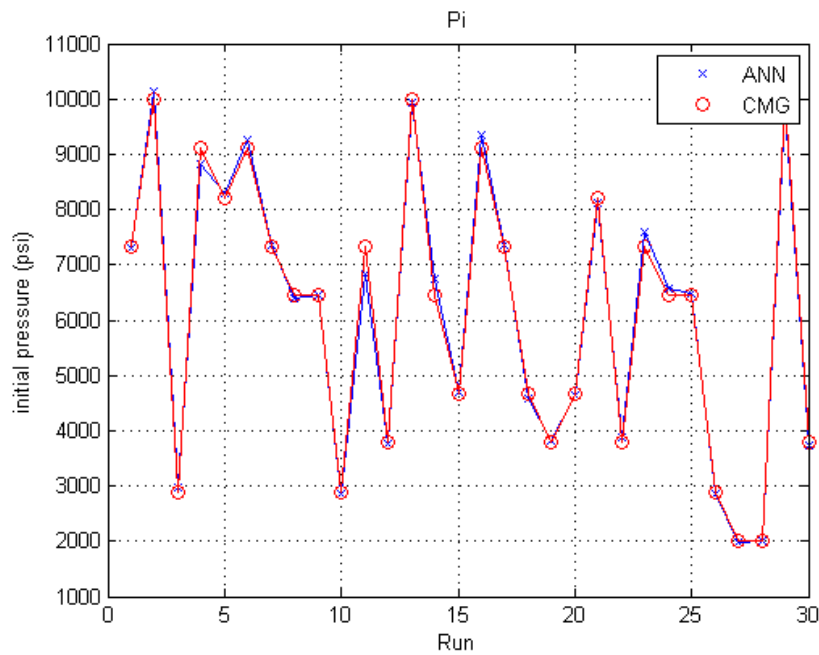


Figure 48 Initial Reservoir pressure plots for CMG Vs ANN

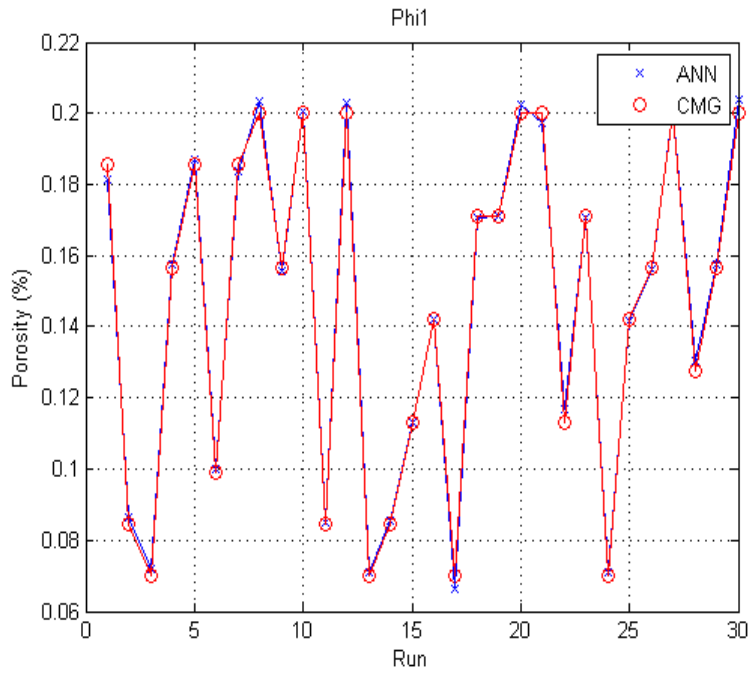


Figure 49 porosity layer 1 and porosity layer 1 plots for CMG Vs ANN

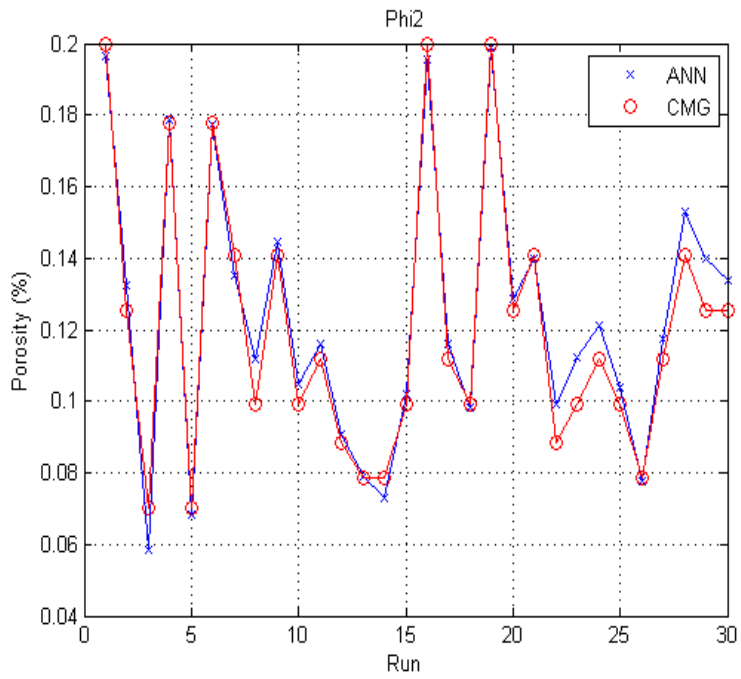


Figure 50 porosity layer 2 plots for CMG Vs ANN

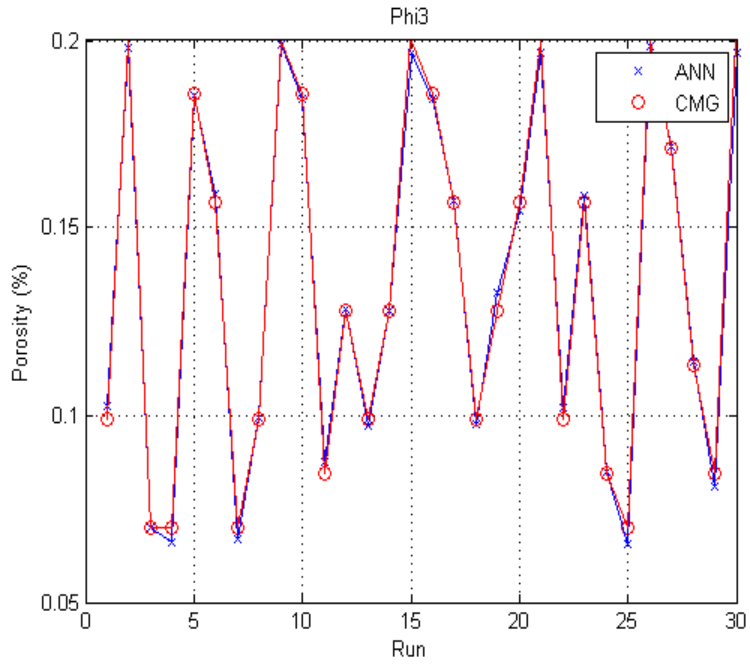


Figure 51 porosity layer 3 plots for CMG Vs ANN

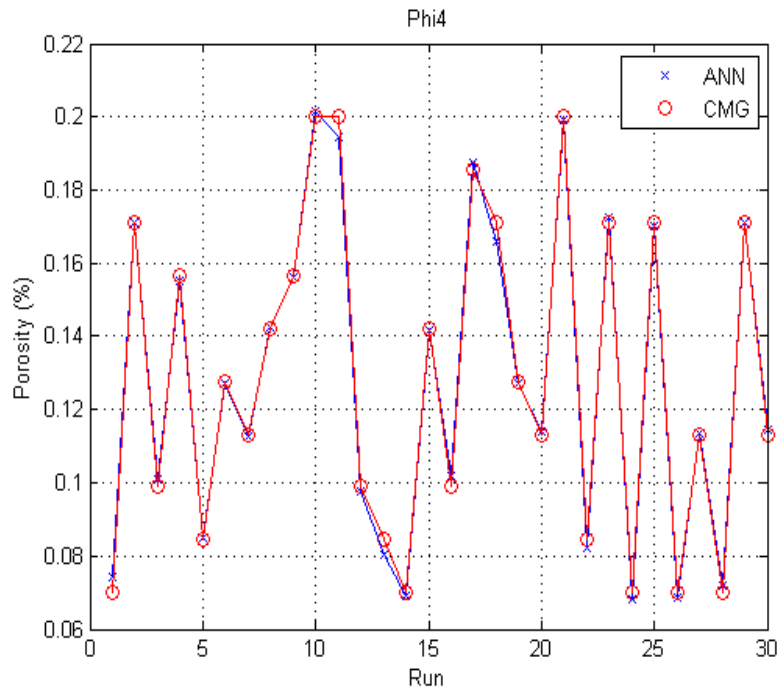


Figure 52 porosity layer 4 plots for CMG Vs ANN

6.4 Results of network for blind data within the range

To test the model that has been trained, 70 blind data sets have been generated using CMG-CMOST. These data sets are generated within the range of the model and will be used to check whether the trained model is reliable. These data sets are called blind sets in which they have not been introduced or seen by the tool. The two sample results for production rate and cumulative production are shown in Figure 137 and Figure 138. The following plots are for 30 values from each curve showing very good alignments and most importantly, a similar trend.

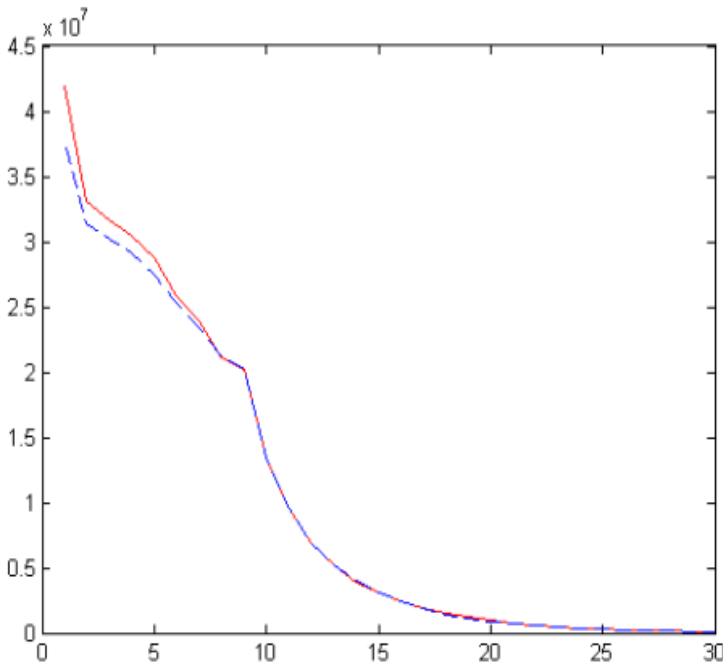


Figure 53 Two plots represent two data sets of production rate for blind data set and trained ANN data set with similar trend

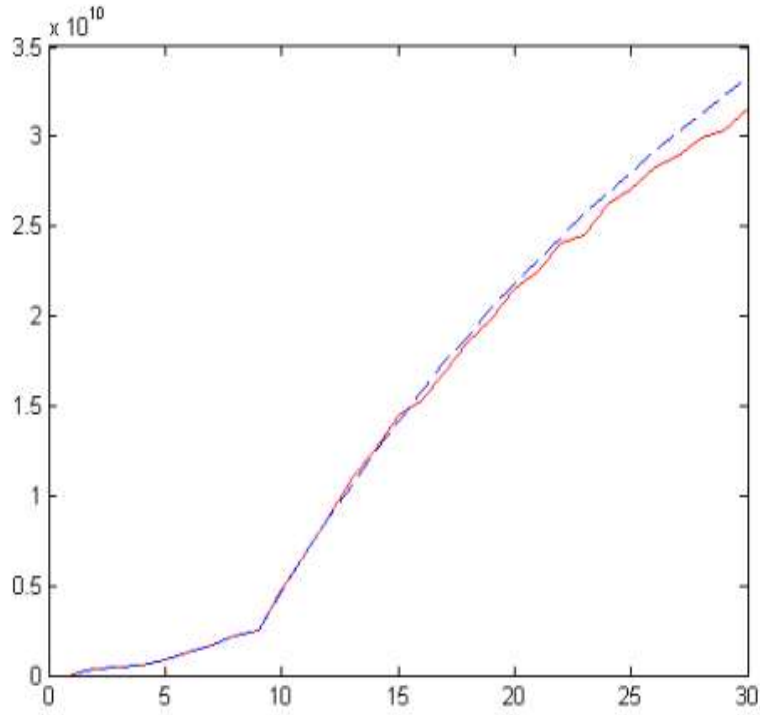


Figure 54 Two plots represent two data set of cumulative production for blind data set and trained ANN data set

The Forward solution for three-layered reservoir has been tested and the network results are shown in Table 29. The average error for 70 data set of production rate and cumulative production are 7 and 11 percent respectively.

Table 29 Network results for 70 blind data set

Forward Output	Cumulative production	Production rate
Error %	7	11

To show that ANN and CMG plots are following the same trend , Figure 139 and Figure 140 prepared that includes all 70 data sets curves in blue and red resembling simulator and ANN results respectively.

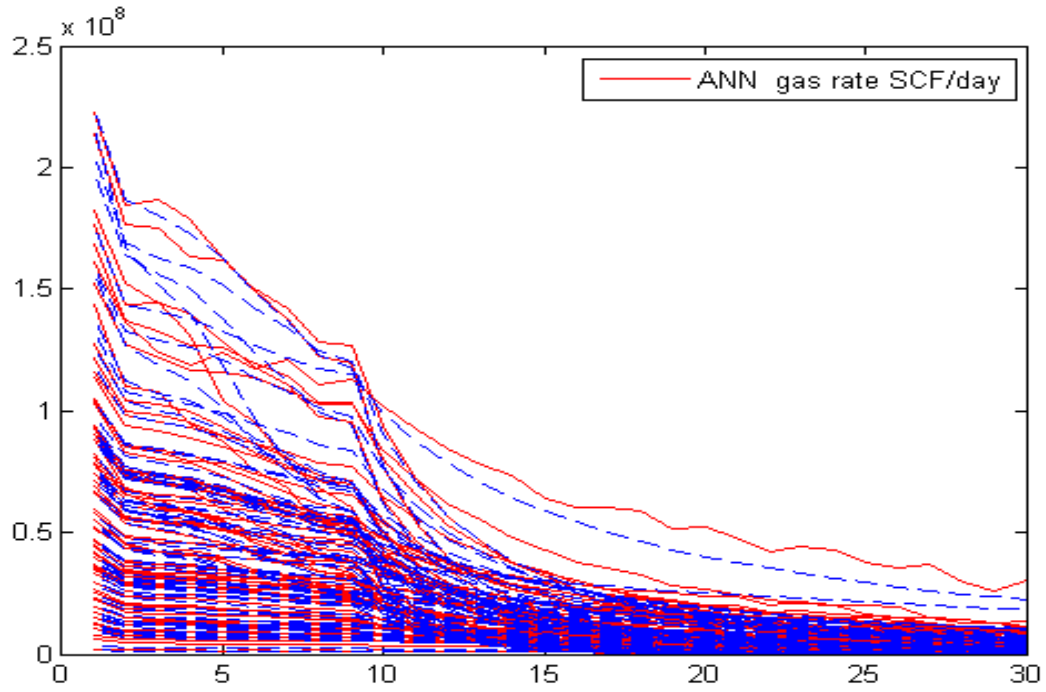


Figure 55 ANN results in red compare to CMG results in blue for gas rate for 70 data sets

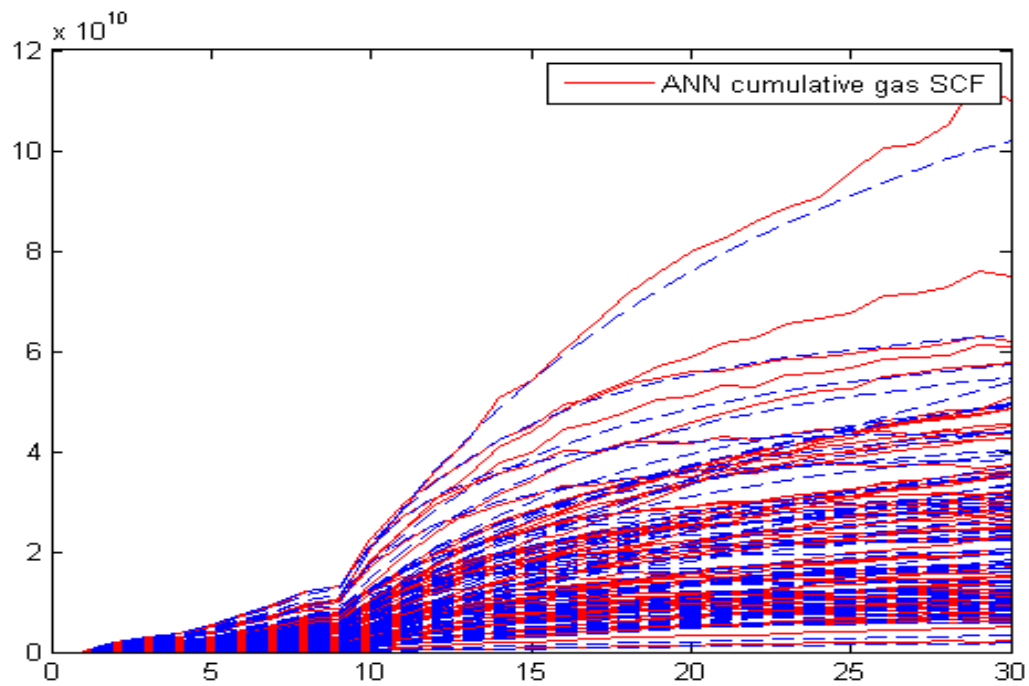


Figure 56 ANN results in red compare to CMG results in blue for cumulative gas for 70 data sets

In Figure 141 and Figure 142 , error distribution for 70 data sets that tested with the forward three-layered system have been presented for cumulative production and gas rate values. According to these figures, majority of the results belong to 5%-10% and less than 5% categories.

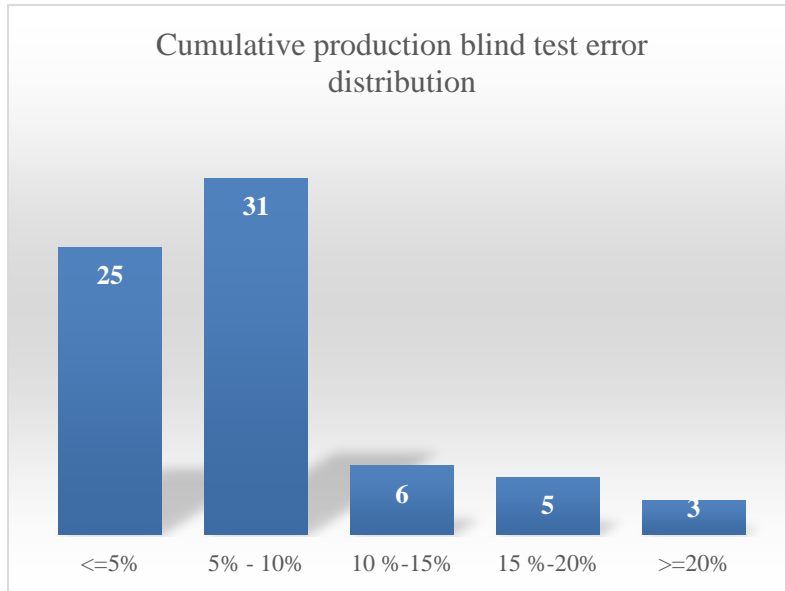


Figure 57 Error distribution map for 70 blind data sets as for 30 values Cumulative production

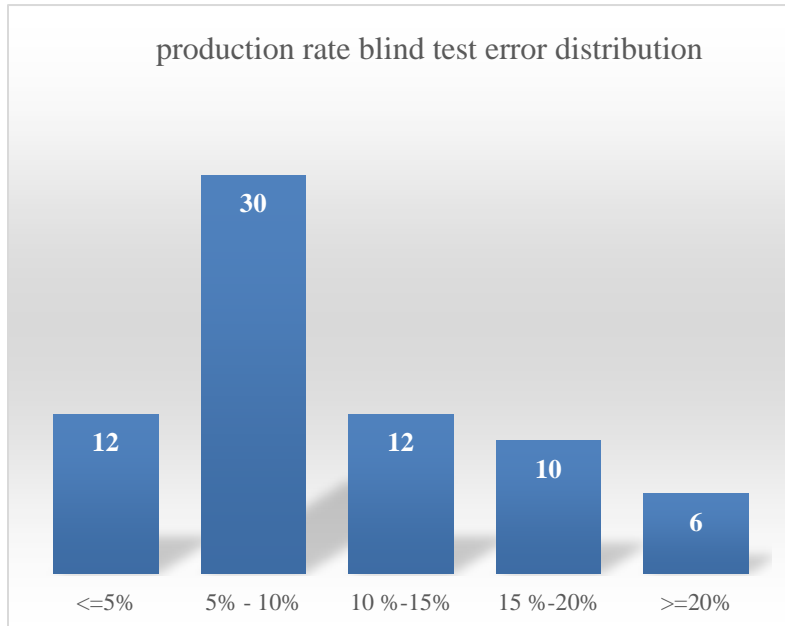


Figure 58 Error distribution map for 70 blind data sets for 30 values of Cumulative production

6.5 Supplemental Approach

In order to enhance the practicality of the ANN model, a new approach has been considered that can solve more problems in the field. Considering the homogenous layers in a reservoir, there is a possibility that a single layer have similar property to another. The model can predict the properties of reservoir with heterogeneity regarding layers properties and will be useful to predict the similar layers within the reservoir.

Without well testing operation and coring samples, the uncertainty regarding multilayered reservoirs is likely to a concern .Developing a model than can predict not only the properties of all layers but also determine the number of layers constituting the reservoir is the goal of this section. In this section, a new approach has been undertaken to evaluate the reservoir layers and come up with a solution to possible problem.

Three-layered reservoir has been selected as an example to solve the uncertainty of reservoir layers. Similar properties have been assigned to two-layereds while the third layer has unique properties. Using artificial neural network that has been trained previously, two different 70 data sets, one for three-layered reservoir with two similar layers properties and second for a two-layered reservoir with similar properties to three-layered system have been created. Using forward solution tool, the production profile of both two-layered system and three-layered system have been generated. The results have been presented in figure 141 and conclude the similarity that exist for both three and two-layered reservoir in trend. One possible answer for the difference in magnitude of data resulted is the vertical permeability value of the data set.

If the vertical permeability of the layers is large enough to create crossflow in between layers, the two adjacent layers with similar properties will most likely to behave like a single-layer reservoir. Another explanation for the data differences for this case can be explained by non-uniqueness concept where a set of reservoir properties may belong to more than one production profile. A result of this approach has been shown in Figure 143 and Figure 144 for gas rate data and cumulative gas data presenting the same trend.

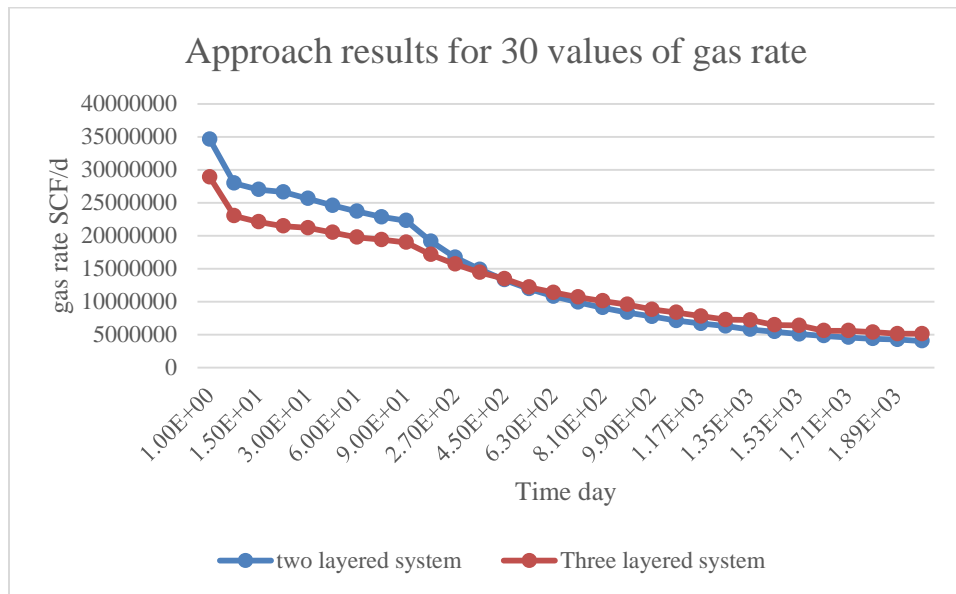


Figure 59 Two-layered and three-layered similarity approach in gas rate

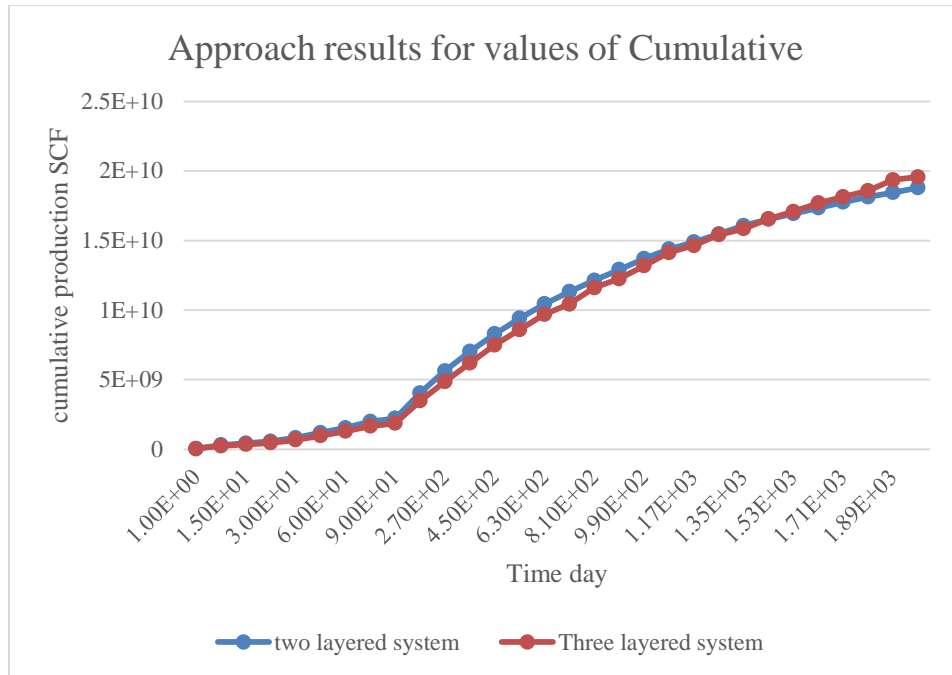


Figure 60 Two-layered and three-layered similarity approach in cumulative production

Chapter 7 Summary, conclusion and recommendation

7.1 Results Summary

The Artificial Neural Network has proved to be a powerful tool in predicting and analyzing data needed in wide range of science and engineering fields and specifically in petroleum industry. So far in this study, the rate transient analysis has been modeled and the tool enables the user to forecast production for each well in a multilayered reservoir. Skipping rate transient analysis or other field practices for obtaining required data is now possible with the artificial neural network based expert tool.

Three types of solution tools have been embedded into this model such as forward production profile, inverse reservoir properties and inverse well design parameters. In the first solution, the cumulative production and production rate have been predicted. Comparing the simulator results to the ANN expert tool, the average error for cumulative production and gas rate of a two-layered system were 1% and 3% respectively with the optimum network consists of six hidden layers with 84,8,87,90,89 and 86 number of neurons for each hidden layer. The transfer function for the entire process is selected to be Tansig for nonlinear and Purelin for a linear relationship. The algorithm used to create the model is Trainscg. The average error for cumulative production and gas rate of a three-layered system were 2 and 4 percent respectively with the optimum network consists of six hidden layers with 72,78,77,80,75 and 75 number of neurons for each hidden layer. The average error for cumulative production and gas rate of a four-layered system were approximately 1 and 5 percent, respectively, with the optimum

network consists of six hidden layers with 89,99,93,99,91 and 93 number of neurons for each hidden layer.

For the inverse well design tool, the network was able to predict two variables such as bottom hole pressure and drainage area. It yields results with very low error of 4 and 1 percent, respectively. The optimum network consists of two hidden layers with 41 and 42 number of neurons in each. For a three-layered system, the errors are 6 and 2 percent for bottom hole pressure and drainage area with the optimum network consists of two hidden layers with 78 and 84 neurons in each. For the four-layered system, the errors are 6 and 2 percent for bottom hole pressure and drainage area with the optimum network consists of two hidden layers with 34 and 35 neurons in each.

In inverse tool forecasting reservoir properties, the results have shown an increase in error which can be related to an increase in the number of reservoir layers. This tool was the most challenging one within the ANN model since the number of unknowns was greater. For a two-layered system, the error of CMG and ANN for $k_1, k_2, kv_1, kv_2, \pi, \phi_1$ and ϕ_2 were 1, 5, 4, 10, 1, 1 and 1 percent respectively with the optimum network consists of five hidden layers of 95, 100, 109, 96 and 98 neurons in each layer. It is important to note that the smaller the value, the larger the error seems to be. In the case where K_v or vertical permeability ranges from 0.001 to 10 percent of horizontal permeability, the error is expected to be higher than that of the larger values. The expert tool has been tested using 70 blind data sets within the range and the result is favorable. In the forward tool for instance, the cumulative and gas rate error is approximately 7 and 11 percent.

7.2 Conclusion

- This expert tool is able to better predict the properties that have more influence on production compared to properties with less impact.
- Vertical permeability is a factor to determine the boundary and crossflow condition of the reservoir and due to its small value, has the largest error compared to other variables.
- Hyperbolic tangent sigmoid is proven to be the best transfer function for tool.
- The number of hidden layers is very critical to optimize the network structure and it increases with the complexity of the network.
- There are an optimum number of hidden layers and neurons for each tool that will be determined by trial and error, and for neurons some rules of thumb can be helpful.
- This model is able to predict the number of reservoir layers in an indirect way substituting inputs and outputs in multiple tools.
- Functional links are found to be very decisive for linking the neurons and layers. The number of links needed for any network increases with the complexity of the network.

7.3 Future recommendations

- Due to the low permeability of an unconventional reservoir which requires hydraulic fracturing, a fractured multilayered reservoir can be modeled using ANN.
- A model that predicts properties of a directional well in a multilayered reservoir.

References

1. Alajmi ,M, The development of an artificial neural network as pressure transient analysis tool for applications in double porosity behaviors , Master's thesis in petroleum and natural gas engineering, The Pennsylvania State University, (2003)
2. Al-Fattah. S.M., Startzman .R.A., Predicting Natural gas production using Artificial Neural network. SPE 68593
3. Automatic Parameter Estimation from Well Test Data Using Artificial Neural Network. Arhichanagorn, Suwat. Dallas: SPE, 1995. SPE 30556.
4. Almousa, T. S. Development and Utilization of Integrated Artificial Expert Systems For designing multilateral well configurations, estimating reservoir properties and forecasting reservoir performance. The Pennsylvania State University,(2013)
5. Bailey, D., & Thompson, D. (1990). How to Develop Neural Network. 5(6): 38-47.
6. Beale. M. H., Hagan, M.T., Demuth H.B., Neural Network Toolbox^{MT} Users's Guide R2014a
7. Bidaux. P., Whittle. T.M. Analysis of Pressure and rate Transient Data from Wells in Multilayered Reservoirs: Theory and Application, SPE 24679
8. Bourdet ,D, pressure behavior of layered reservoir with crossflow, SPE paper 13628,1985
9. Chaudhry, Amanat U. Gas Well Testing Handbook, Elsevier, 2003

10. Cleveland, Cutler , Encyclopedia of energy, Volume 1-6, Principles of Artificial Neural networks, Elsevier 2007
11. CMG IMEX. (2012).<http://www.cmgl.ca/software/soft-imex>
12. D.G, Russel, M, Prats (1962) The Practical Aspects of Interlayer Crossflow, 369-PA SPE Journal Paper
13. Demuth, Beale Hagan, Beale, Mark and Hagan, Martin T. Neural Network Toolbox for use with Matlab. Natick, MA: The MathWorks Inc., 2009.
14. Ehlig-Economides C.A, and Joseph J, “A new test for determination of individual layer properties in a multilayered reservoir, SPE paper 14167, 1987
15. Ertekin, T., Abou-Kassem, J. H., & King, G. R. (2001). Basic Applied Reservoir Simulation. Richardson: Society of Petroleum Engineers.
16. Graupe, D. (2007). Principles of Artificial Neural Networks. 2nd Ed. Hackensack: World Scientific .Publishing Co. Pte. Ltd.82
17. I.A. Basheer , M. Hajmeer ,.Artificial neural networks: fundamentals, computing, design, and application. Journal of Microbiological Methods 43 (2000) 3–31
18. Hagan, M. T., Demuth, H. B., & Beale, M. (2002). Neural Network Design. University of Colorado .Bookstore: Campus Pub. Service.
19. Kulga, Ihsan Burak. Development of an artificial neural network for hydraulically fractured horizontal wells in tight gas sands. Master's Thesis: Pennsylvania State University, 2010.

20. Park.H., Well Test Analysis of Multilayered Reservoir with Formation Cross Flow, Stanford University,1989
21. Prats.M., Vogiatzis.J.P., Calculation of Wellbore Pressures and Rate Distribution in Multilayered Reservoirs, 57241-PA SPE Journal Paper - 1999
22. Sui.W , Zhu ,D., Ehlig-Economides., Determining multilayer formation properties from transient temperature and pressure measurements, SPE 57452
23. S.S.Dakshindas, T. Ertekin, and A.S. Grader, Virtual Well Testing, The Pennsylvania State University, SPE 57452
24. Torcuk, M. A., Fakcharoenphol, P., & Kazemi, H. (2013). Theory and Application of Pressure and Rate Transient Analysis in Unconventional Reservoirs. ATCE. New Orleans, LA: SPE.
25. Tarman ,M, The development of an artificial neural network as pressure transient analysis tool for multilayered reservoir with or without cross flow , Master's thesis in petroleum and natural gas engineering, The Pennsylvania State University, University Park, (2003)

Appendix A

Data sample of the three-layered reservoir generated by the simulator

INUNIT FIELD

WSRF WELL 1

WSRF GRID TIME

WSRF SECTOR TIME

OUTSRF WELL LAYER NONE

OUTSRF RES ALL

OUTSRF GRID SO SG SW PRES OILPOT BPP SSPRES WINFLUX

WPRN GRID 0

OUTPRN GRID NONE

OUTPRN RES NONE

**\$ Distance units: ft

RESULTS XOFFSET 0.0000

RESULTS YOFFSET 0.0000

RESULTS ROTATION 0.0000 **\$ (DEGREES)

RESULTS AXES-DIRECTIONS 1.0 -1.0 1.0

**\$

**\$ Definition of fundamental cartesian grid

**\$

GRID VARI 50 50 3

KDIR DOWN

DI IVAR

50*59.03

DJ JVAR

50*59.03

DK ALL

2500*40 2500*50 2500*60

DTOP

2500*9000

PERMI KVAR

.5 1 4

**\$ 0 = null block, 1 = active block

NULL CON 1

POR KVAR

0.15 0.1 .08

PERMJ KVAR

.5 1 4

PERMK KVAR

.009 0.09 .5

**\$ 0 = pinched block, 1 = active block

PINCHOUTARRAY CON 1

CPOR .000001

MODEL GASWATER

TRES 200

**\$ p Eg visg

PVTG EG 1

14.696 4.44274 0.0135995
813.716 259.805 0.0144494
1612.74 533.708 0.015895
2411.76 805.071 0.0177671
3210.78 1052.62 0.019882
4009.8 1266.59 0.0220641
4808.82 1447.48 0.0242007
5607.84 1600.05 0.0262373
6406.86 1729.63 0.0281546
7205.88 1840.91 0.0299522
8004.9 1937.64 0.0316377
8803.92 2022.73 0.0332221
9602.94 2098.42 0.0347164
10402 2166.4 0.0361312
11201 2228.01 0.0374755
12000 2284.28 0.0387577

BWI 1.02776

CVW 0

CW 3.3202e-006

DENSITY WATER 60.5501

REFPW 14.696

VWI 0.219053

GRAVITY GAS .7

ROCKFLUID

RPT 1

**\$ Sw krw Pcgw

SWT

0 0 0

1 1 0

**\$ Sl krg

SLT

0 1

1 0

RTYPE CON 1

INITIAL

VERTICAL DEPTH_AVE WATER_GAS EQUIL NOTRANZONE

REFDEPTH 9000

REFPRES 7000

DWGC 20000

GOC_PC 0

WOC_PC 0

NUMERICAL

RUN

DATE 2014 1 1

**\$

WELL 'Well-1'

PRODUCER 'Well-1'

OPERATE MIN BHP 3500 CONT

**\$ rad geofac wfrac skin

GEOMETRY K 0.25 0.37 1. 0.

PERF GEOA 'Well-1'

**\$ UBA ff Status Connection

25 25 1 1. OPEN FLOW-TO 'SURFACE' REFLAYER

25 25 2 1. OPEN FLOW-TO 1

25 25 3 1. OPEN FLOW-TO 2

DATE 2014 2 1.00000

DATE 2014 3 1.00000

DATE 2014 4 1.00000

DATE 2014 5 1.00000

DATE 2014 6 1.00000

DATE 2014 7 1.00000

DATE 2014 8 1.00000

DATE 2014 9 1.00000

DATE 2014 10 1.00000

DATE 2014 11 1.00000

DATE 2014 12 1.00000

DATE 2015 1 1.00000

DATE 2015 2 1.00000

DATE 2015 3 1.00000

DATE 2015 4 1.00000

DATE 2015 5 1.00000

DATE 2015 6 1.00000

DATE 2015 7 1.00000

DATE 2015 8 1.00000
DATE 2015 9 1.00000
DATE 2015 10 1.00000
DATE 2015 11 1.00000
DATE 2015 12 1.00000
DATE 2016 1 1.00000
DATE 2016 2 1.00000
DATE 2016 3 1.00000
DATE 2016 4 1.00000
DATE 2016 5 1.00000
DATE 2016 6 1.00000
DATE 2016 7 1.00000
DATE 2016 8 1.00000
DATE 2016 9 1.00000
DATE 2016 10 1.00000
DATE 2016 11 1.00000
DATE 2016 12 1.00000
DATE 2017 1 1.00000
DATE 2017 2 1.00000
DATE 2017 3 1.00000
DATE 2017 4 1.00000
DATE 2017 5 1.00000
DATE 2017 6 1.00000
DATE 2017 7 1.00000
DATE 2017 8 1.00000

DATE 2017 9 1.00000
DATE 2017 10 1.00000
DATE 2017 11 1.00000
DATE 2017 12 1.00000
DATE 2018 1 1.00000
DATE 2018 2 1.00000
DATE 2018 3 1.00000
DATE 2018 4 1.00000
DATE 2018 5 1.00000
DATE 2018 6 1.00000
DATE 2018 7 1.00000
DATE 2018 8 1.00000
DATE 2018 9 1.00000
DATE 2018 10 1.00000
DATE 2018 11 1.00000
DATE 2018 12 1.00000
DATE 2019 1 1.00000
DATE 2019 2 1.00000
DATE 2019 3 1.00000
DATE 2019 4 1.00000
DATE 2019 5 1.00000
DATE 2019 6 1.00000
DATE 2019 7 1.00000
DATE 2019 8 1.00000
DATE 2019 9 1.00000

DATE 2019 10 1.00000
DATE 2019 11 1.00000
DATE 2019 12 1.00000
DATE 2020 1 1.00000
DATE 2020 2 1.00000
DATE 2020 3 1.00000
DATE 2020 4 1.00000
DATE 2020 5 1.00000
DATE 2020 6 1.00000
DATE 2020 7 1.00000
DATE 2020 8 1.00000
DATE 2020 9 1.00000
DATE 2020 10 1.00000
DATE 2020 11 1.00000
DATE 2020 12 1.00000
DATE 2021 1 1.00000
DATE 2021 2 1.00000
DATE 2021 3 1.00000
DATE 2021 4 1.00000
DATE 2021 5 1.00000
DATE 2021 6 1.00000
DATE 2021 7 1.00000
DATE 2021 8 1.00000
DATE 2021 9 1.00000
DATE 2021 10 1.00000

DATE 2021 11 1.00000
DATE 2021 12 1.00000
DATE 2022 1 1.00000
DATE 2022 2 1.00000
DATE 2022 3 1.00000
DATE 2022 4 1.00000
DATE 2022 5 1.00000
DATE 2022 6 1.00000
DATE 2022 7 1.00000
DATE 2022 8 1.00000
DATE 2022 9 1.00000
DATE 2022 10 1.00000
DATE 2022 11 1.00000
DATE 2022 12 1.00000
DATE 2023 1 1.00000
DATE 2023 2 1.00000
DATE 2023 3 1.00000
DATE 2023 4 1.00000
DATE 2023 5 1.00000
DATE 2023 6 1.00000
DATE 2023 7 1.00000
DATE 2023 8 1.00000
DATE 2023 9 1.00000
DATE 2023 10 1.00000
DATE 2023 11 1.00000

DATE 2023 12 1.00000

DATE 2024 1 1.00000

DATE 2024 2 1.00000

DATE 2024 3 1.00000

DATE 2024 4 1.00000

DATE 2024 5 1.00000

DATE 2024 6 1.00000

DATE 2024 7 1.00000

DATE 2024 8 1.00000

DATE 2024 9 1.00000

DATE 2024 10 1.00000

DATE 2024 11 1.00000

DATE 2024 12 1.00000

DATE 2025 1 1.00000

DATE 2025 2 1.00000

DATE 2025 3 1.00000

DATE 2025 4 1.00000

DATE 2025 5 1.00000

DATE 2025 6 1.00000

DATE 2025 7 1.00000

DATE 2025 8 1.00000

DATE 2025 9 1.00000

DATE 2025 10 1.00000

DATE 2025 11 1.00000

DATE 2025 12 1.00000
DATE 2026 1 1.00000
DATE 2026 2 1.00000
DATE 2026 3 1.00000
DATE 2026 4 1.00000
DATE 2026 5 1.00000
DATE 2026 6 1.00000
DATE 2026 7 1.00000
DATE 2026 8 1.00000
DATE 2026 9 1.00000
DATE 2026 10 1.00000
DATE 2026 11 1.00000
DATE 2026 12 1.00000
DATE 2027 1 1.00000
DATE 2027 2 1.00000
DATE 2027 3 1.00000
DATE 2027 4 1.00000
DATE 2027 5 1.00000
DATE 2027 6 1.00000
DATE 2027 7 1.00000
DATE 2027 8 1.00000
DATE 2027 9 1.00000
DATE 2027 10 1.00000
DATE 2027 11 1.00000
DATE 2027 12 1.00000

DATE 2028 1 1.00000
DATE 2028 2 1.00000
DATE 2028 3 1.00000
DATE 2028 4 1.00000
DATE 2028 5 1.00000
DATE 2028 6 1.00000
DATE 2028 7 1.00000
DATE 2028 8 1.00000
DATE 2028 9 1.00000
DATE 2028 10 1.00000
DATE 2028 11 1.00000
DATE 2028 12 1.00000
DATE 2029 1 1.00000

Appendix B

Forward network and simulator comparison plots in two-layered reservoir

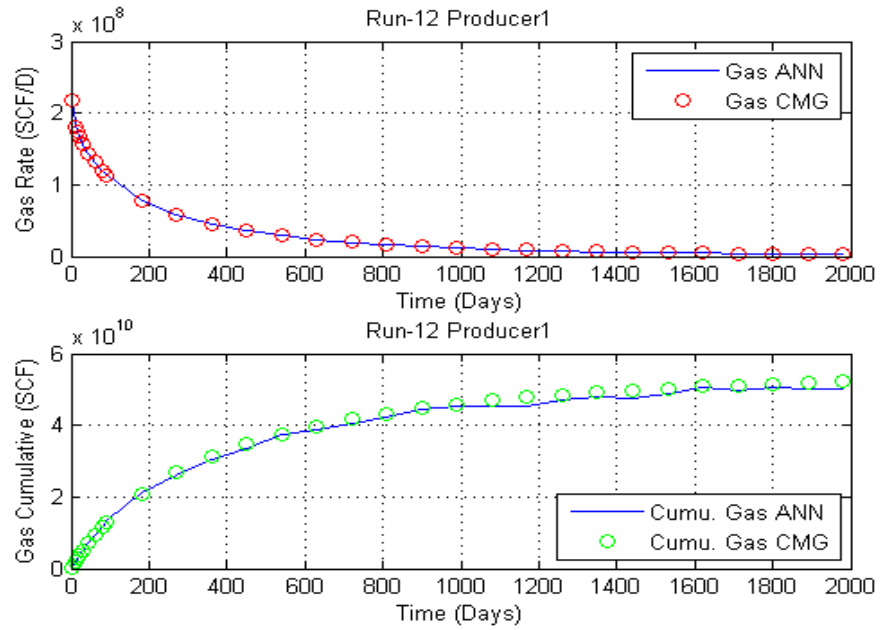


Figure 61 data set 12 of gas rate and cumulative production data of ANN and CMG

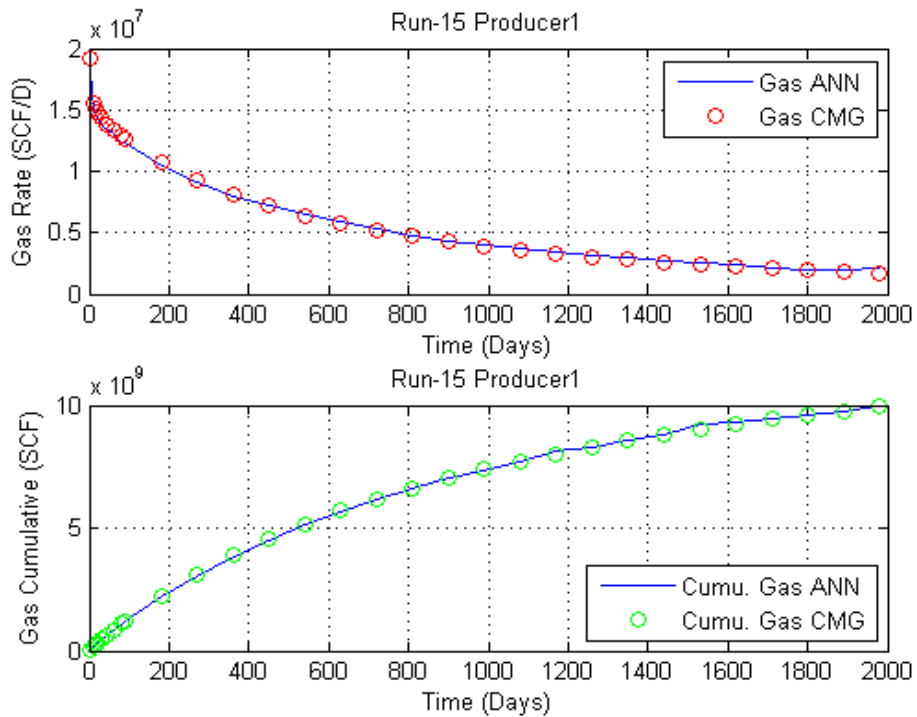


Figure 62 data set 15 of gas rate and cumulative production data of ANN and CMG

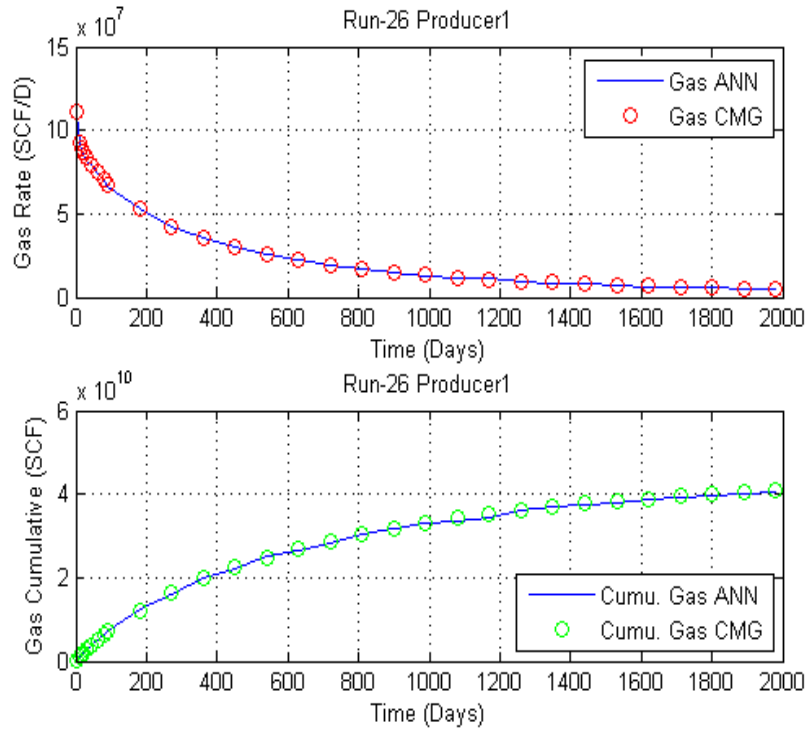


Figure 63 data set 26 of gas rate and cumulative production data of ANN and CMG

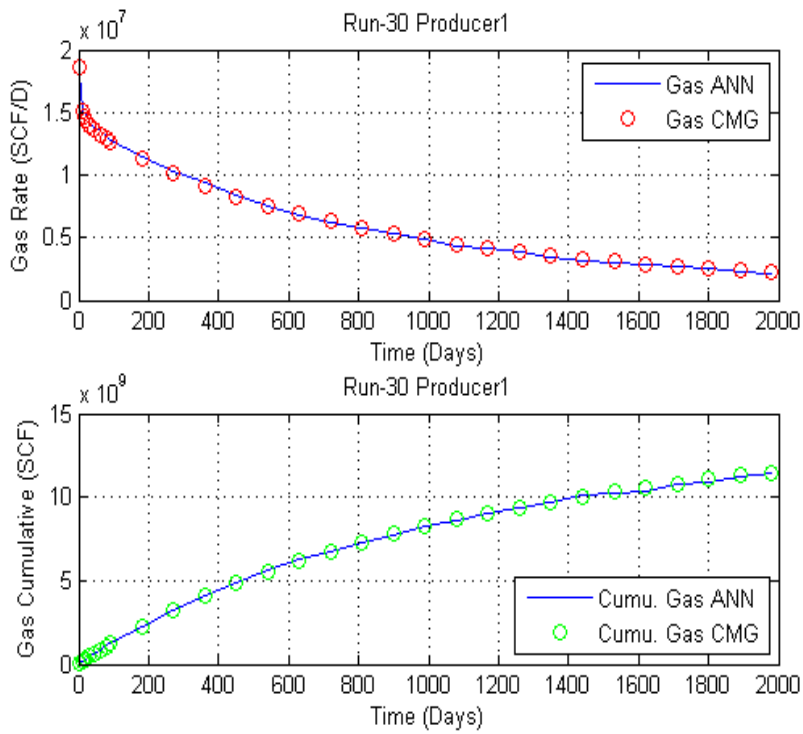


Figure 64 data set 30 of gas rate and cumulative production data of ANN and CMG

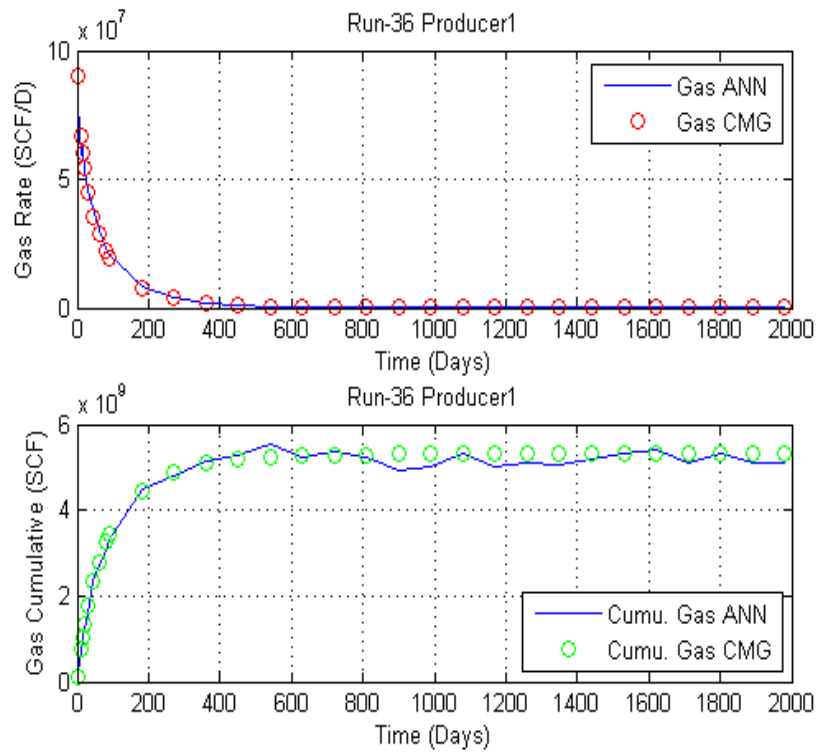


Figure 65 data set 36 of gas rate and cumulative production data of ANN and CMG

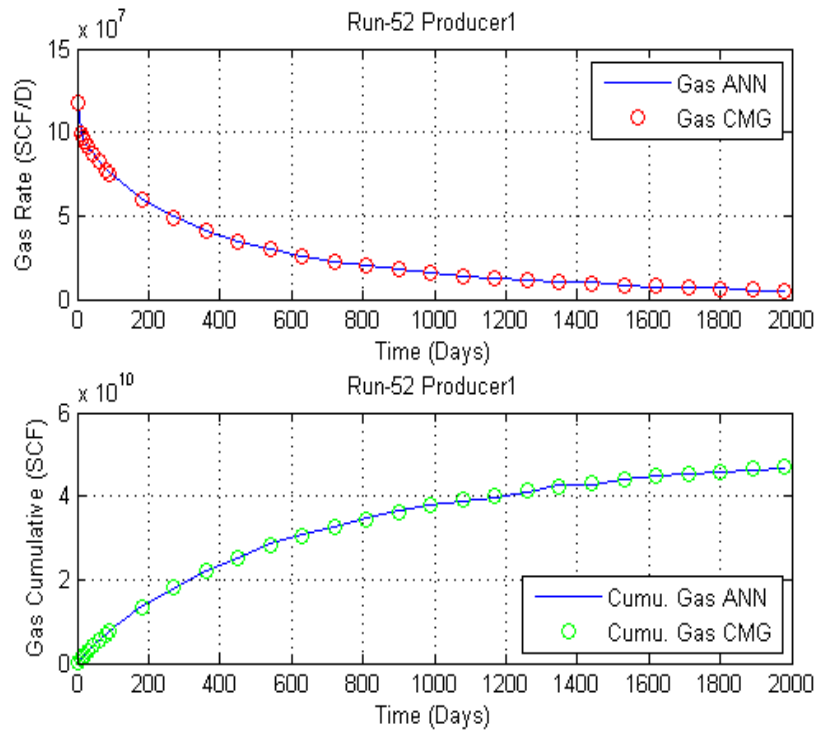


Figure 66 data set 52 of gas rate and cumulative production data of ANN and CMG

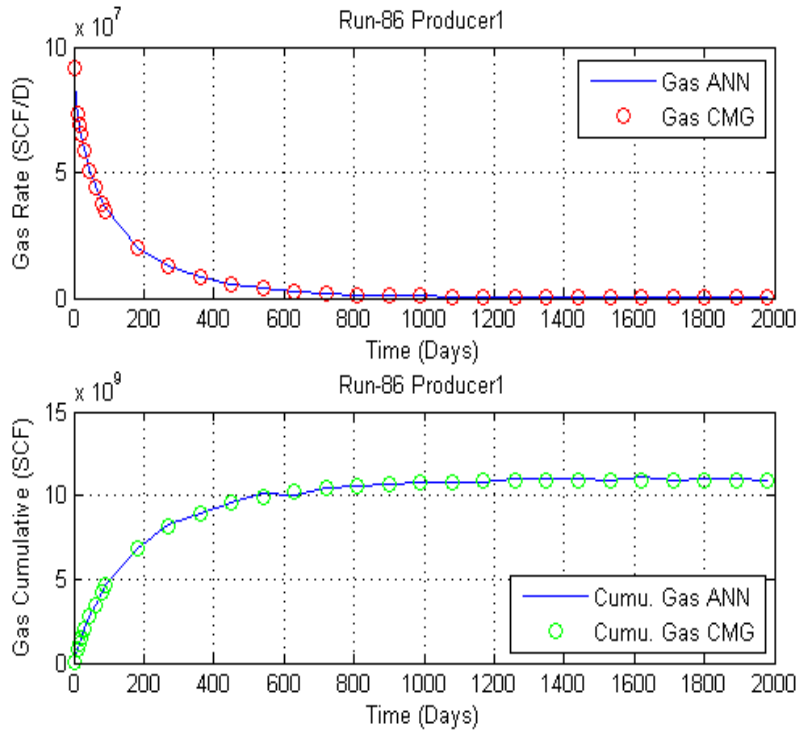


Figure 67 data set 86 of gas rate and cumulative production data of ANN and CMG

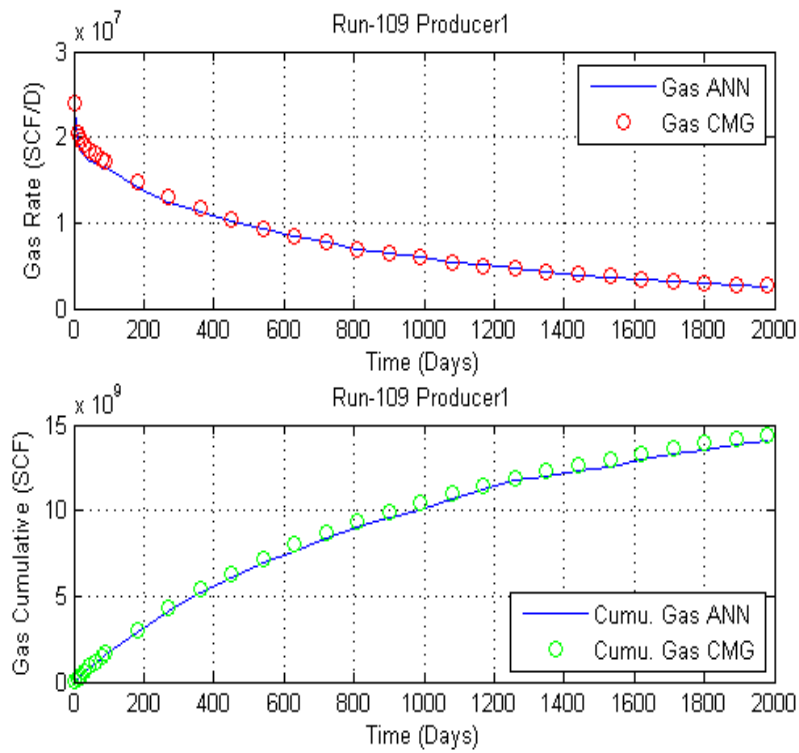


Figure 68 data set 109 of gas rate and cumulative production data of ANN and CMG

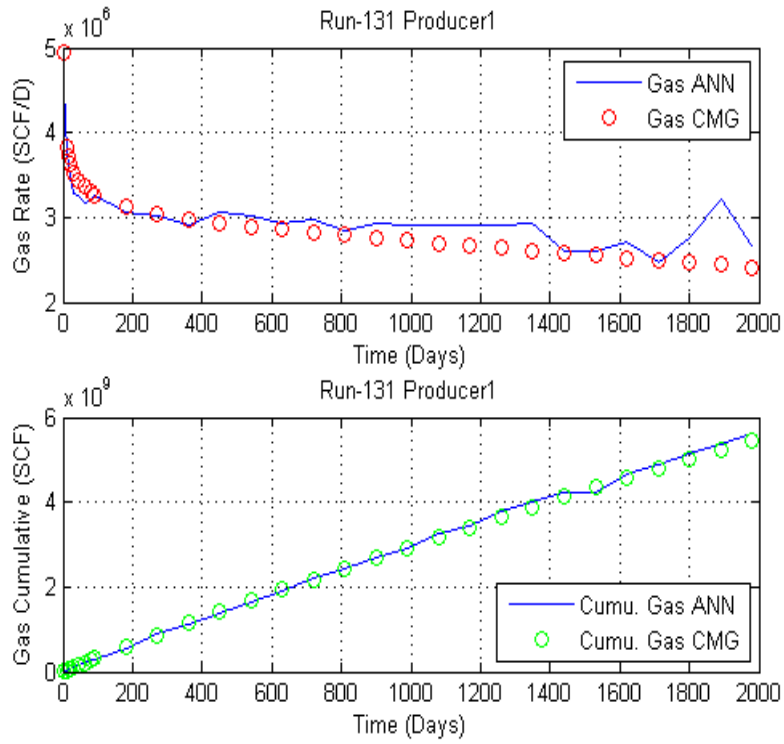


Figure 69 data set 131 of gas rate and cumulative production data of ANN and CMG

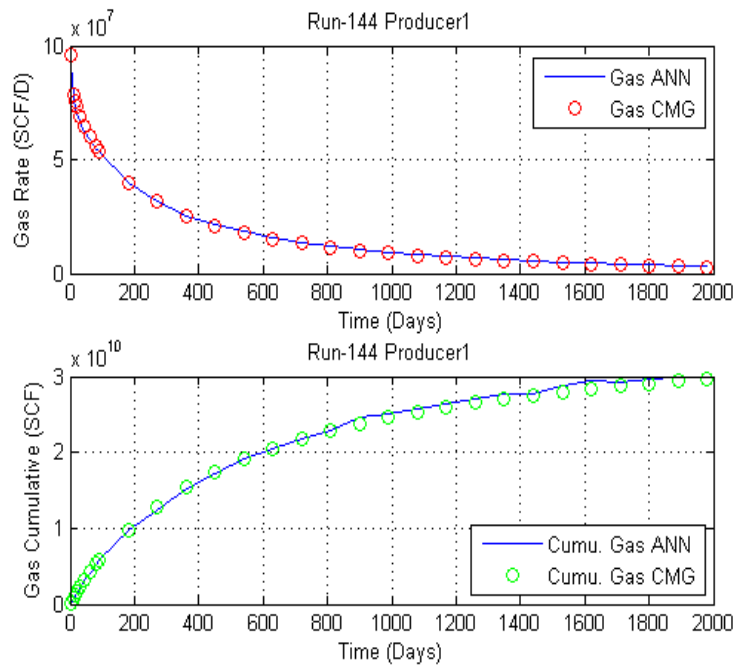


Figure 70 data set 144 of gas rate and cumulative production data of ANN and CMG

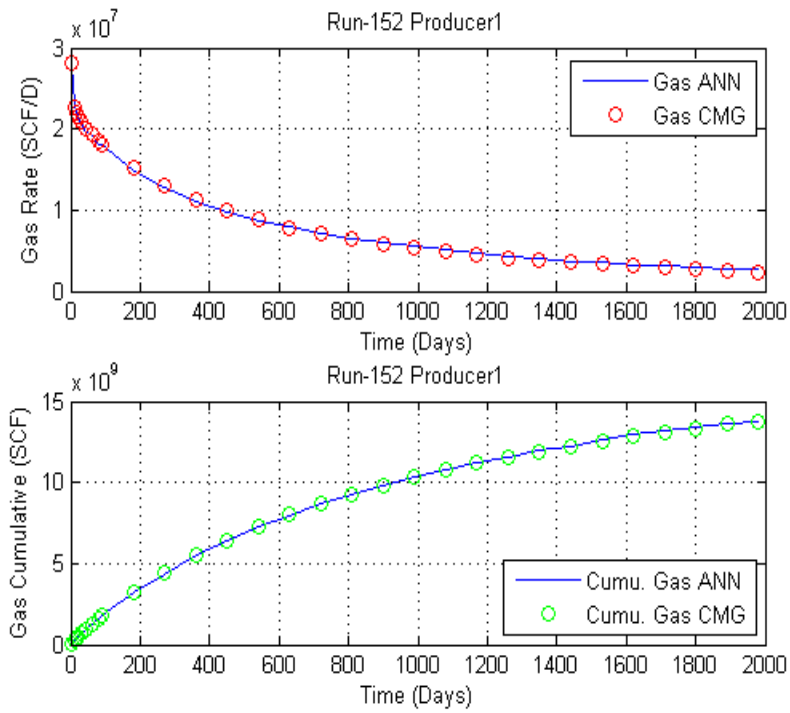


Figure 71 data set 152 of gas rate and cumulative production data of ANN and CMG

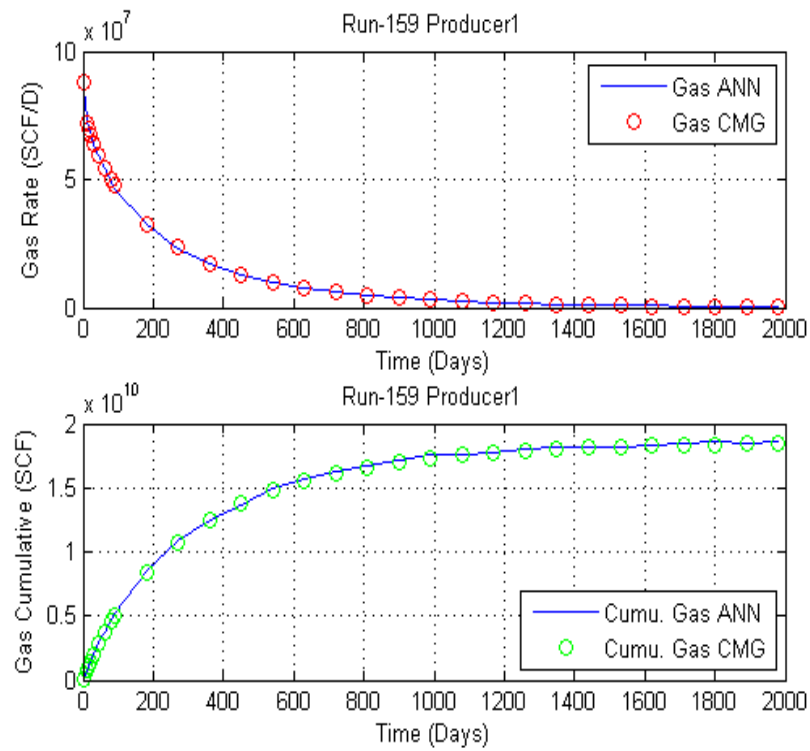


Figure 72 data set 159 of gas rate and cumulative production data of ANN and CMG

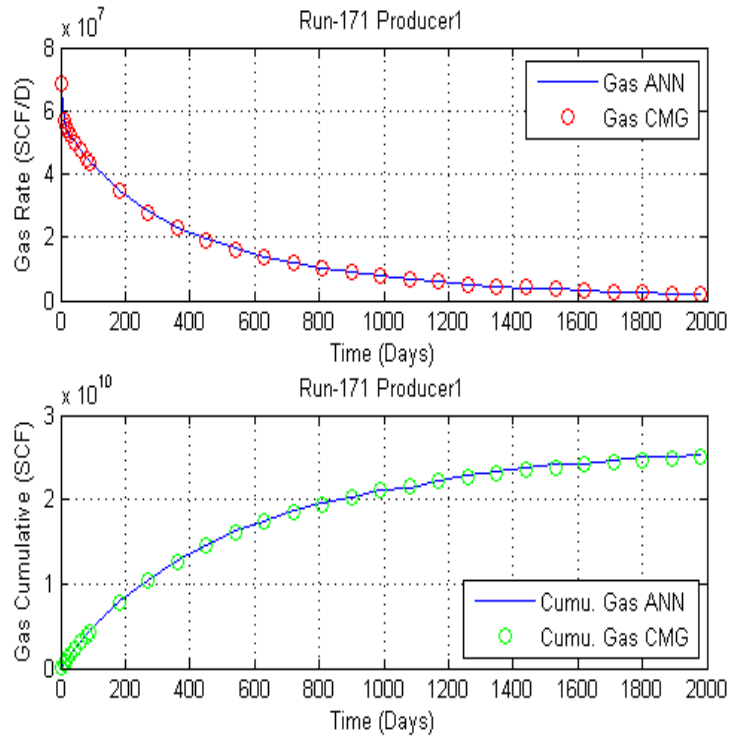


Figure 73 data set 171 of gas rate and cumulative production data of ANN and CMG

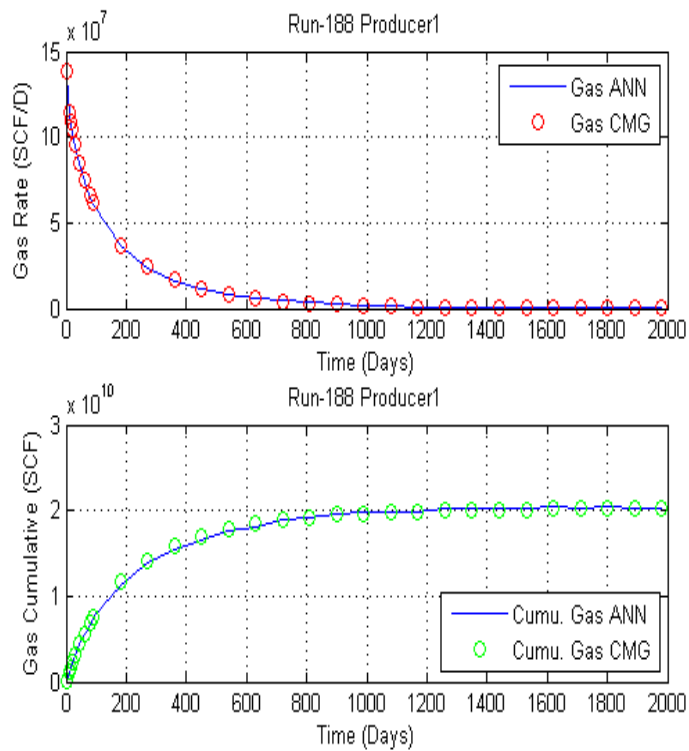


Figure 74 data set 188 of gas rate and cumulative production data of ANN and CMG

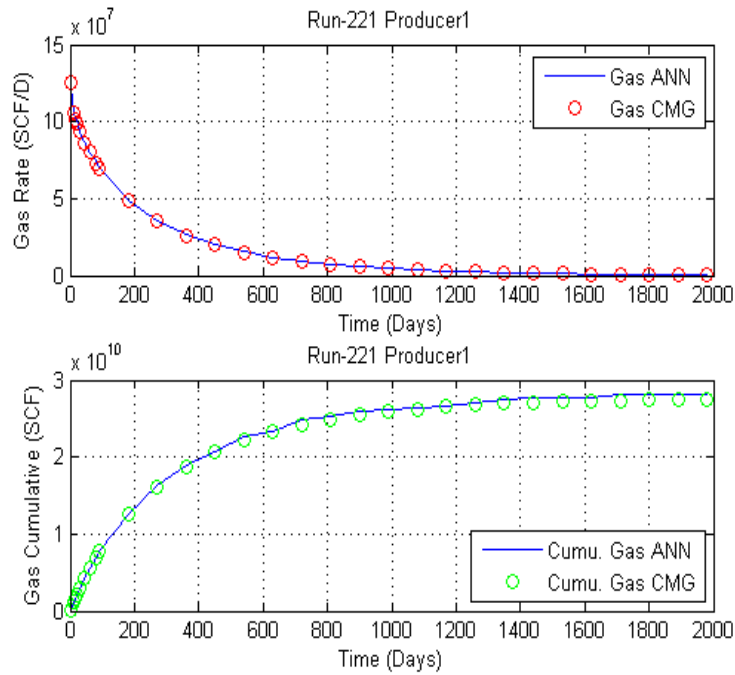


Figure 75 data set 221 of gas rate and cumulative production data of ANN and CMG

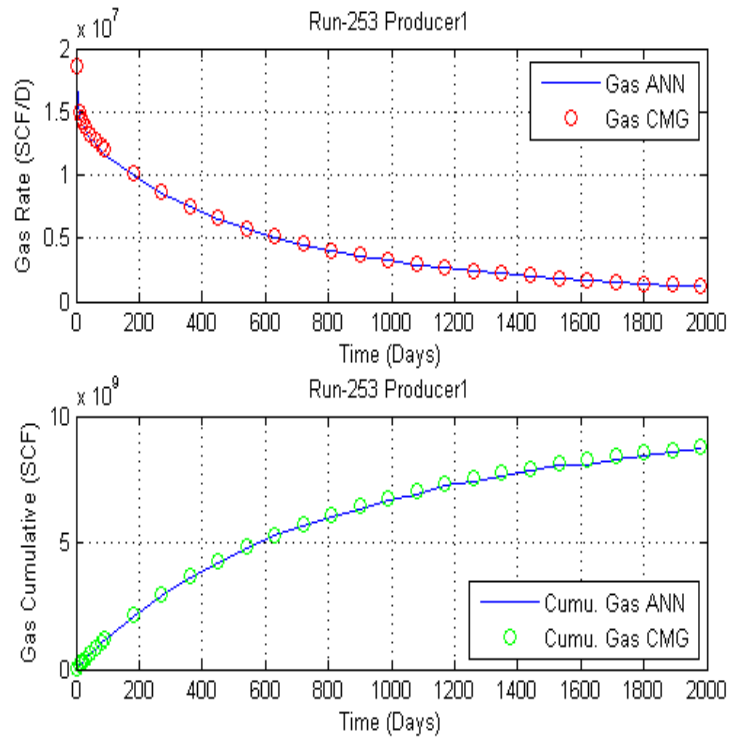


Figure 76 data set 253 of gas rate and cumulative production data of ANN and CMG

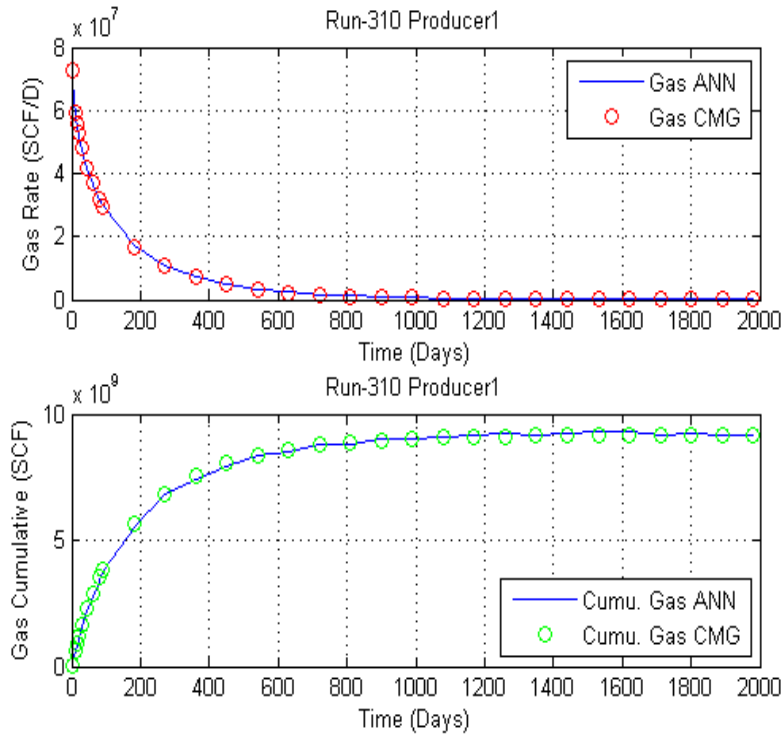


Figure 77 data set 310 of gas rate and cumulative production data of ANN and CMG

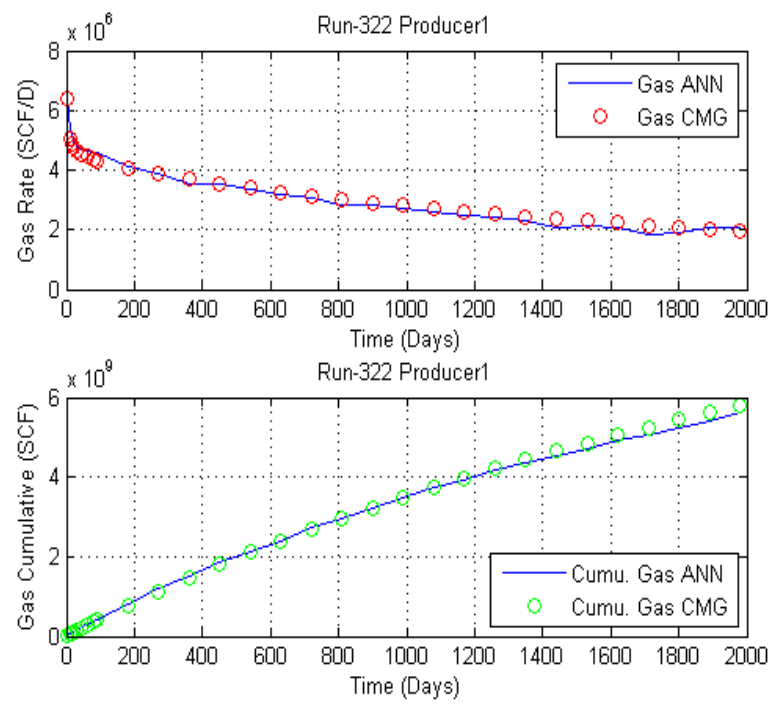


Figure 78 data set 322 of gas rate and cumulative production data of ANN and CMG

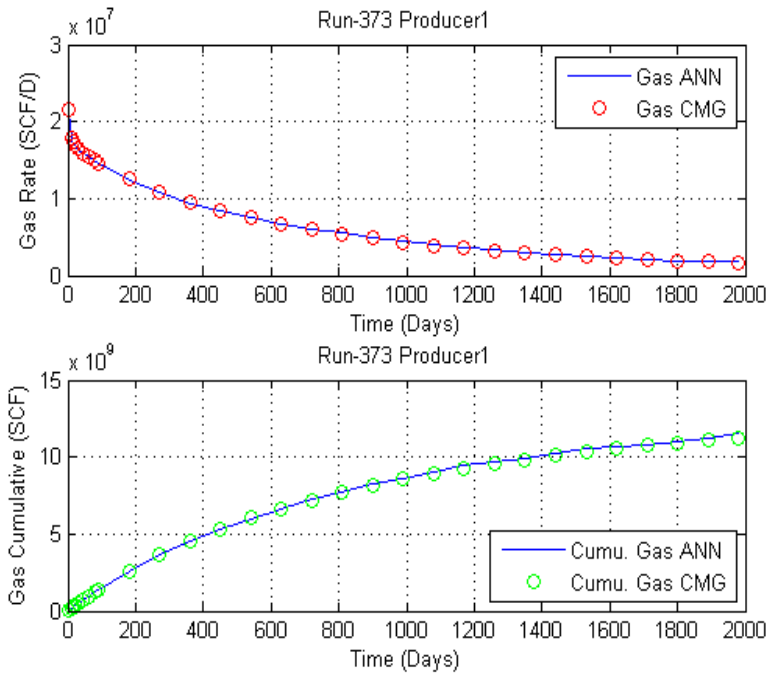


Figure 79 data set 373 of gas rate and cumulative production data of ANN and CMG

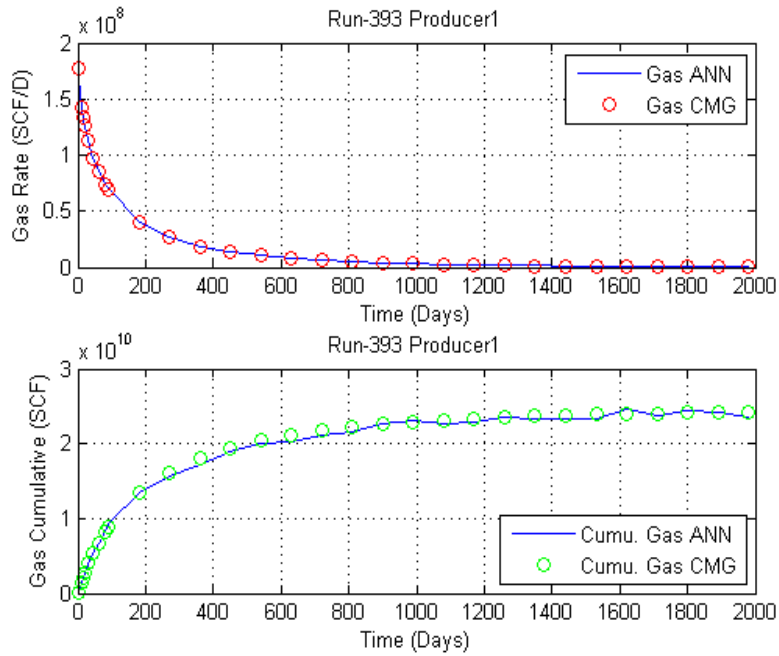


Figure 80 data set 393 of gas rate and cumulative production data of ANN and CMG

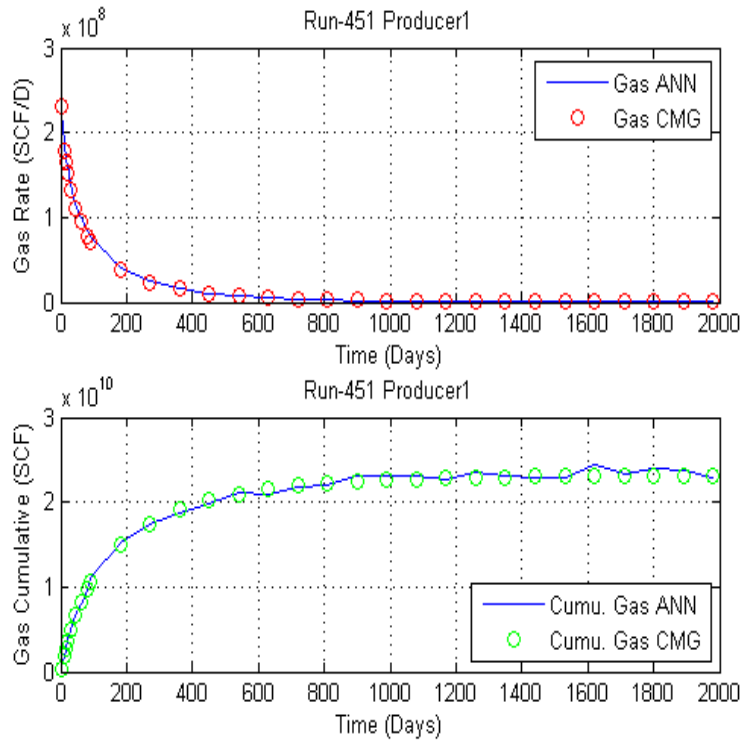


Figure 81 data set 451 of gas rate and cumulative production data of ANN and CMG

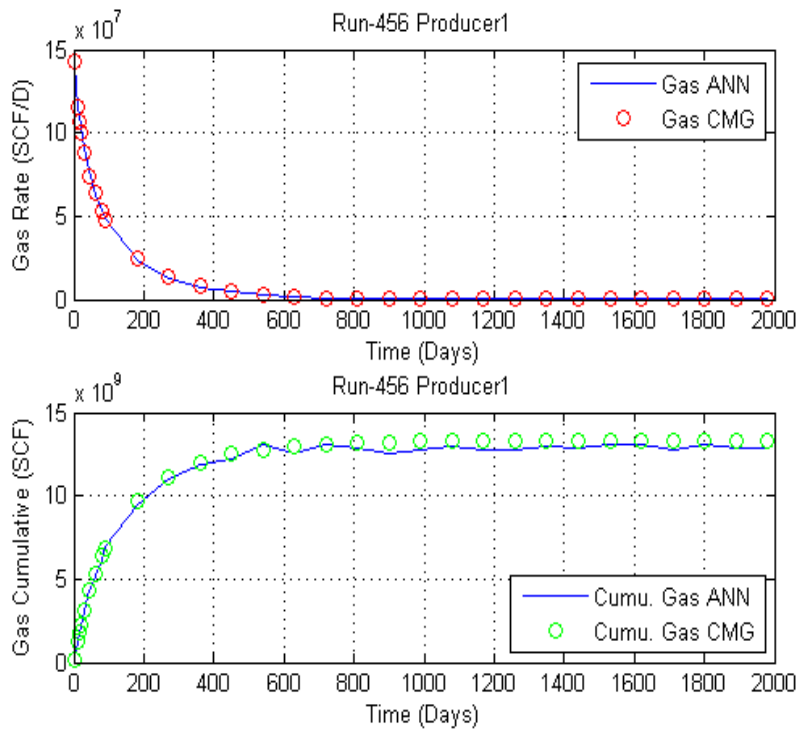


Figure 82 data set 456 of gas rate and cumulative production data of ANN and CMG

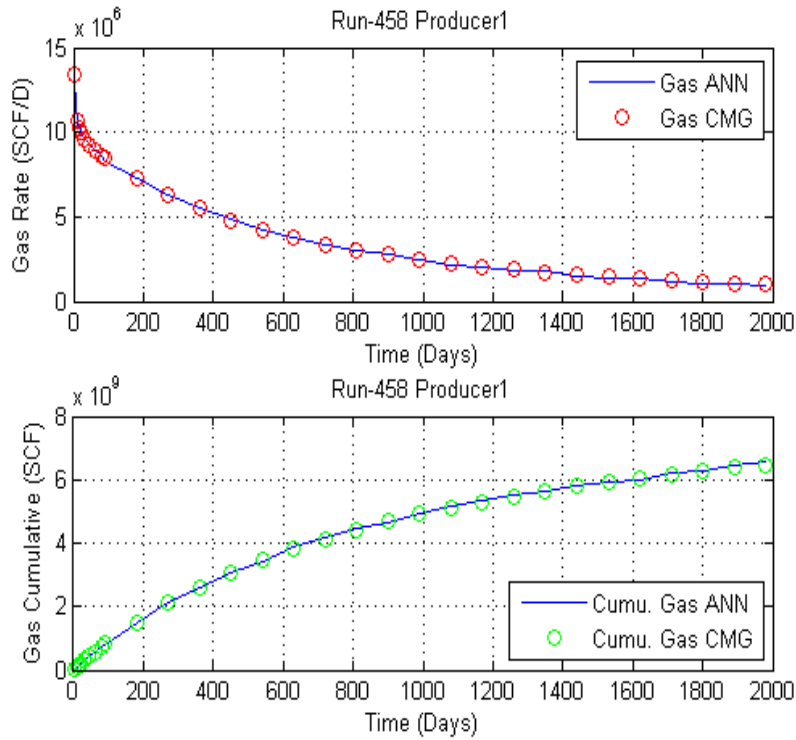


Figure 83 data set 458 of gas rate and cumulative production data of ANN and CMG

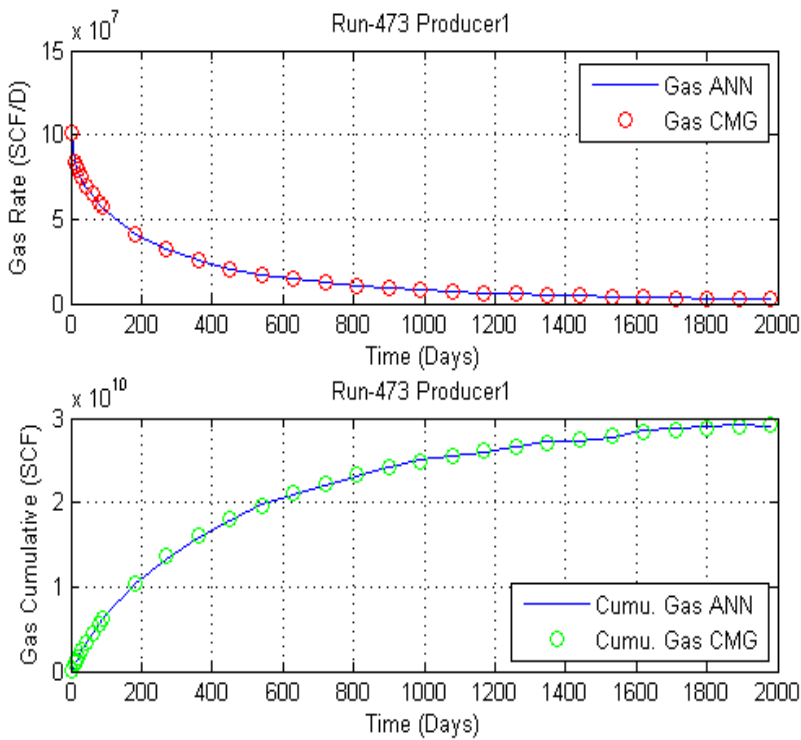


Figure 84 data set 473 of gas rate and cumulative production data of ANN and CMG

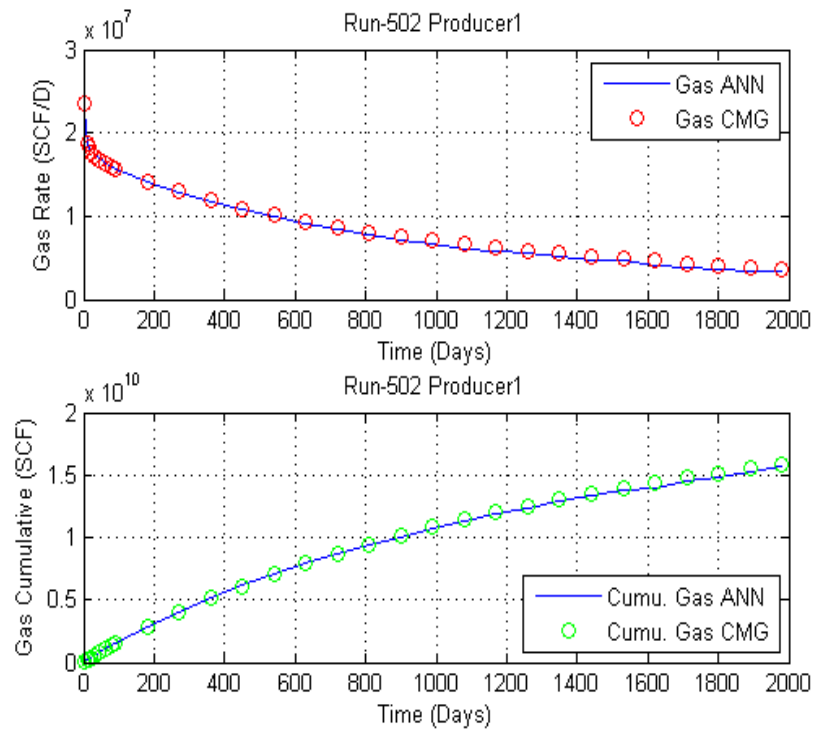


Figure 85 data set 502 of gas rate and cumulative production data of ANN and CMG

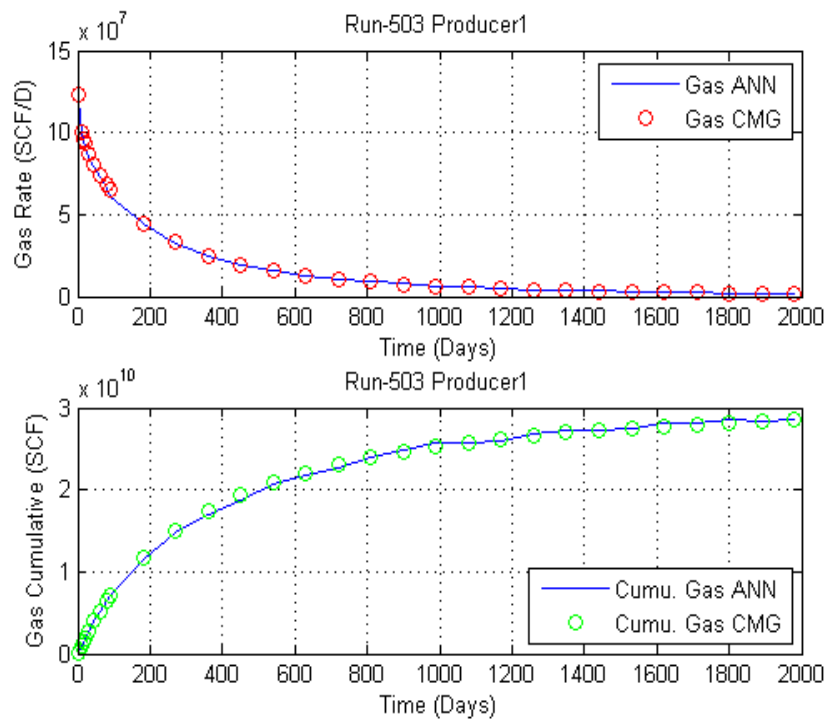


Figure 86 data set 503 of gas rate and cumulative production data of ANN and CMG

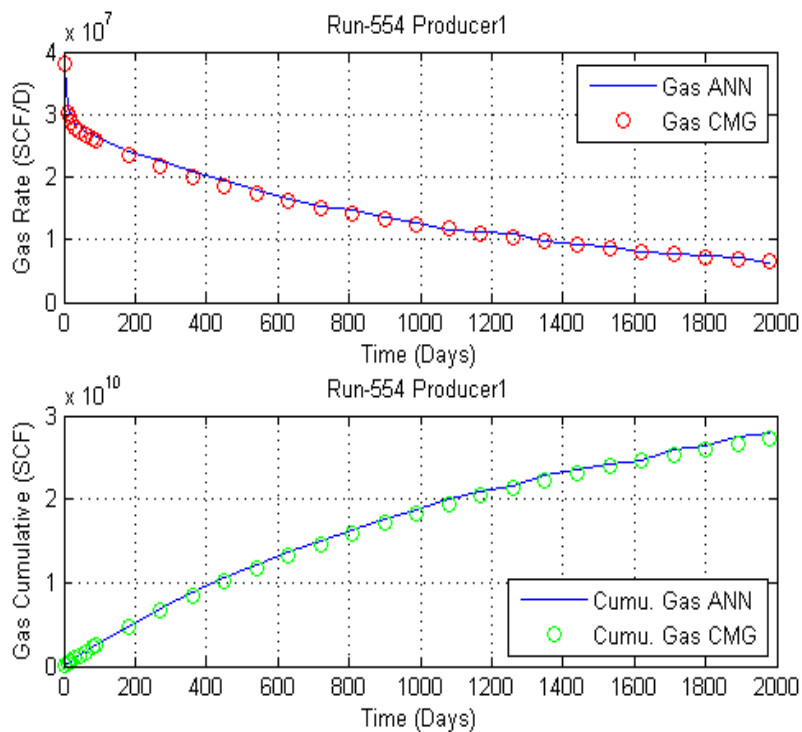


Figure 87 data set 554 of gas rate and cumulative production data of ANN and CMG

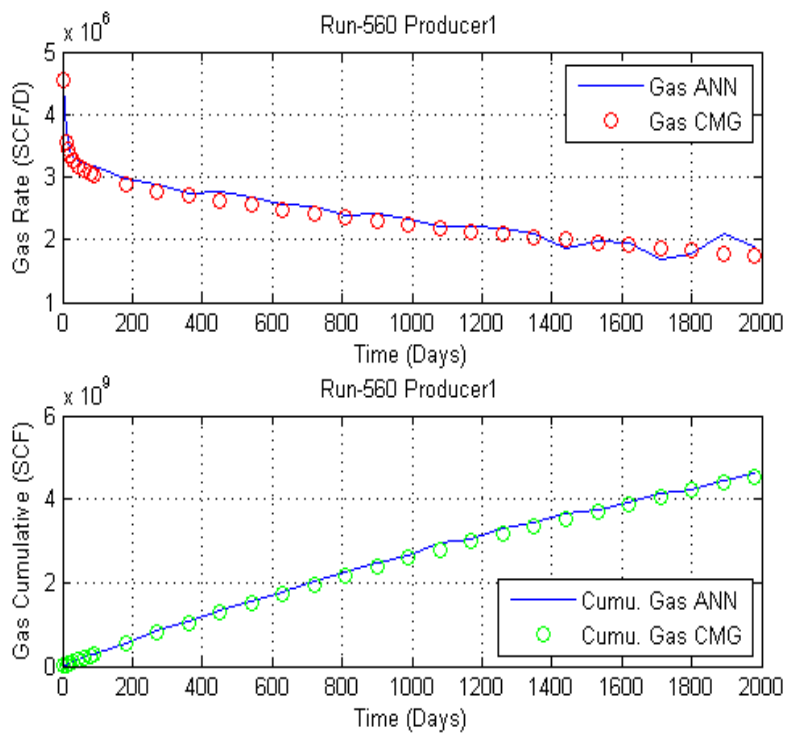


Figure 88 data set 560 of gas rate and cumulative production data of ANN and CMG

Appendix C

Forward network and simulator comparison plots in three-layered reservoir

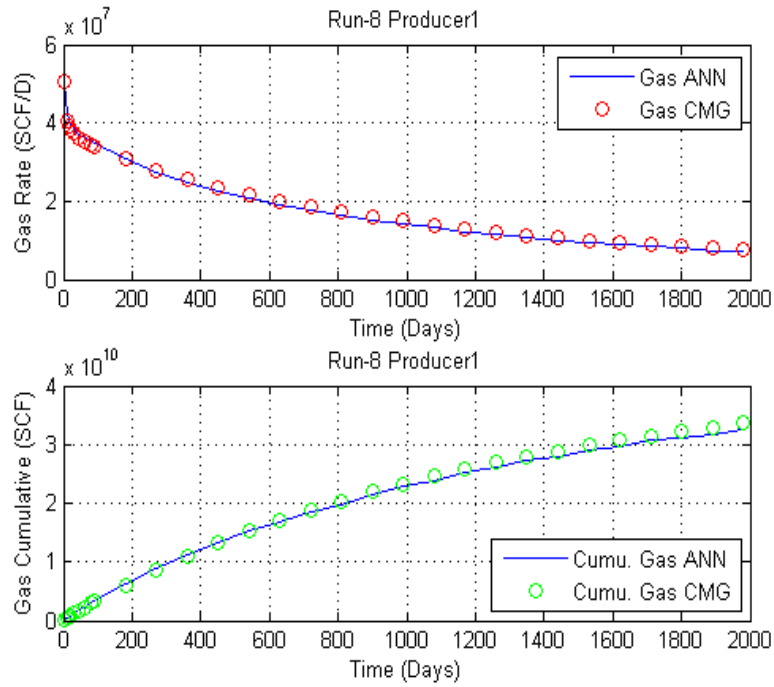


Figure 89 Data set 8 of forward network for three-layered system

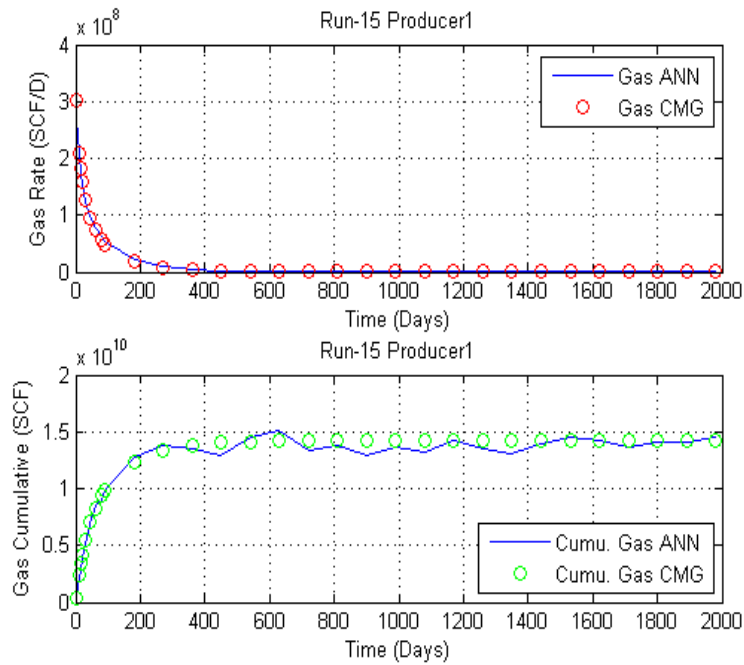


Figure 90 Data set 15 of forward network for three-layered system

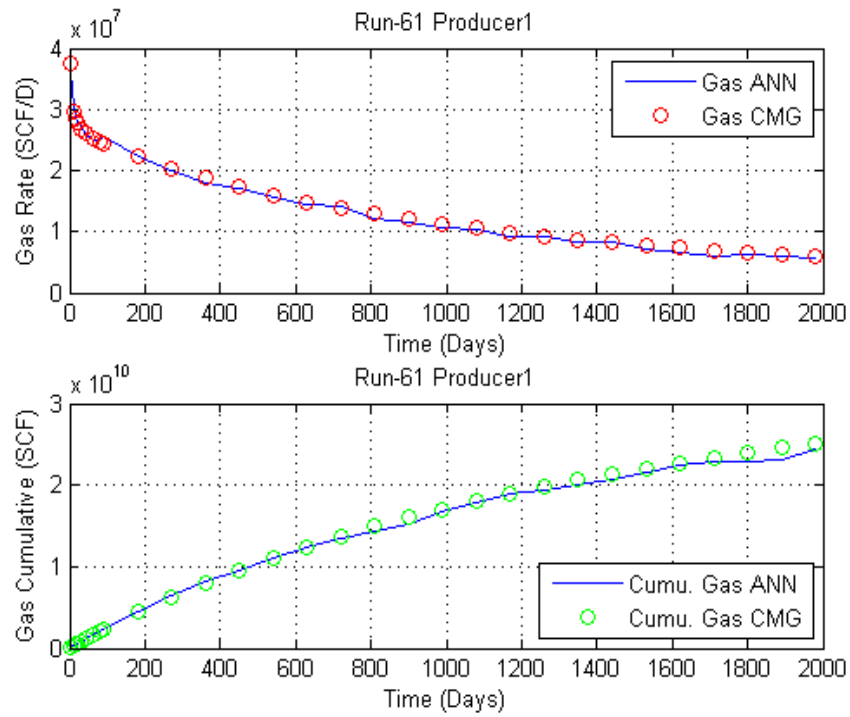


Figure 91 Data set 61 of forward network for three-layered system

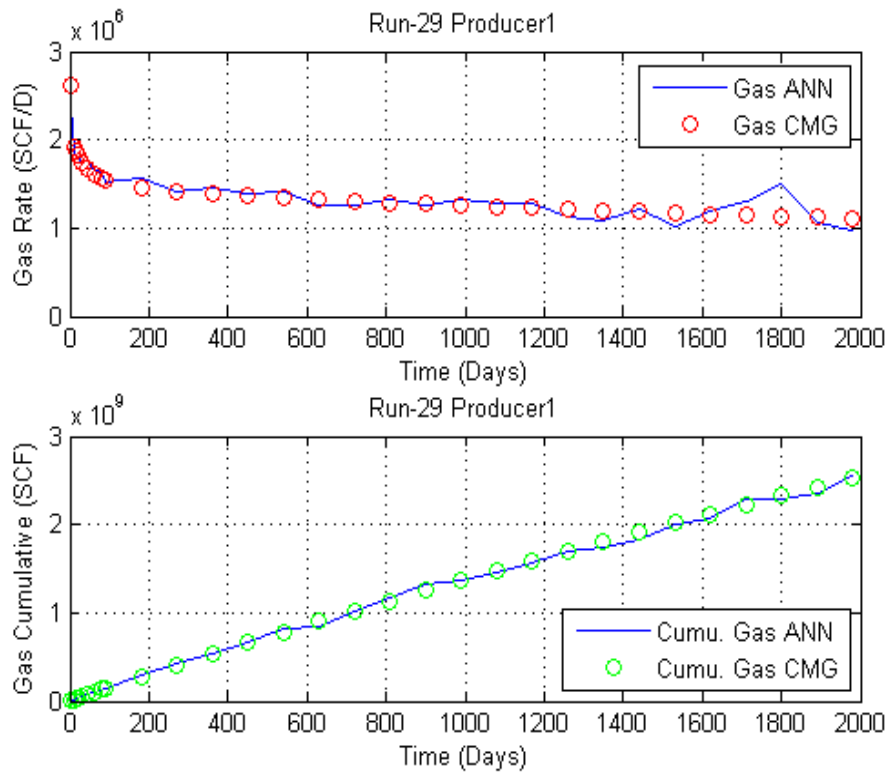


Figure 92 Data set 29 of forward network for three-layered system

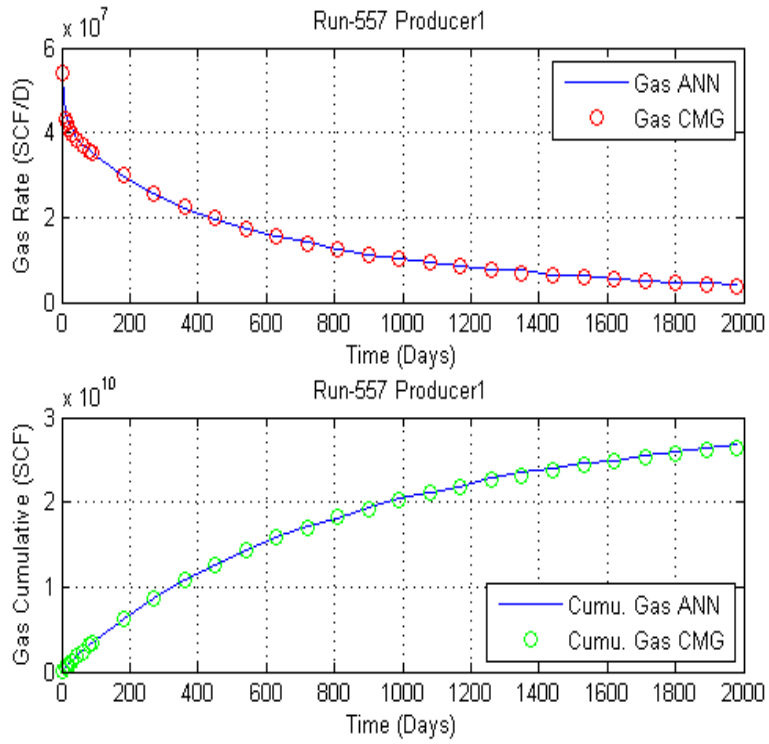


Figure 93 Data set 557 of forward network for three-layered system

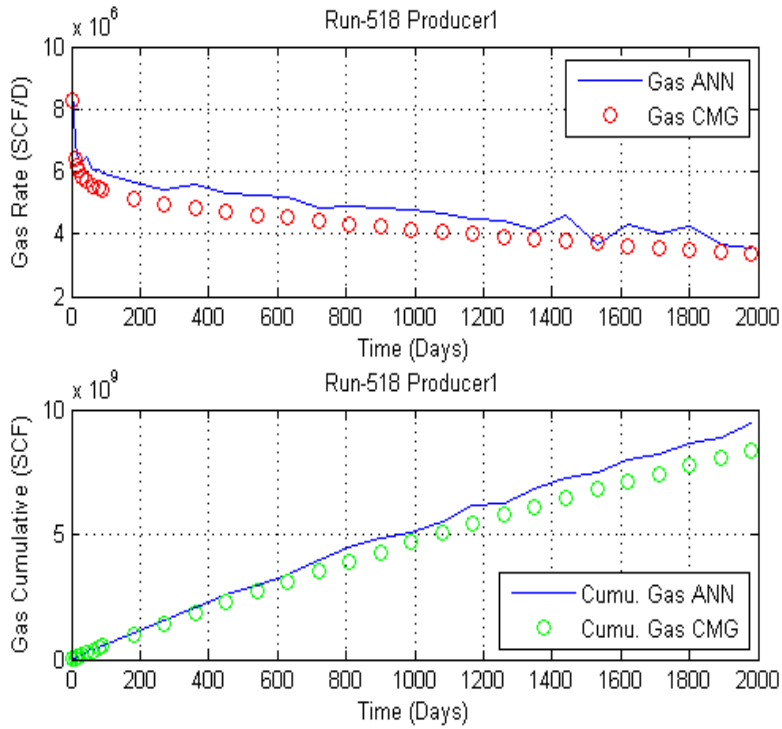


Figure 94 Data set 518 of forward network for three-layered system

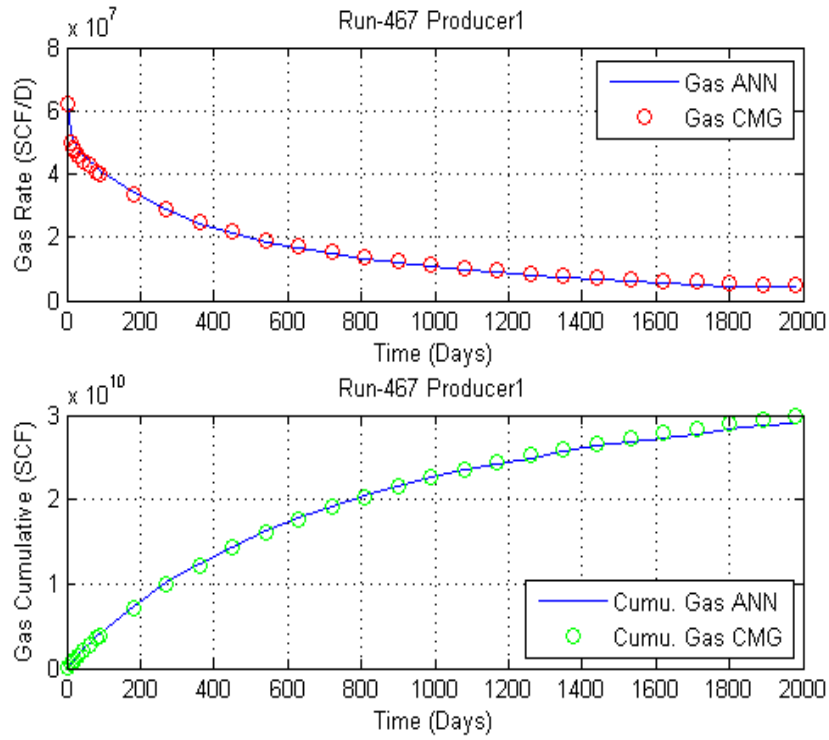


Figure 95 Data set 467 of forward network for three-layered system

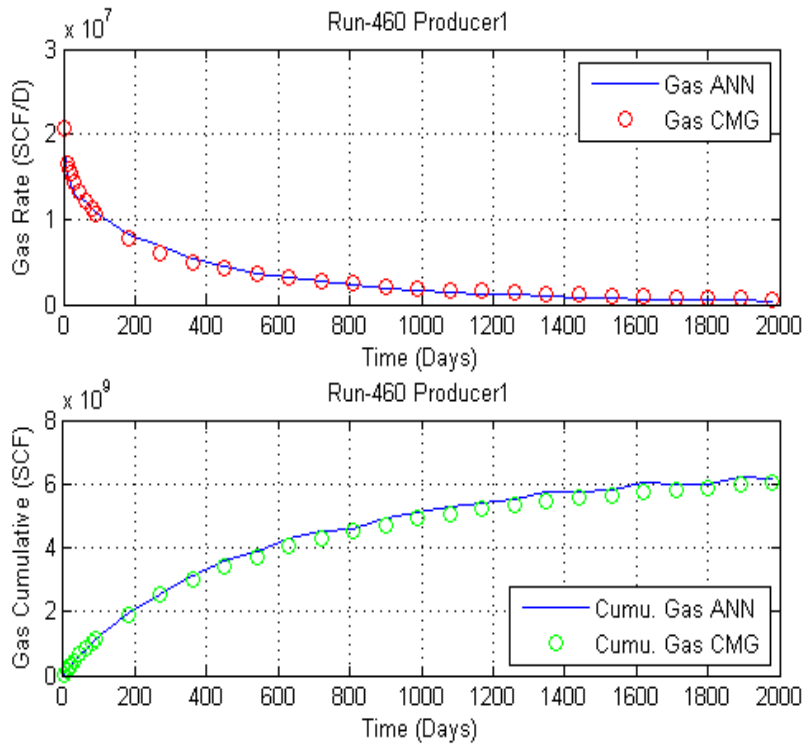


Figure 96 Data set 460 of forward network for three-layered system

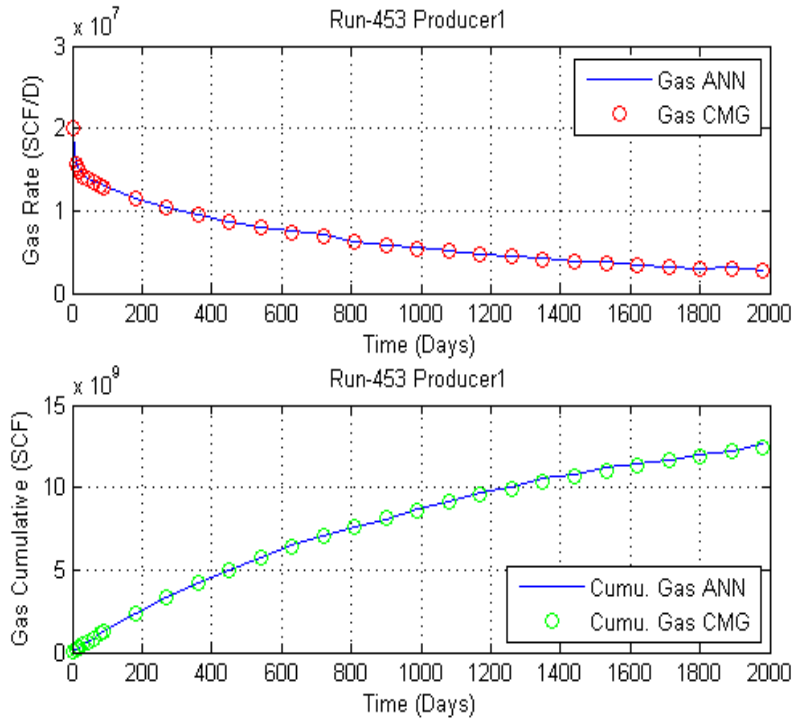


Figure 97 Data set 453 of forward network for three-layered system

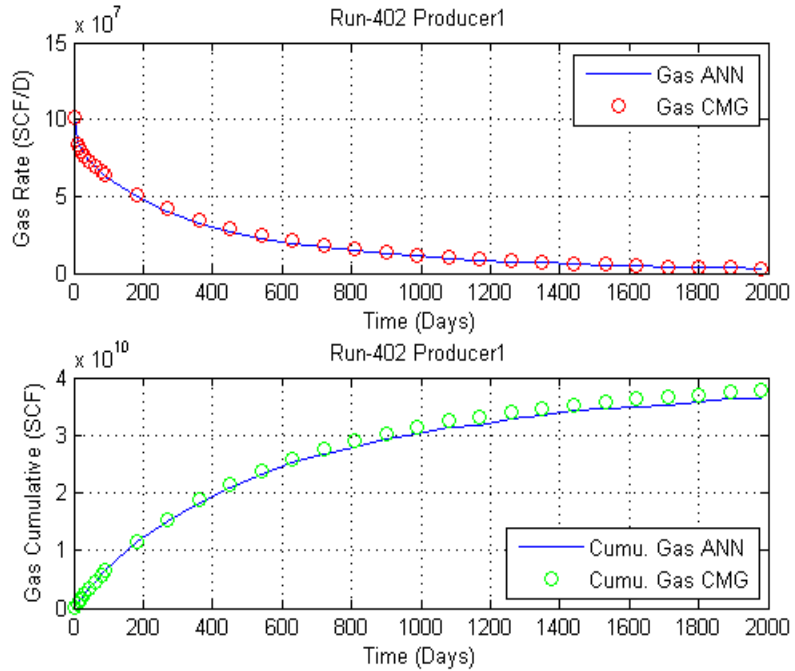


Figure 98 Data set 402 of forward network for three-layered system

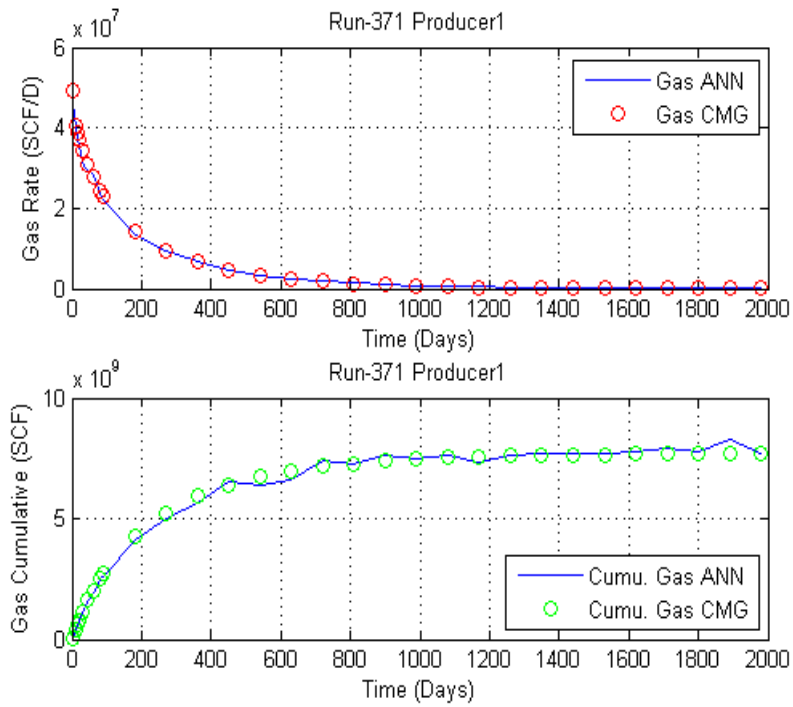


Figure 99 Data set 371 of forward network for three-layered system

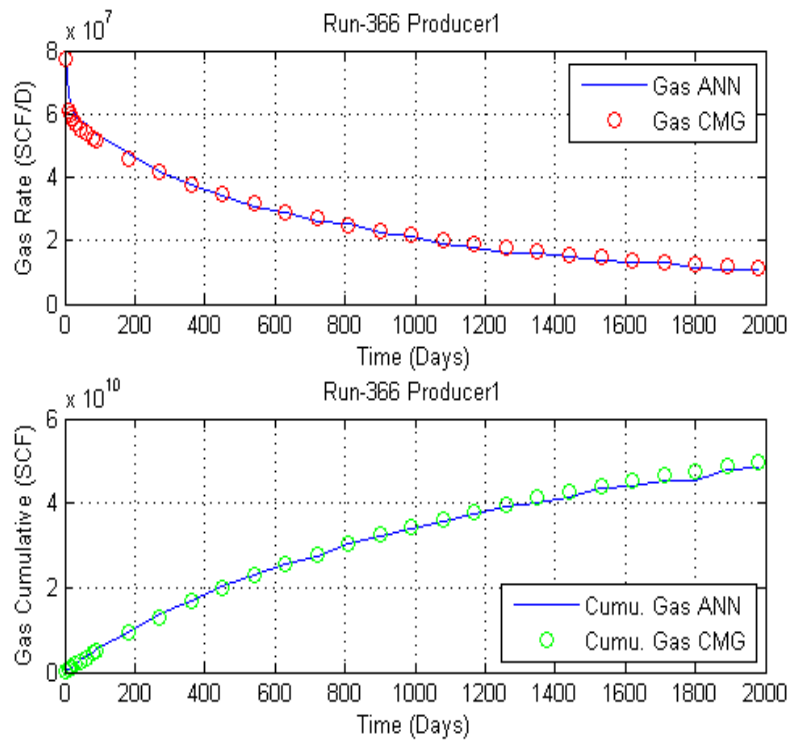


Figure 100 Data set 366 of forward network for three-layered system

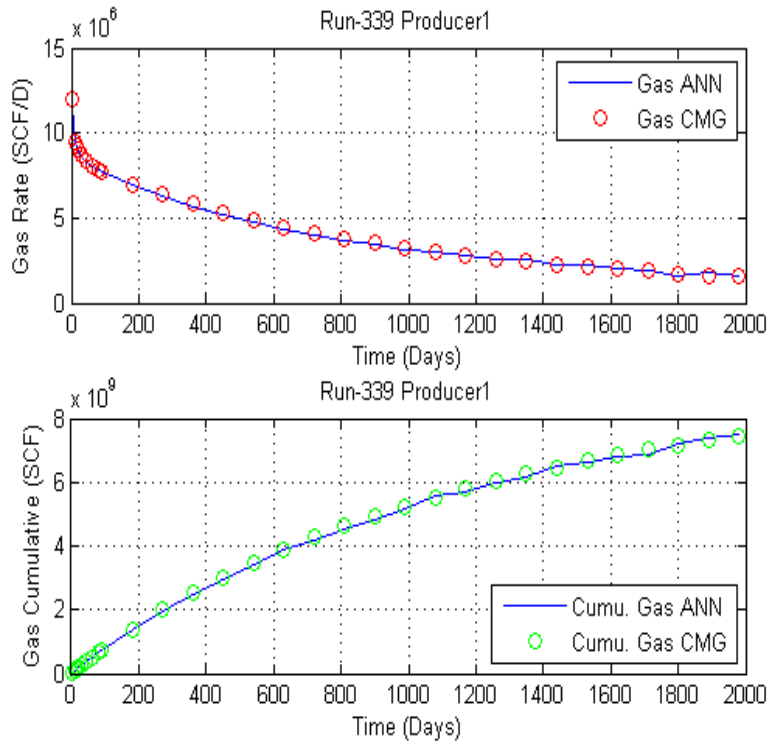


Figure 101 Data set 339 of forward network for three-layered system

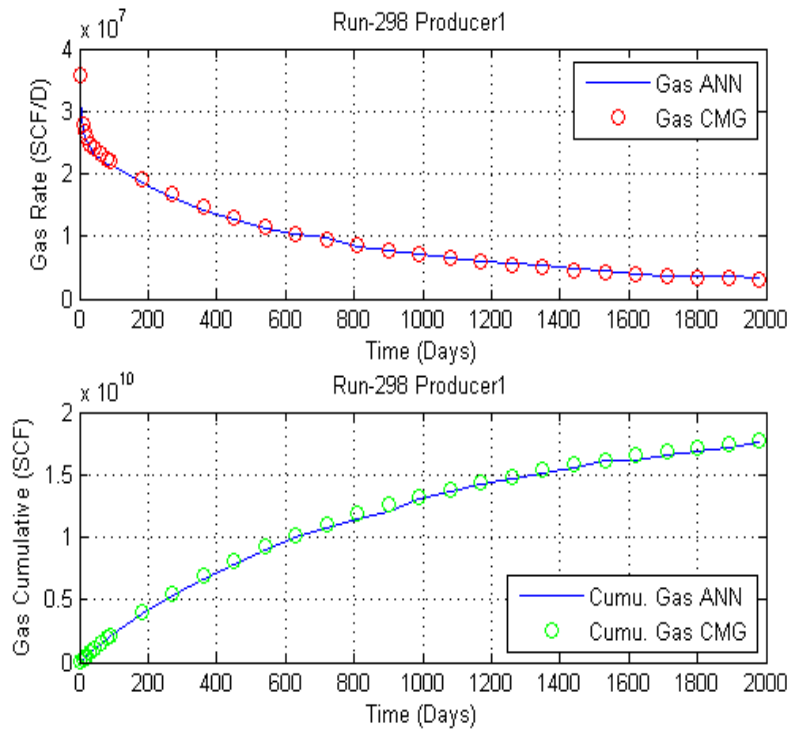


Figure 102 Data set 298 of forward network for three-layered system

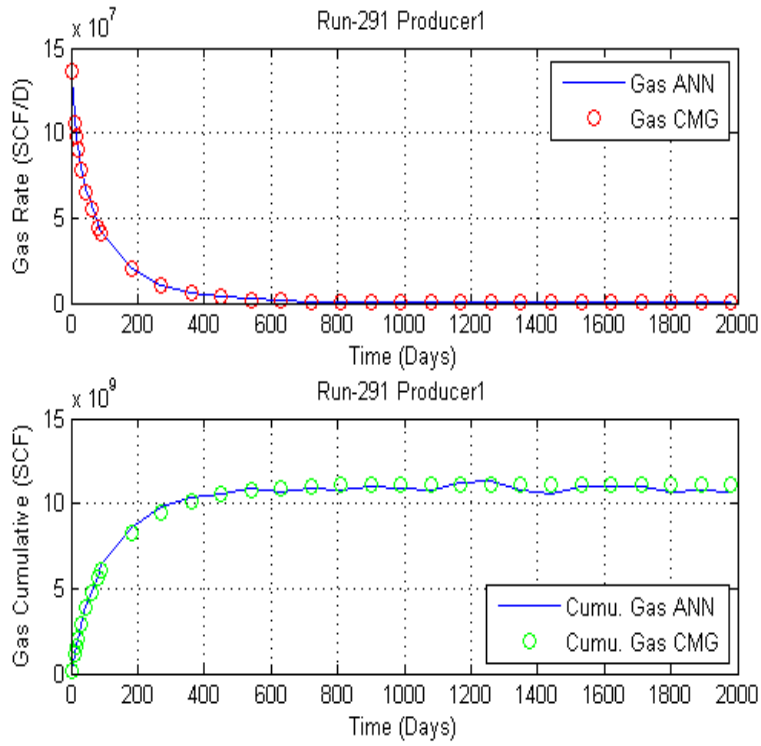


Figure 103 Data set 291 of forward network for three-layered system

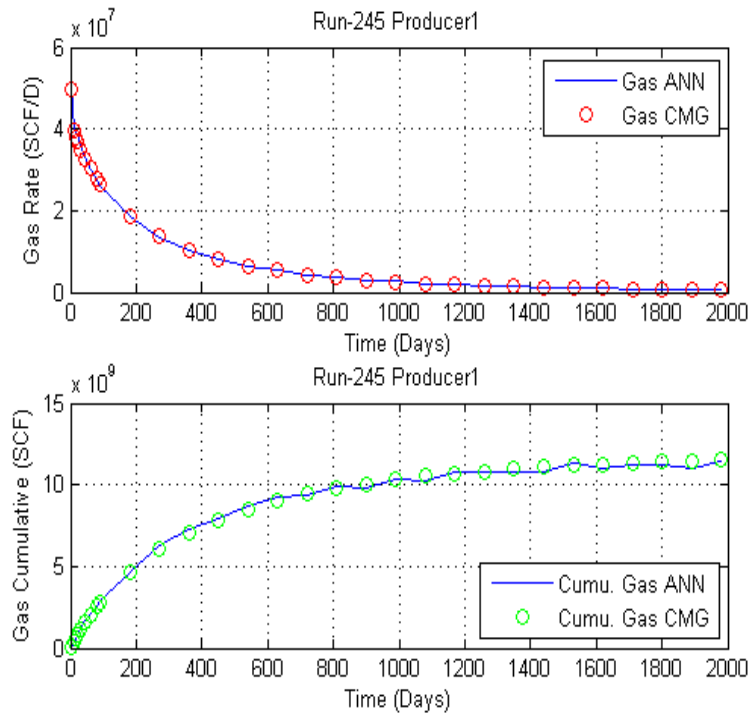


Figure 104 Data set 245 of forward network for three-layered system

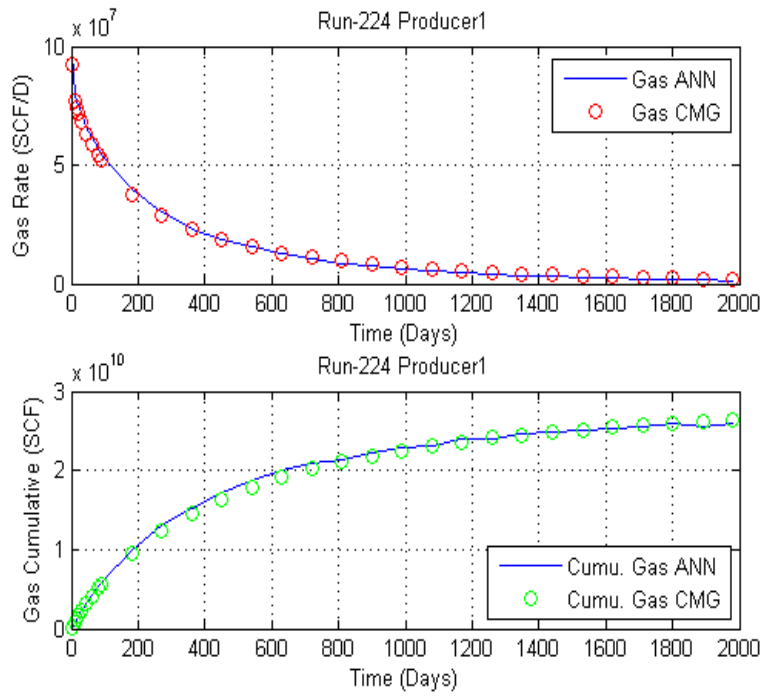


Figure 105 Data set 224 of forward network for three-layered system

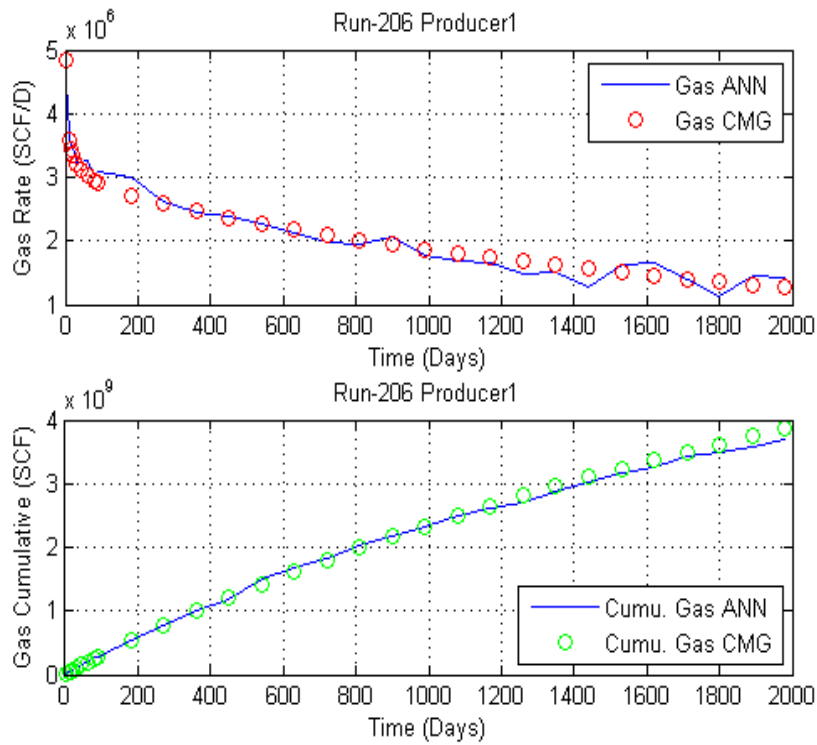


Figure 106 Data set 206 of forward network for three-layered system

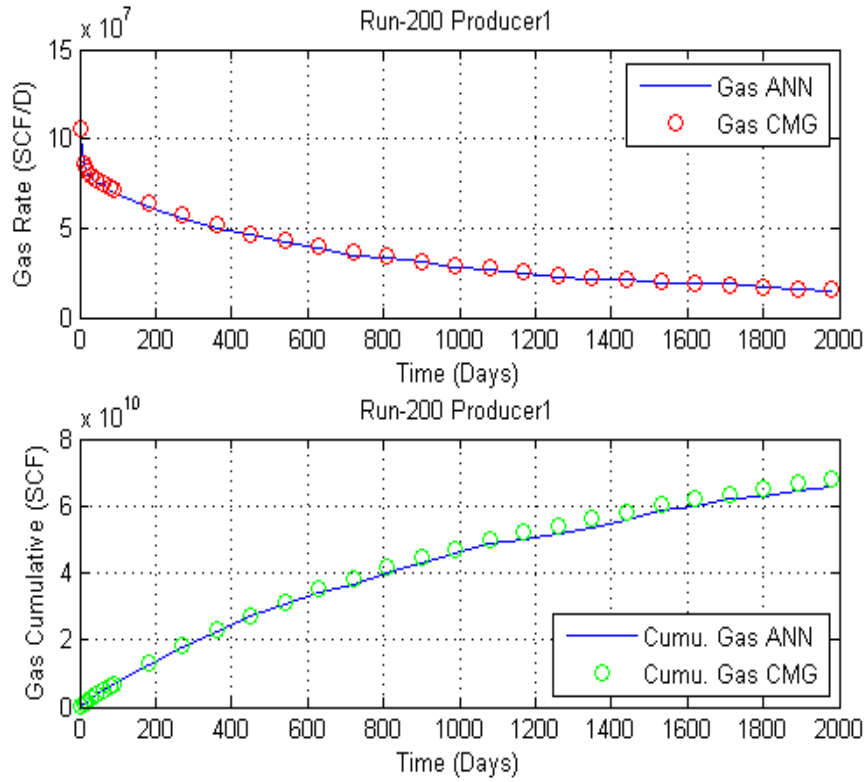


Figure 107 Data set 200 of forward network for three-layered system

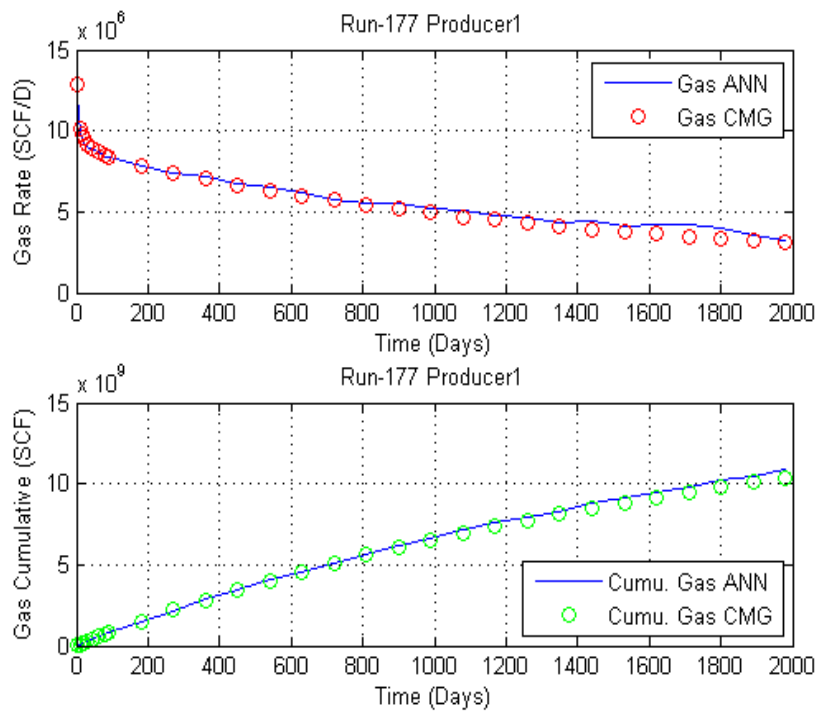


Figure 108 Data set 177 of forward network for three-layered system

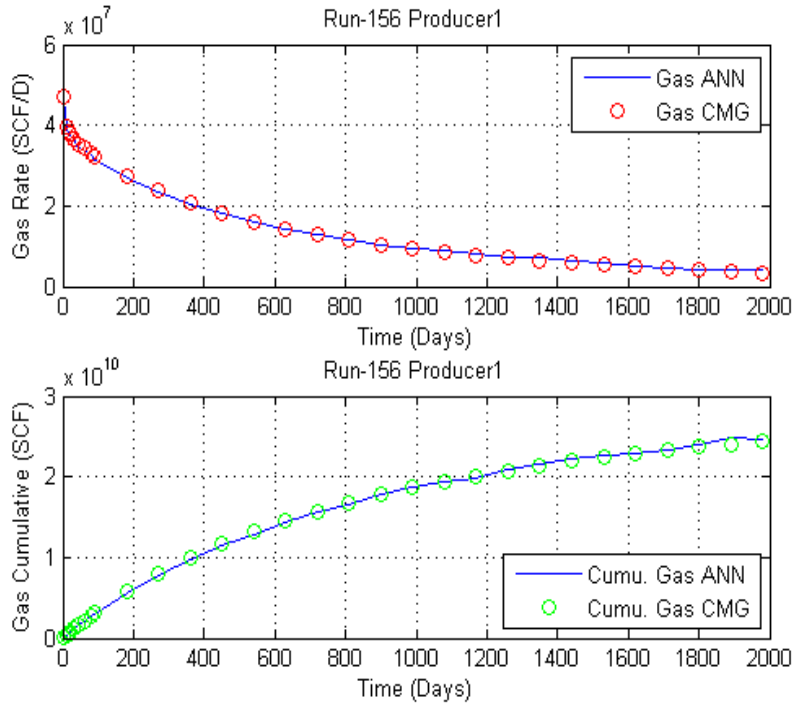


Figure 109 Data set 156 of forward network for three-layered system

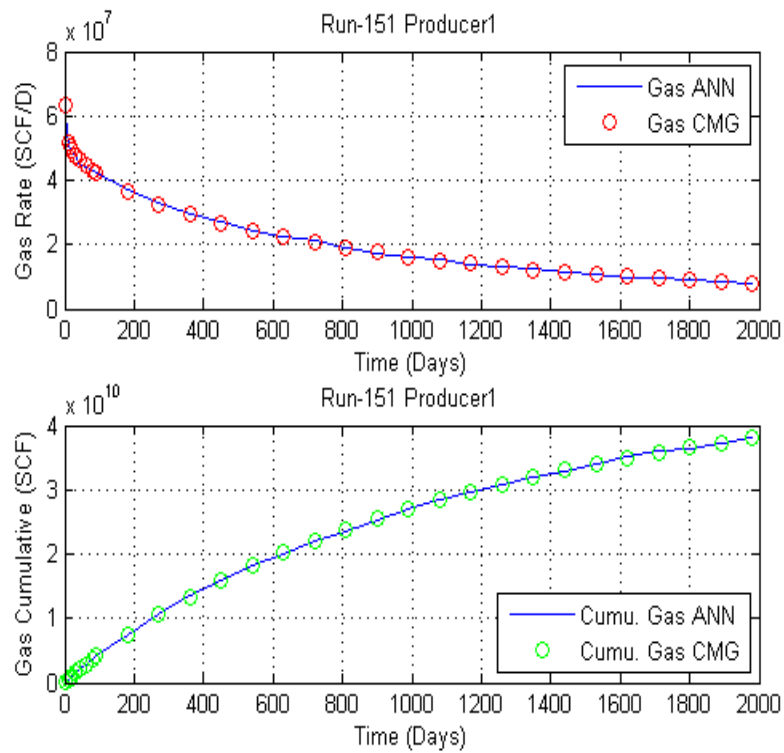


Figure 110 Data set 151 of forward network for three-layered system

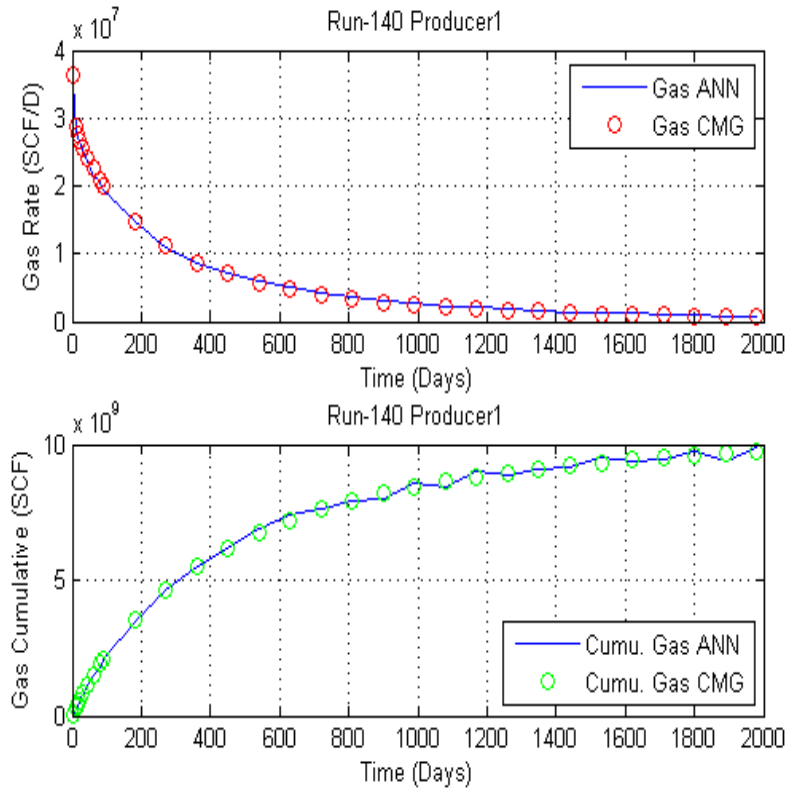


Figure 111 Data set 140 of forward network for three-layered system

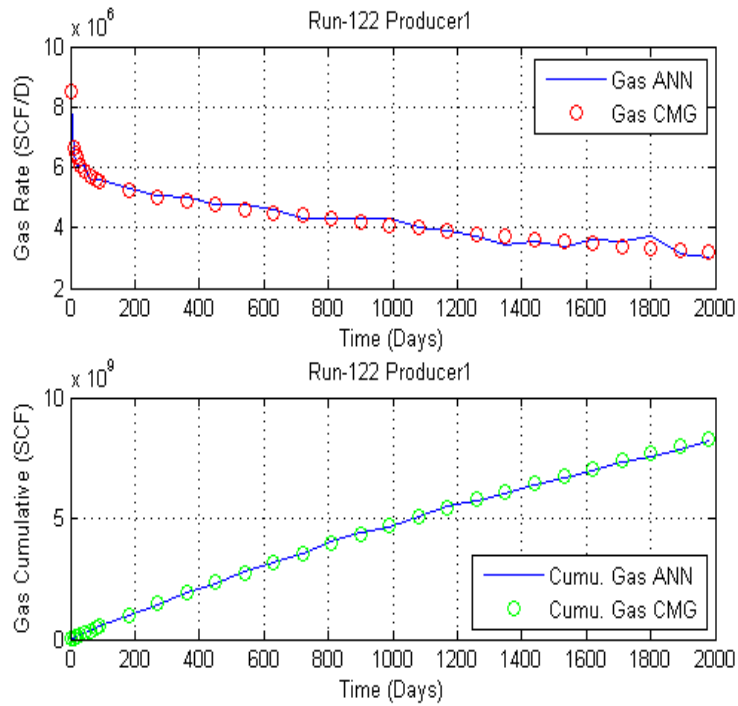


Figure 112 Data set 122 of forward network for three-layered system

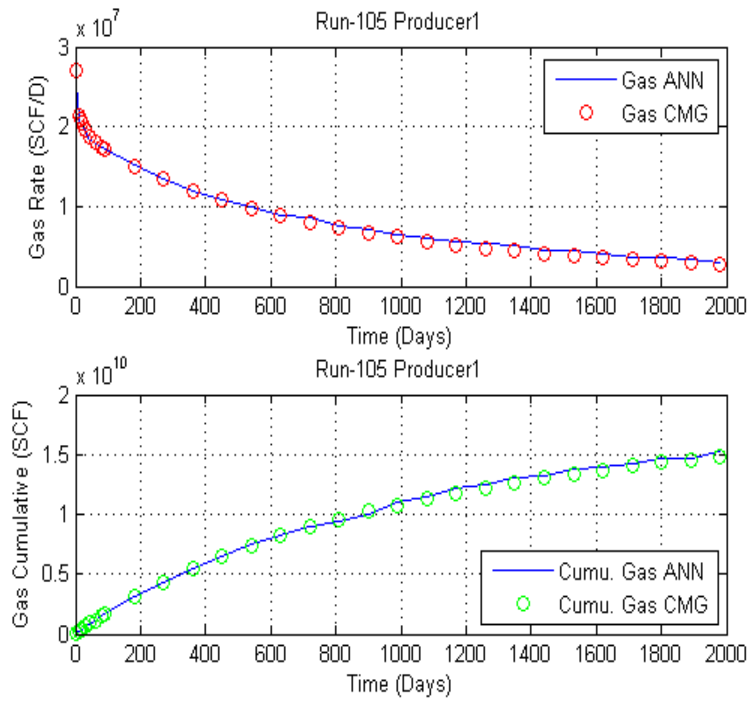


Figure 113 Data set 105 of forward network for three-layered system

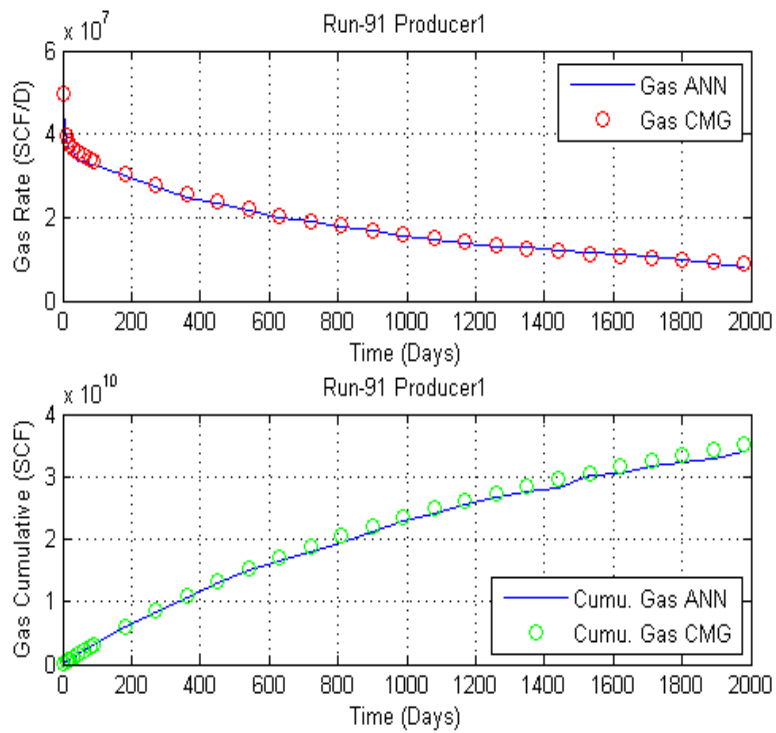


Figure 114 Data set 91 of forward network for three-layered system

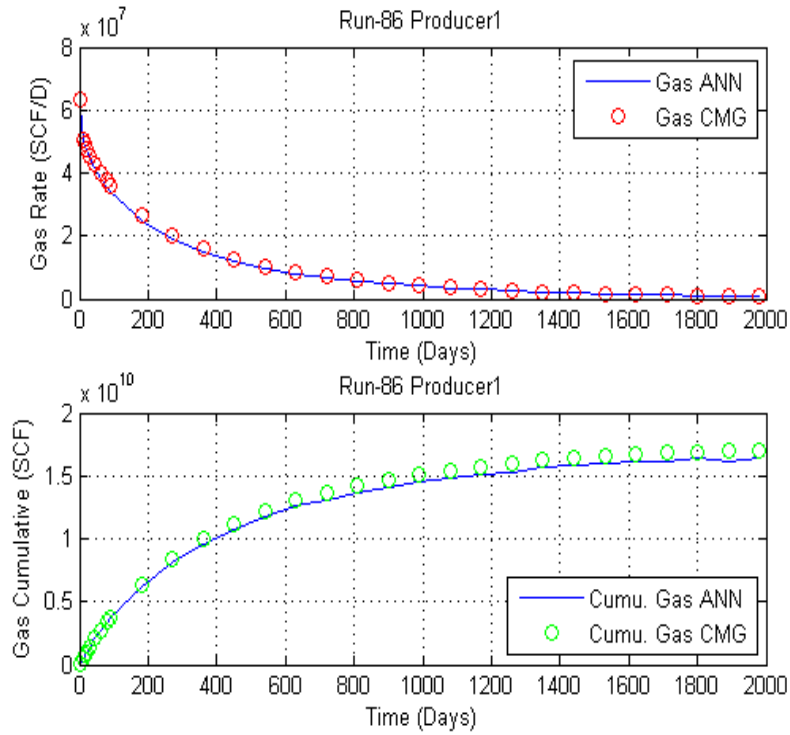


Figure 115 Data set 86 of forward network for three-layered system

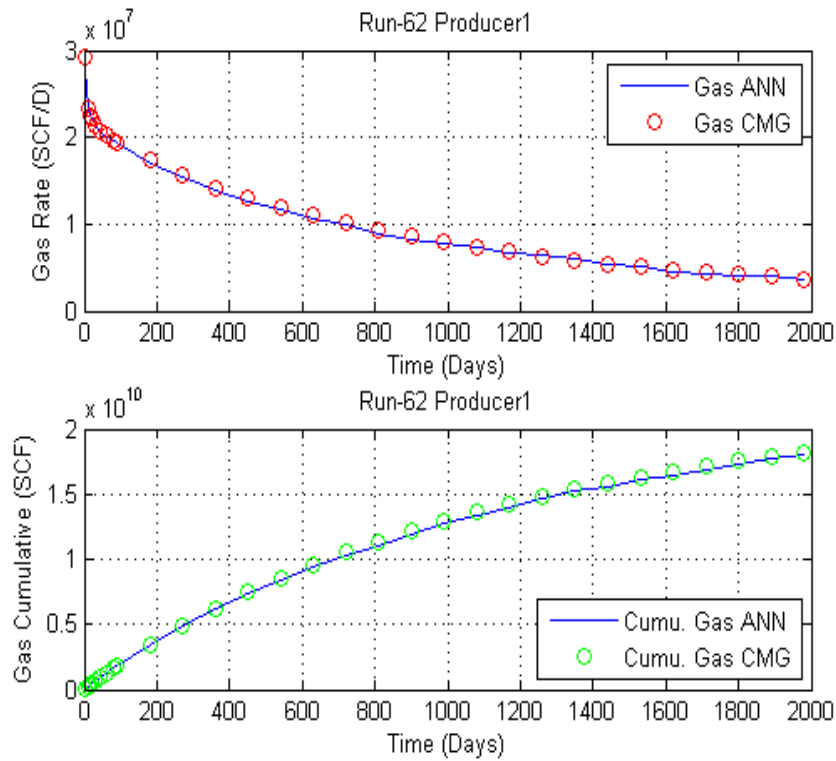


Figure 116 Data set 62 of forward network for three-layered system

Appendix D

Forward network and simulator comparison plots in three-layered reservoir

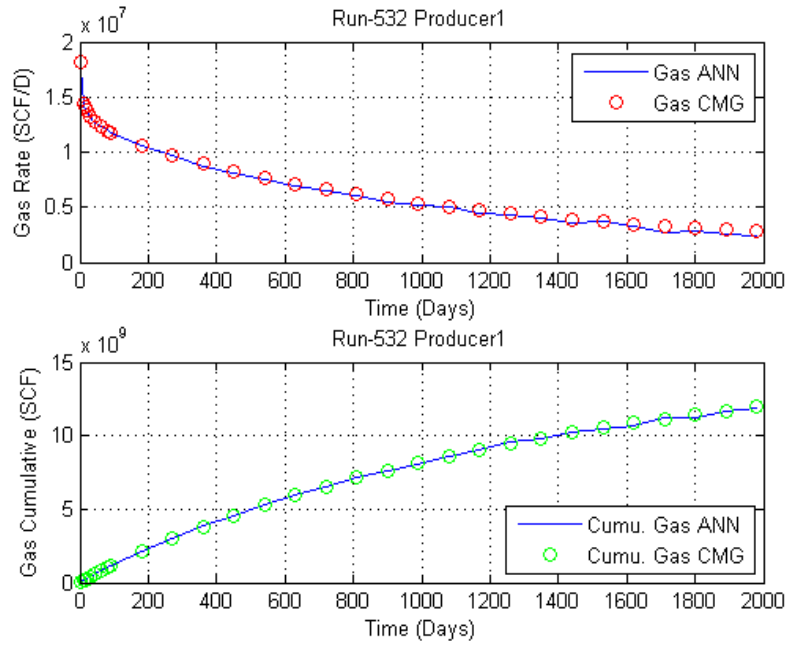


Figure 117 data set 532 forward solution for four-layered reservoir

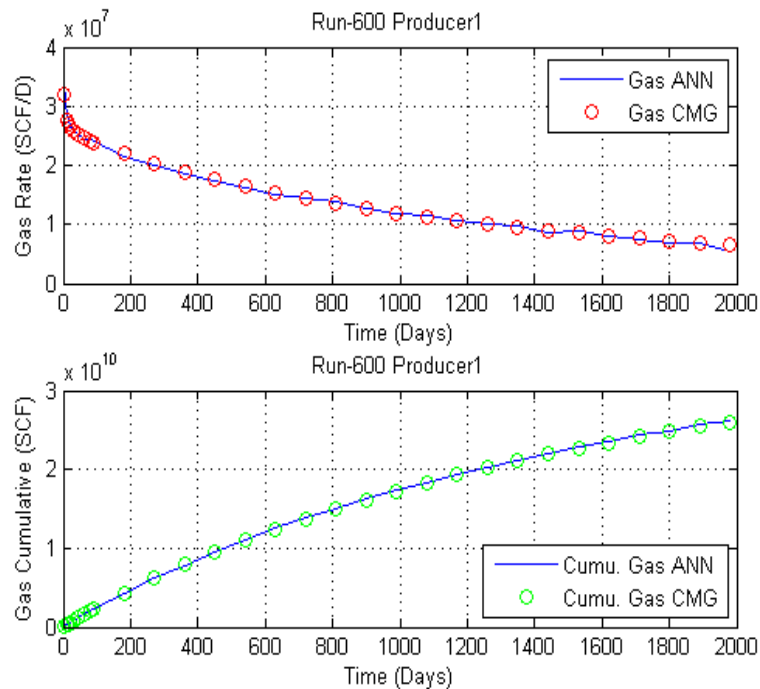


Figure 118 data set 600 forward solution for four-layered reservoir

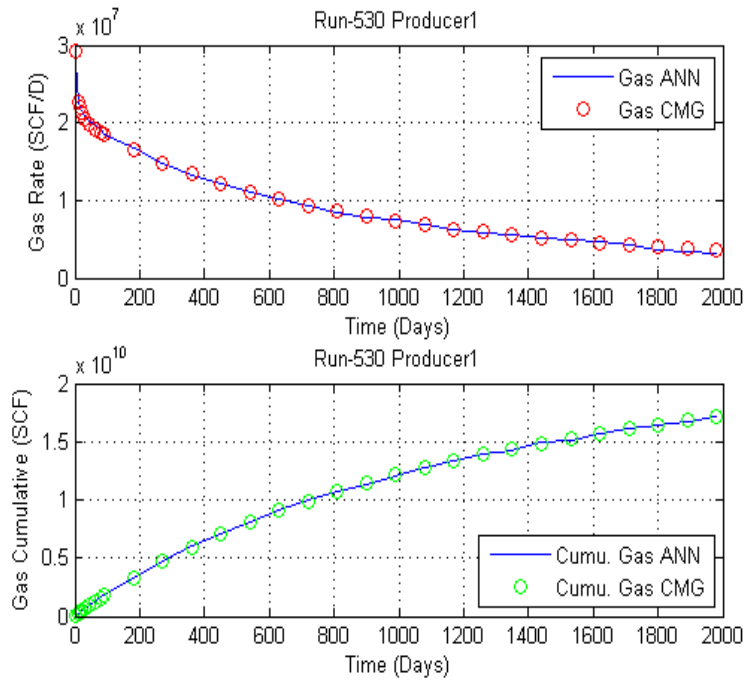


Figure 119 data set 530 forward solution for four-layered reservoir

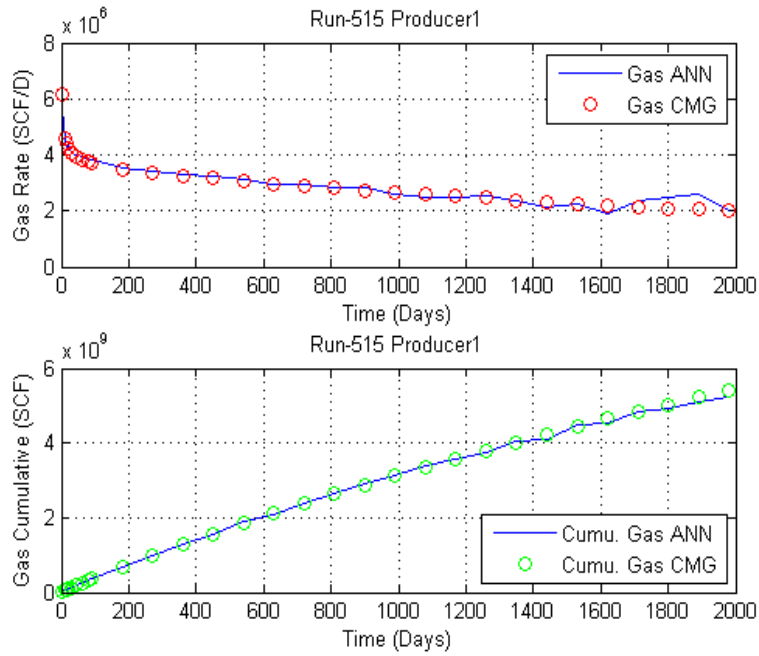


Figure 120 data set 515 forward solution for four-layered reservoir

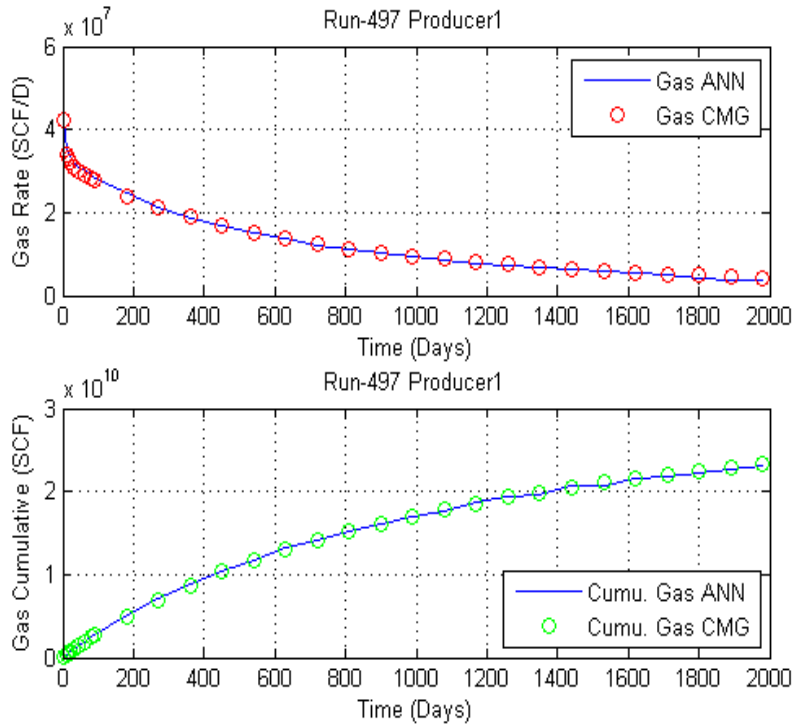


Figure 121 data set 497 forward solution for four-layered reservoir

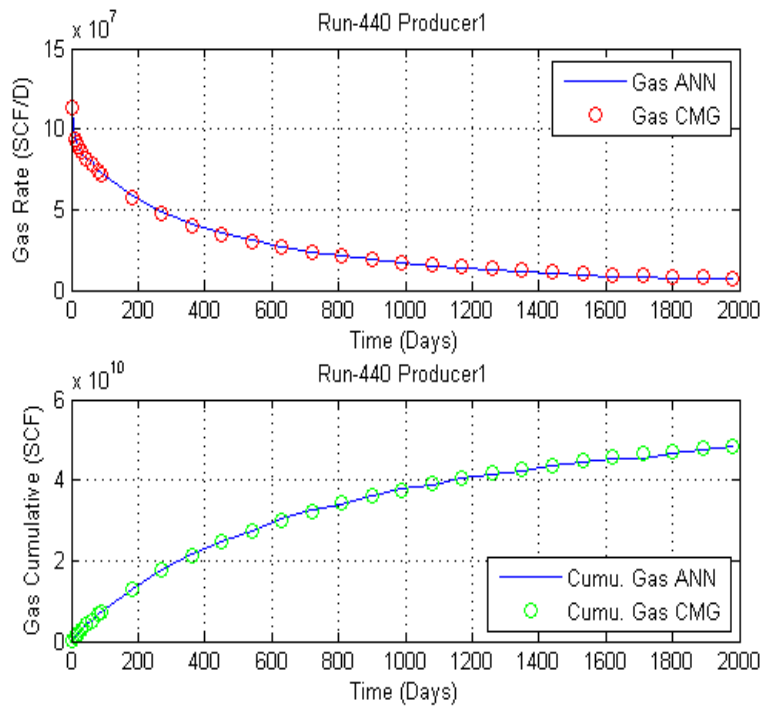


Figure 122 data set 440 forward solution for four-layered reservoir

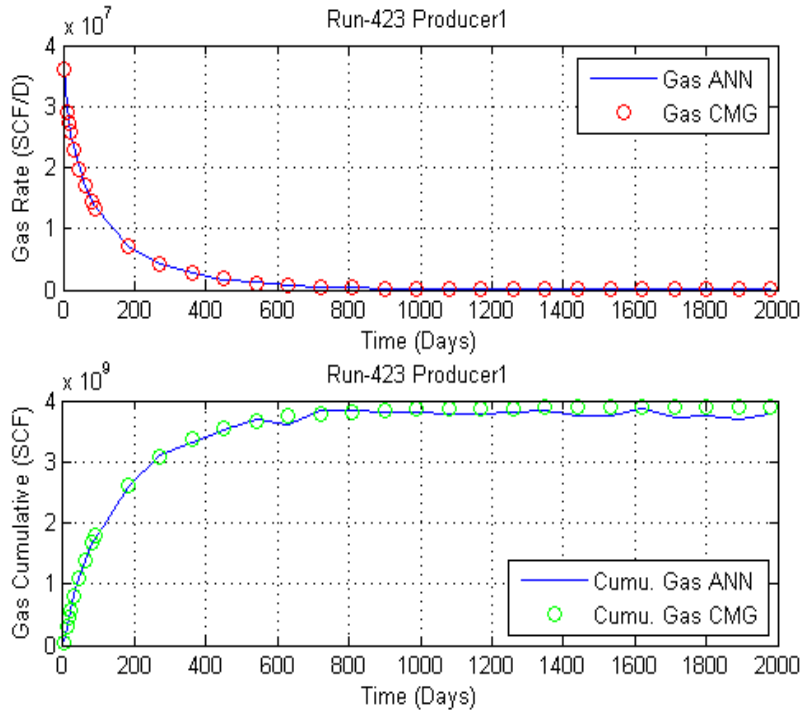


Figure 123 data set 423 forward solution for four-layered reservoir

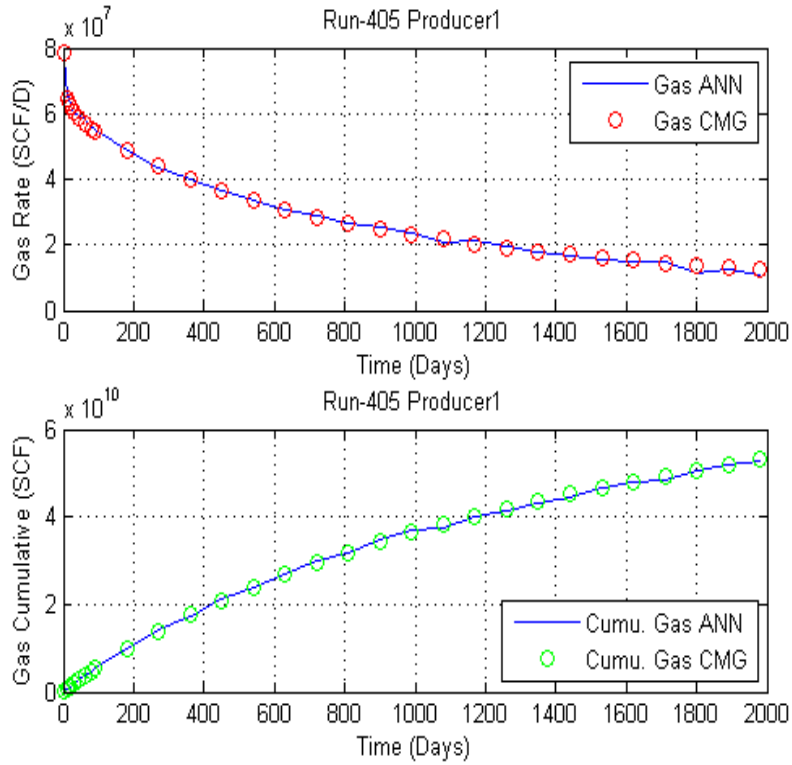


Figure 124 data set 405 forward solution for four-layered reservoir

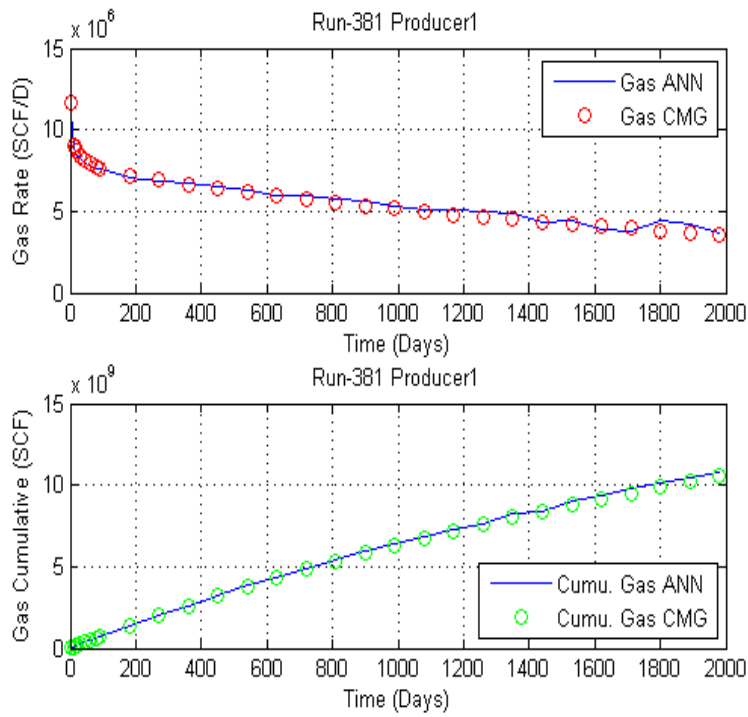


Figure 125 data set 381 forward solution for four-layered reservoir

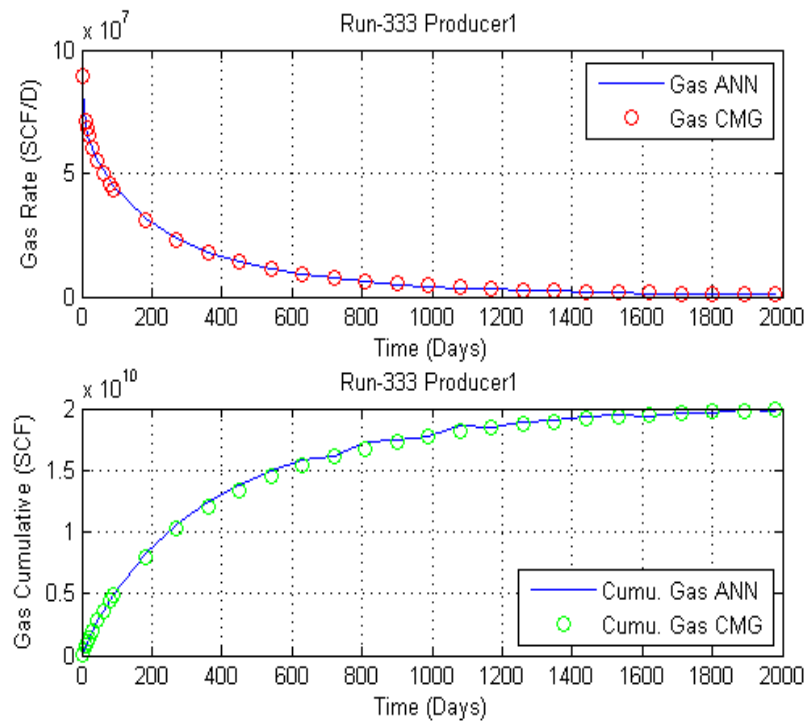


Figure 126 data set 333 forward solution for four-layered reservoir

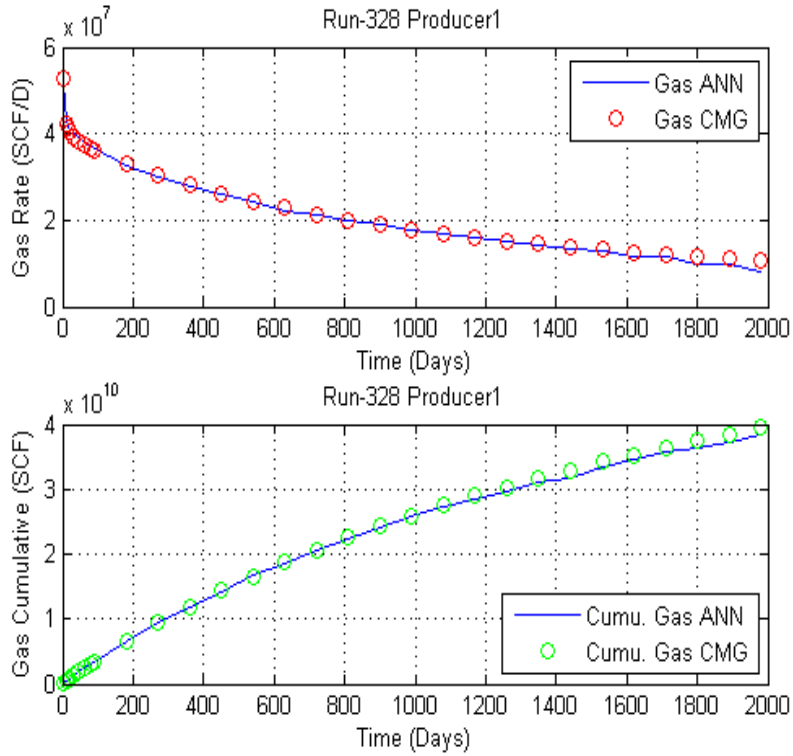


Figure 127 data set 328 forward solution for four-layered reservoir

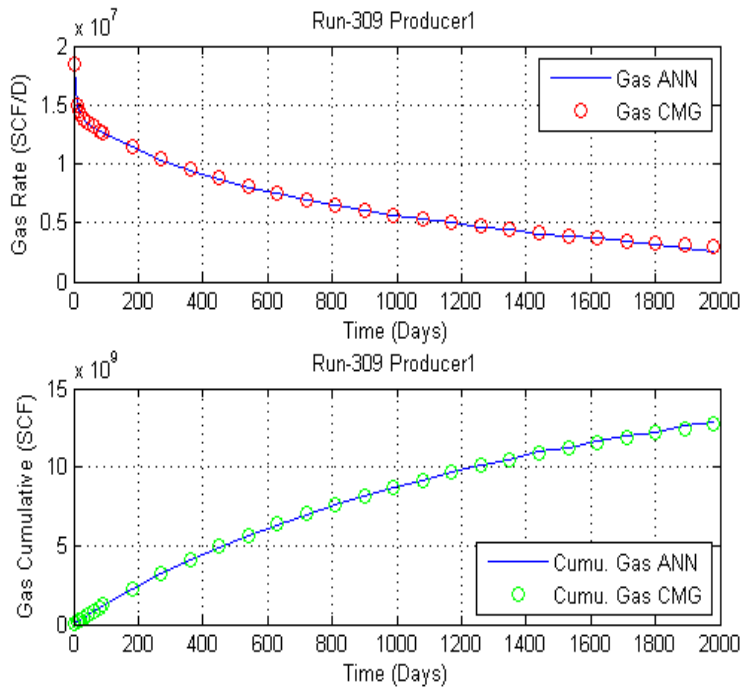


Figure 128 data set 309 forward solution for four-layered reservoir

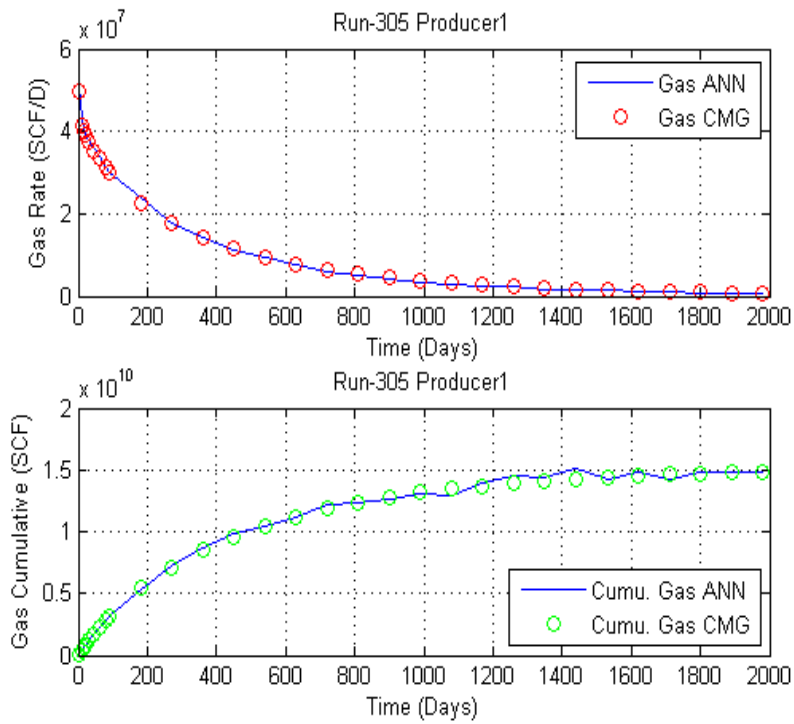


Figure 129 Data set 305 forward solution for four-layered reservoir

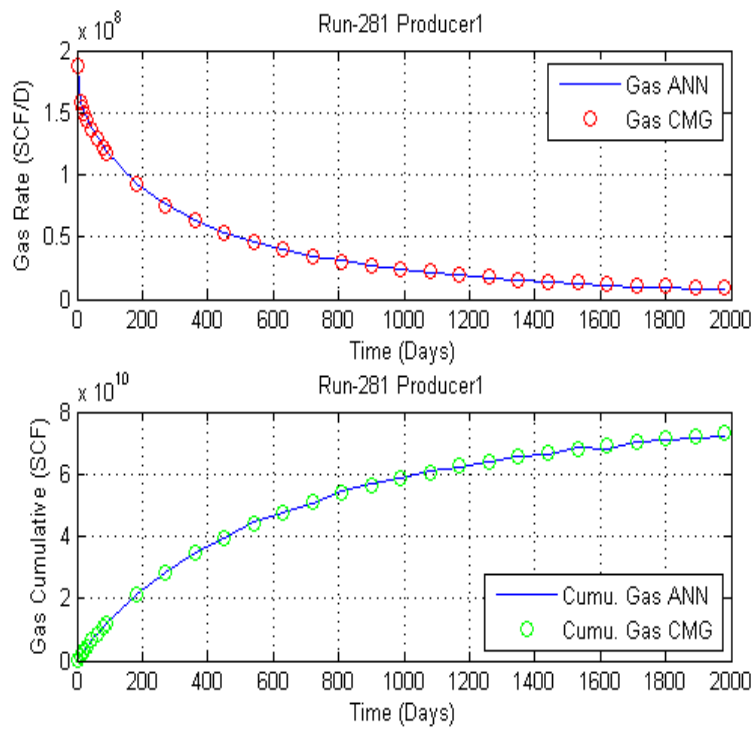


Figure 130 Data set 281 forward solution for four-layered reservoir

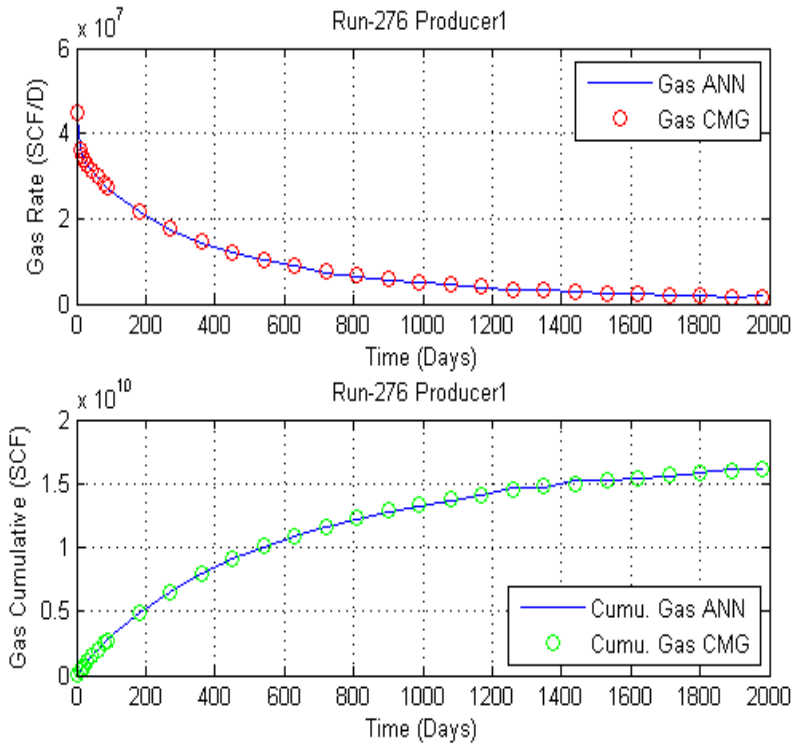


Figure 131 Data set 276 forward solution for four-layered reservoir

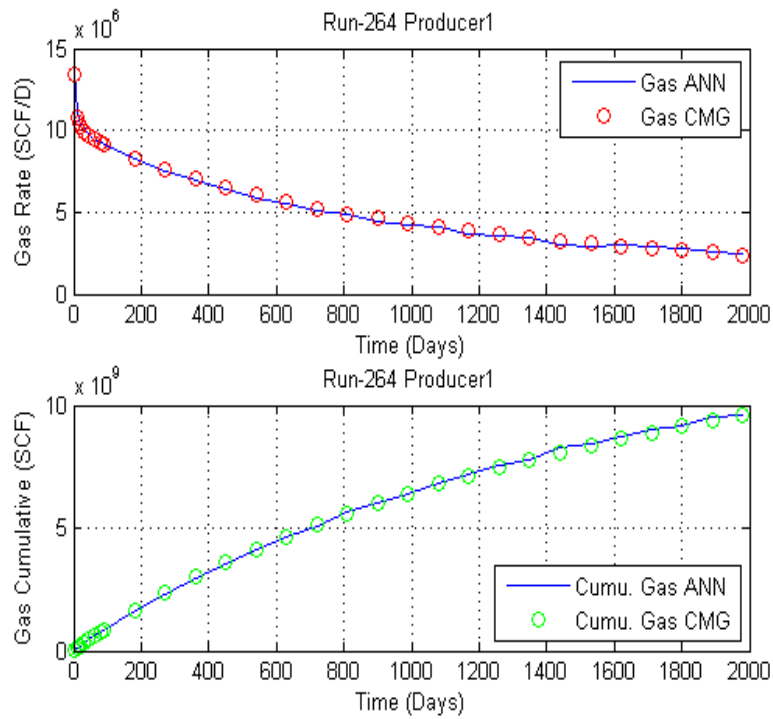


Figure 132 Data set 264 forward solution for four-layered reservoir

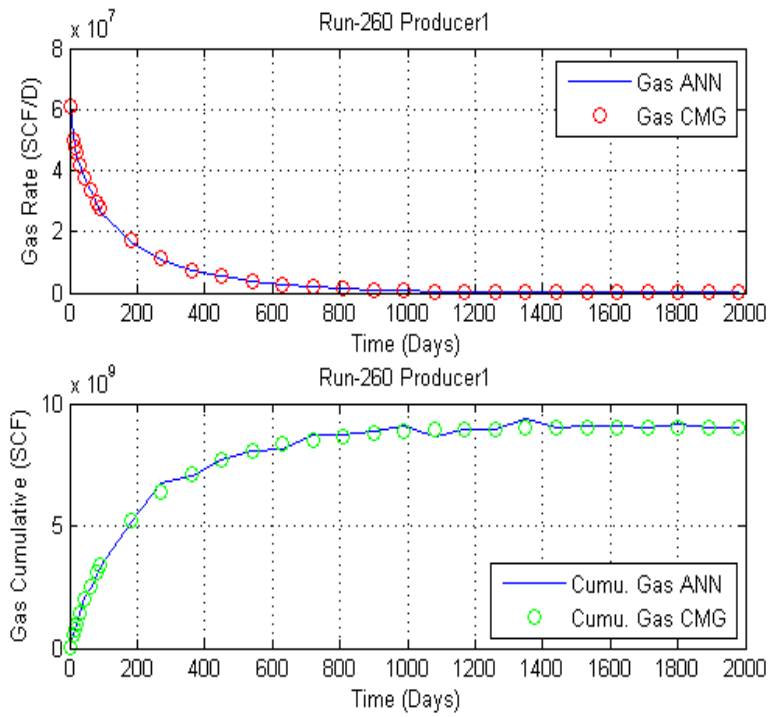


Figure 133 Data set 260 forward solution for four-layered reservoir

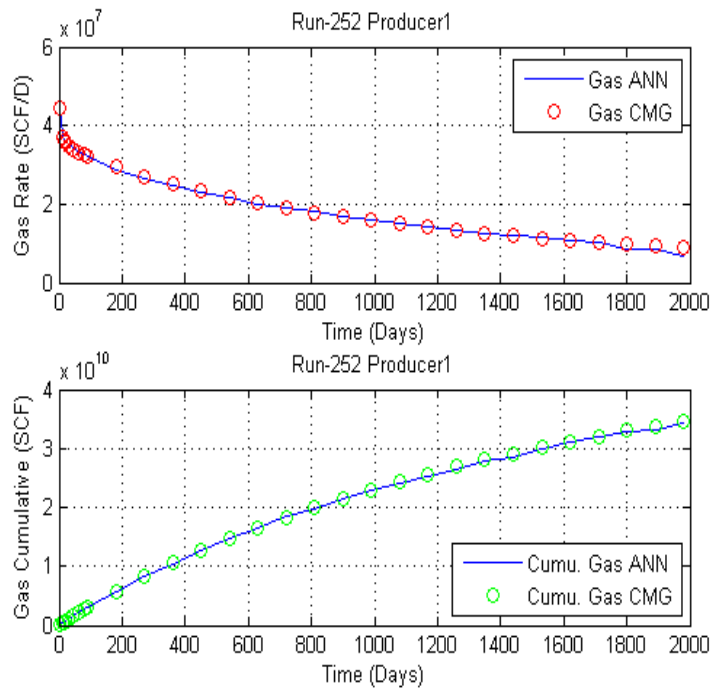


Figure 134 Data set 252 forward solution for four-layered reservoir

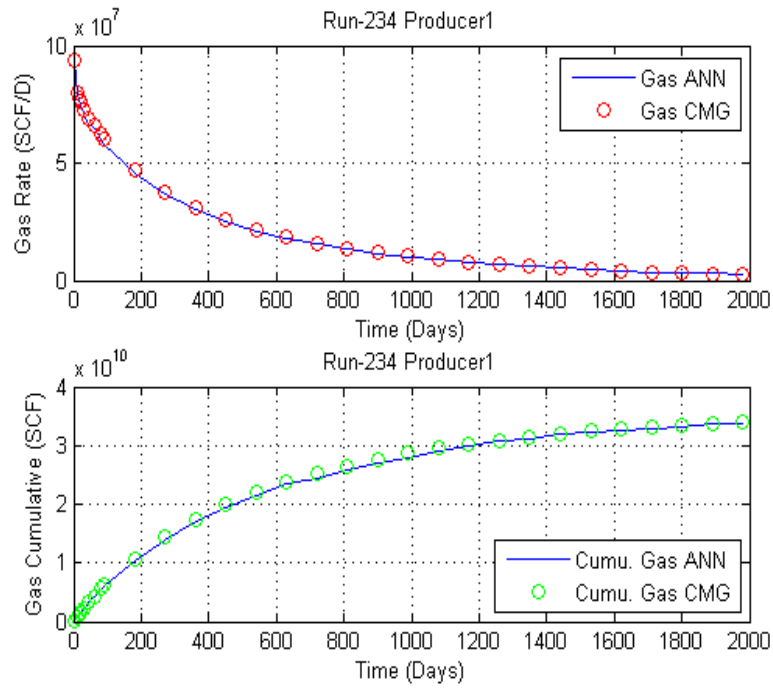


Figure 135 Data 234 set 305 forward solution for four-layered reservoir

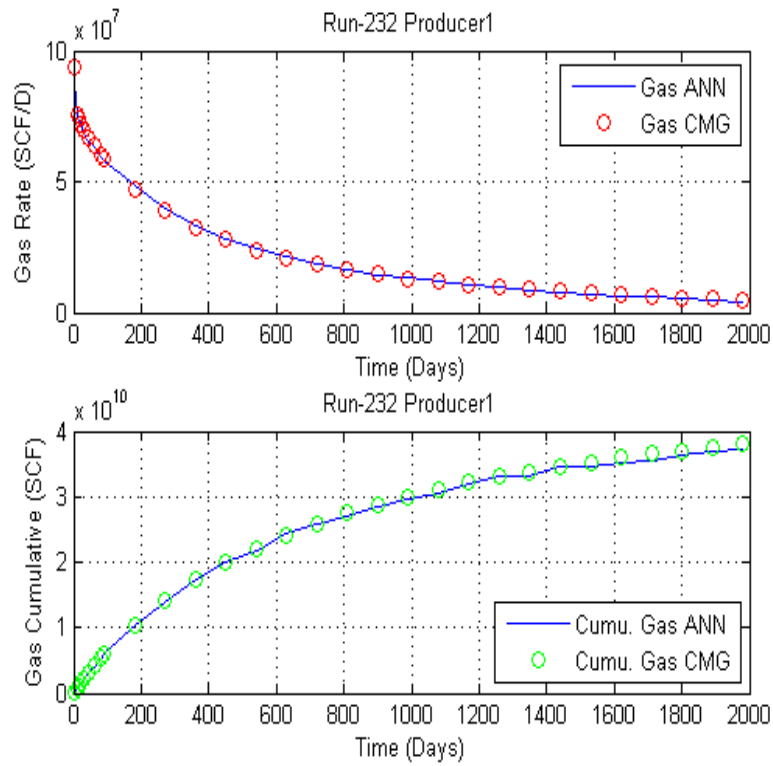


Figure 136 Data set 232 forward solution for four-layered reservoir

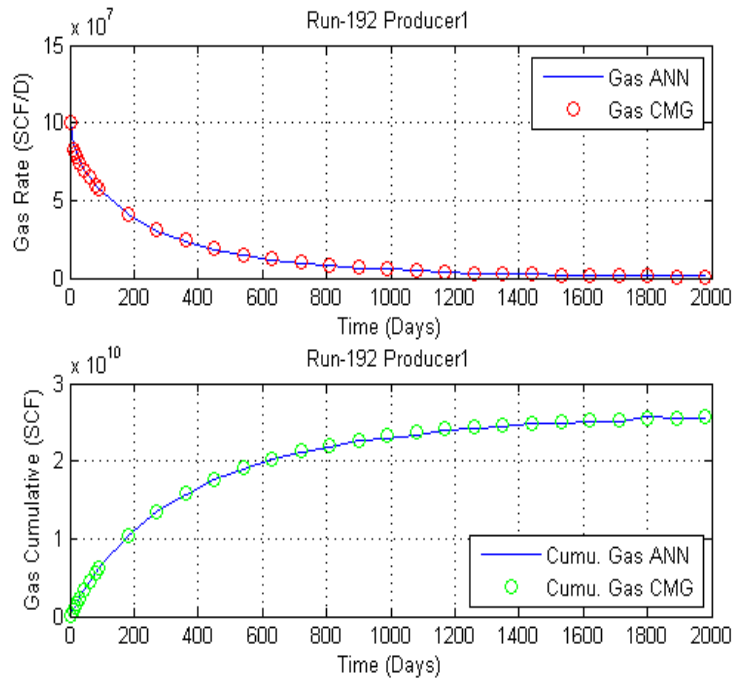


Figure 137 Data set 192 forward solution for four-layered reservoir

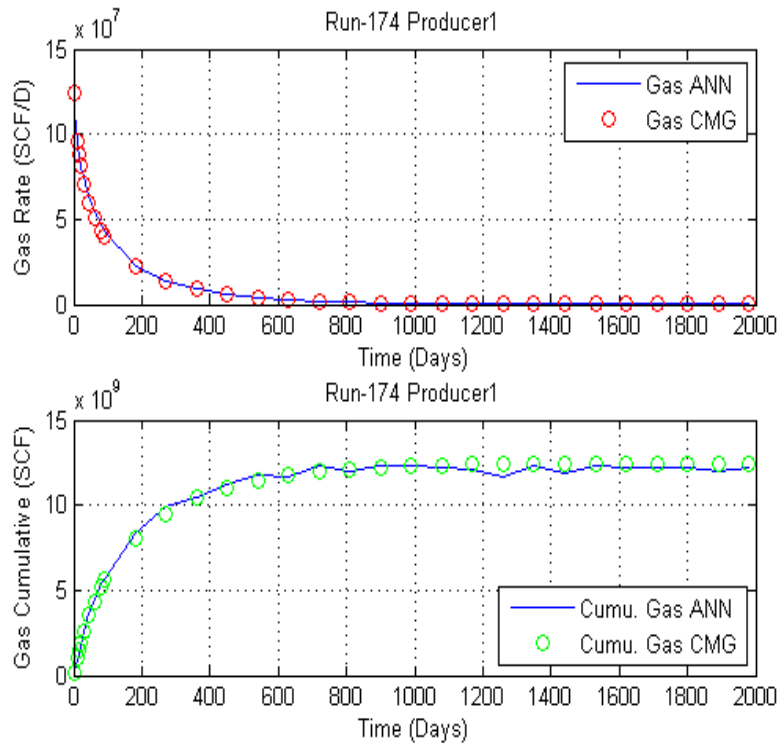


Figure 138 Data set 174 forward solution for four-layered reservoir

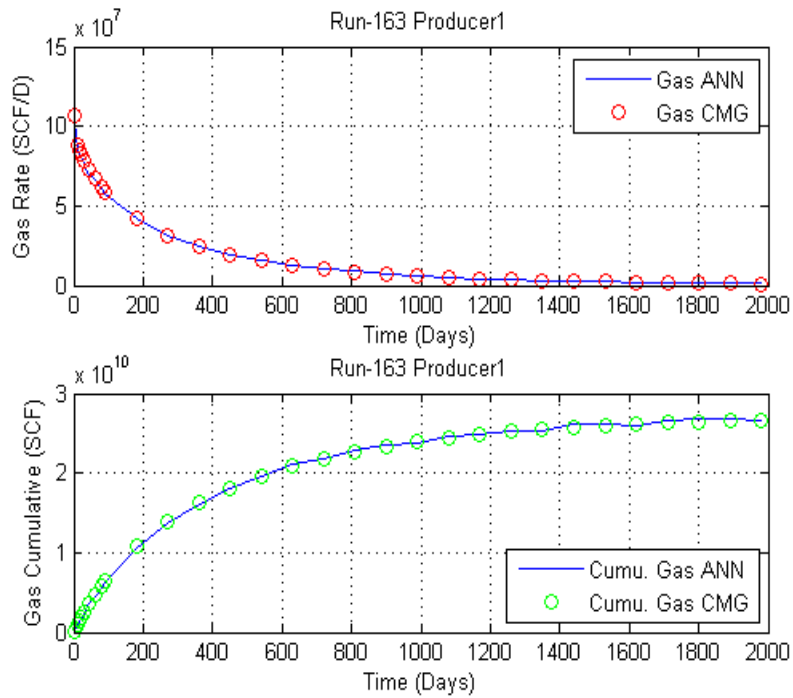


Figure 139 Data set 163 forward solution for four-layered reservoir

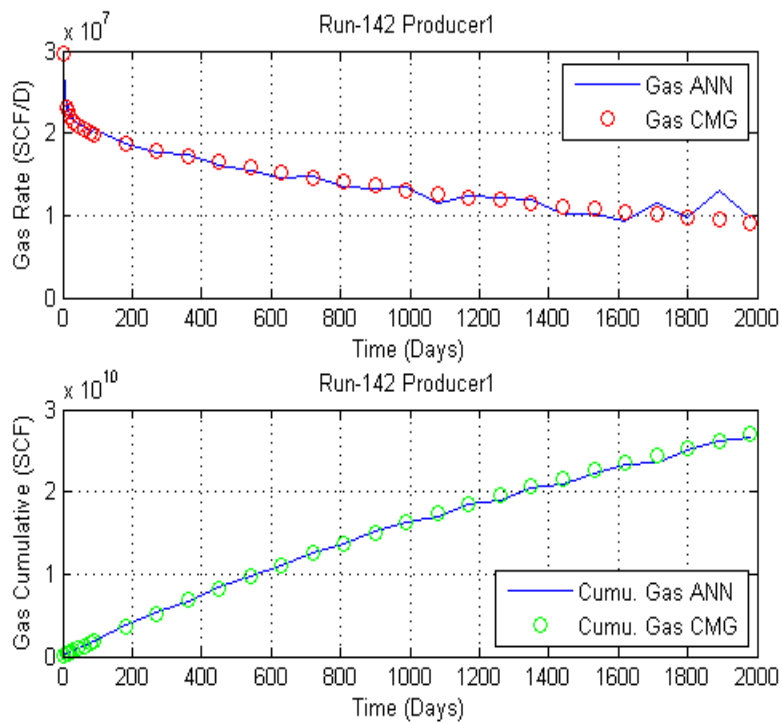


Figure 140 Data set 142 forward solution for the four-layered reservoir

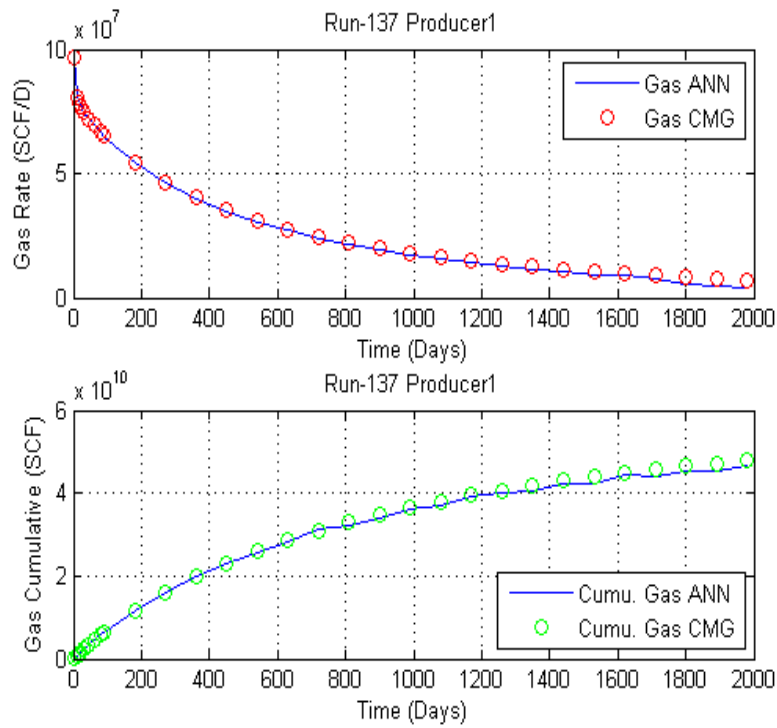


Figure 141 Data set 137 forward solution for the four-layered reservoir

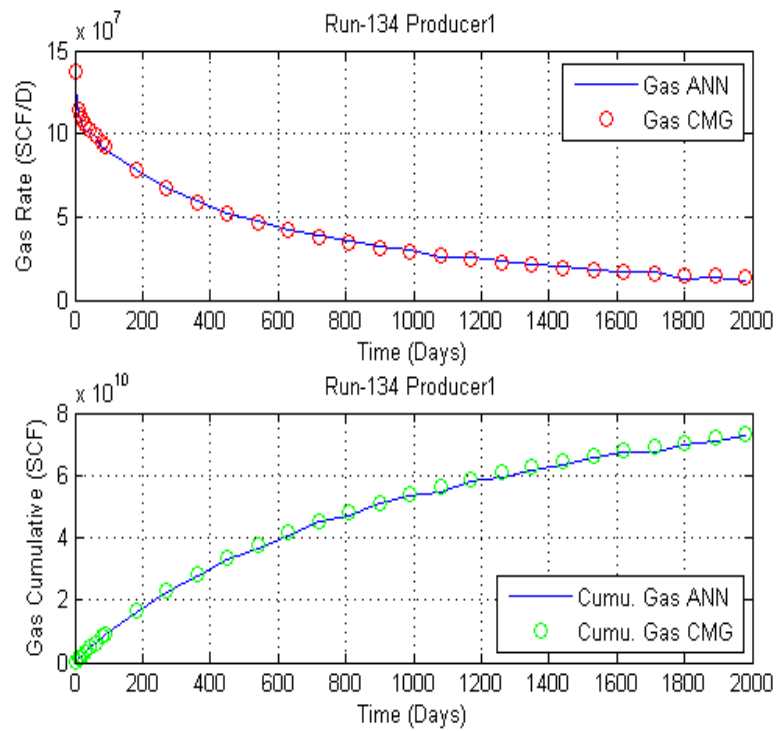


Figure 142 Data set 134 forward solution for the four-layered reservoir

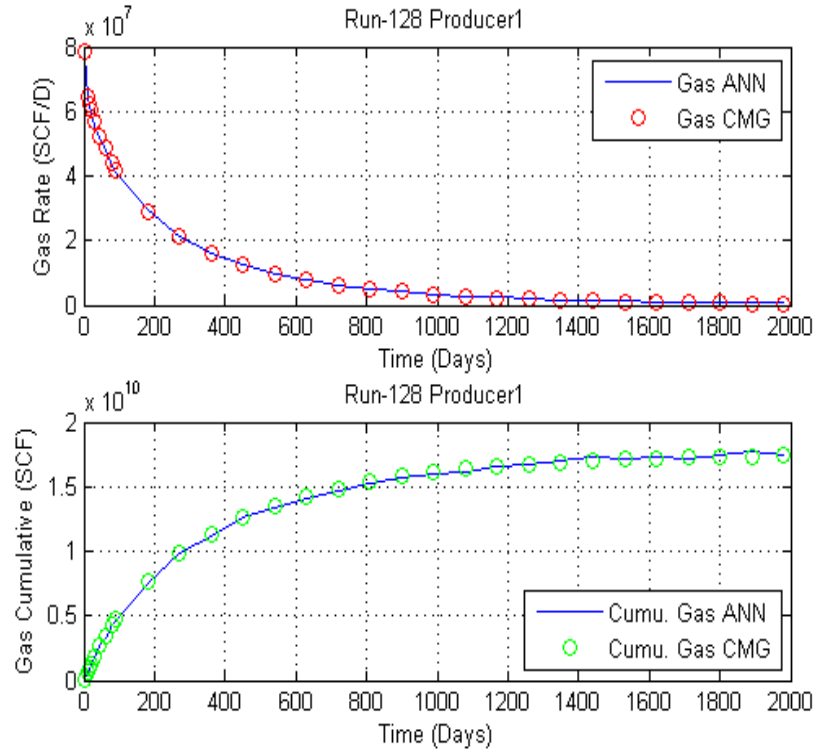


Figure 143 Data set 128 forward solution for the four-layered reservoir

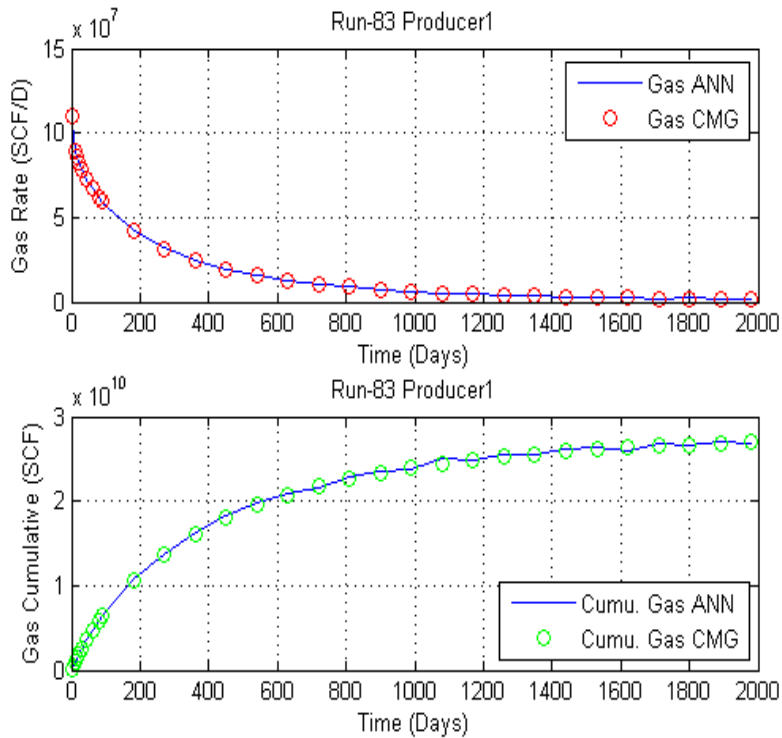


Figure 144 Data set 83 forward solution for the four-layered reservoir

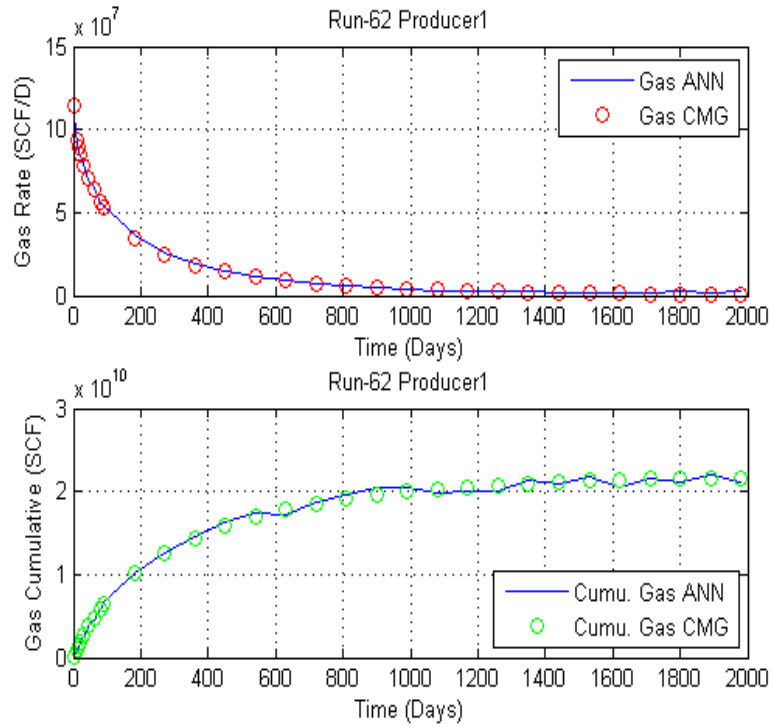


Figure 145 Data set 62 forward solution for the four-layered reservoir

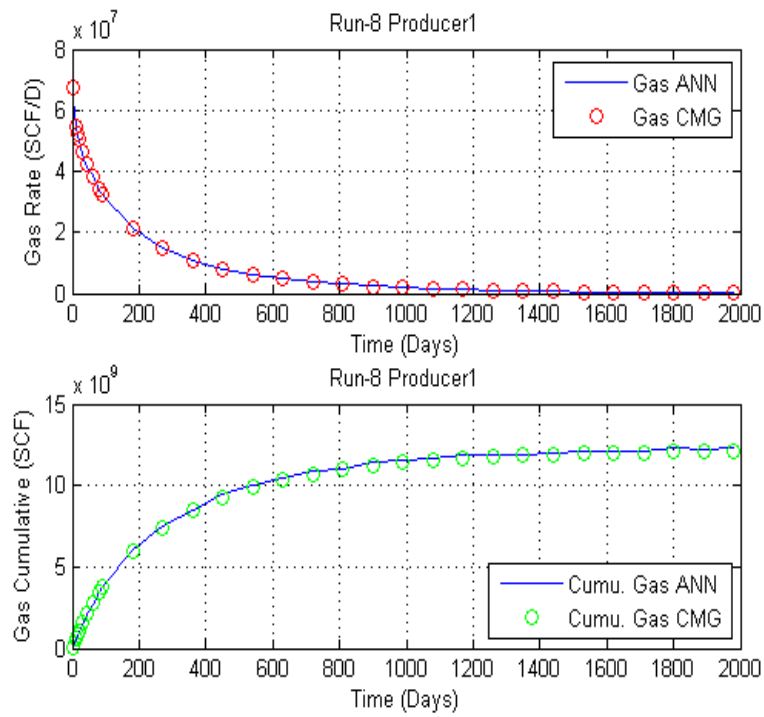


Figure 146 Data set 8 forward solution for the four-layered reservoir